Inland Norway University of Applied Sciences

Faculty of Applied Ecology, Agricultural Sciences and Biotechnology

Sharmin Sultana

Master's thesis

Liquid Array Diagnostics Technology for SARS-CoV-2 variant detection

Masters in applied experimental biotechnology

2024

Consent to lending by University College Library	YES ☒	NO ☐
Consent to accessibility in digital archive Brage	YES ☒	NO ☐

Acknowledgements

In a realm where academic pursuits often diverge from personal passions, I count myself fortunate to have embarked on a master's thesis journey aligned with my deepest interests. I am profoundly grateful for the opportunity to explore my passion within the realm of scholarly inquiry and for the unwavering support that has accompanied me on this extraordinary journey. I am incredibly grateful to my supervisor, Professor Rob Wilson, for his constant encouragement, insightful suggestions, and supportive feedback during my whole research project. This work would not have been possible without his countless guidance, support, and constructive feedback.

Furthermore, I extend my sincere gratitude to Professor Wenche Johansen for her invaluable support and guidance throughout the implementation of cloning technology.

To Wenche Kristiansen and Hanne Greaker, our esteemed lab engineers, I extend my profound appreciation for your remarkable help, time, and patience during my laboratory endeavors. Your support has been indispensable.

I am incredibly grateful to my dear friend Asmita Srestha, whose steady presence and support have been an anchor for me when I've felt feeble.

Words are not enough to thank my beloved family, especially my Mom and Dad, for their boundless love, endless encouragement, and profound understanding throughout this challenging journey. Their steadfast support has been my guiding light and the fuel behind my perseverance. Thank you from the bottom of my heart.

Last but not the least, my greatest gratitude towards Inland Norway University of Applied Sciences, Campus Hamar for fulfilling my aim of studying Biotechnology.

Abbreviations

DNA	Deoxyribonucleic acid
PCR	Polymerase Chain Reaction
qPCR	quantitative Polymerase Chain Reaction
BP	Base Pair
cDNA	Complementary DNA
COVID-19	Coronavirus Disease 2019
CE	Capillary Electrophoresis
SARS-CoV-2	Severe Acute Respiratory Syndrome Coronavirus 2
SNP	Single Nucleotide Polymorphism
SBE	Single Base Extension
FRET	Fluorescence resonance energy transfer
ACE	Angiotensin-Converting Enzyme
ORF	Open Reading Frame
NSP	Nonstructural Protein
PP	Polyprotein
CPE	Common primer extension
LAD	Liquid Array Diagnostics
LP	Labelling probe
RP	Reporter probe
ddNTP	Dideoxynucleotide triphosphate

ddNTP-Q	Quencher labelled ddNTP
ddATP	Dideoxyadenosine triphosphate
ddCTP	Dideoxycytidine triphosophate
ddGTP	Dideoxyguanosine triphosopha
ddUTP	Dideoxyuridine triphosophate
ddATP-Q	Quencher labelled dideoxyadenosine triphosphate
ddCTP-Q	Quencher labelled dideoxycytidine triphosophate
ddGTP-Q	Quencher labelled dideoxyguanosine triphosopha
ddUTP-Q	Quencher labelled dideoxyuridine triphosophate
Tm	Melting Temperature
SDS	Sodium dodecyl sulfate

Table of Contents

Abstract

The appearance of the severe acute respiratory syndrome coronavirus 2 (SARS-CoV-2) in 2020 led to a worldwide pandemic, requiring a collaborative multinational endeavour to understand the virus's behaviour, transmission dynamics, and pathogenicity. The molecular basis for the development of region-specific SARS-CoV-2 diagnostics and therapeutics is provided by SNP genotyping of SARS-CoV-2, which is the most effective technique for researching the genomic epidemiology of COVID-19. The Liquid Array Diagnostics (LAD) approach has recently gained attention as a highly promising platform for multiplex SNP and insertion/deletion (indel) genotyping. By utilizing four-tube multiplex reaction, 18-plex LAD assay allowed for the identification of nine SNPs/indels that are responsible for 18 different allele variants. This permits the differentiation between all viral variants and the wild type.

This study presents the development of a multiplex assay utilizing LAD technology for the precise detection of SARS-CoV-2 variants. Unique SNP sites were identified as the initial step in the method, which is essential for variant discrimination. Consequently, labelling probes were precisely developed to encompass 18 allele variants for nine SNP/indel markers, thereby enabling accurate genotyping. The implementation of single nucleotide extension using the SNaPshot assay ensured successful probe extension. Furthermore, fluorescently labelled RPs were developed to be complementary to the LPs, thereby facilitating the detection procedure. By incorporating short DNA duplexes, each labelled with a fluorophore and a quencher molecule, the LAD approach capitalizes on fluorescence quenching phenomena to achieve high specificity and sensitivity. Four-tube reaction system effectively identified SNPs among variant strains by detecting LP-RP duplexes. The study initially concentrated on 13 specific SARS-CoV-2 variants, but it was subsequently expanded to include variants B.1.1.7, B.1.351, P.1, B.1.617.2, B.1.617.1, B.1.525, C.37, BA.1, BA.2, BA.4&5, BA.2.12.1, BA.2.75, BA.2.86, BQ.1, XBB, XBB.1.5, XBB.1.16, CH.1.1, XBB.1.9, XBB.2.3, EG.5.1, BA.1, BA.2, BF.7, CK.2.1.1, BY.1.1.1, CJ.1, BA.4.6.3, BE.1.1 listed on the GISAID monitoring list.

The LAD multiplex reaction was experimentally validated by analyzing clinical samples that contained a variety of SARS-CoV-2 variants alongside a plasmid clone featuring precise amplicons derived from the clinical sample variant BQ.1. The successful genotyping of the BQ.1 variant was demonstrated by the results, which were confirmed by the detection of the variant in both the FAM and ROX channels on a qPCR equipment. Nevertheless, the necessity of conducting additional research into the quenching mechanisms of fluorescent probes to

enhance assay performance and guarantee consistent detection across a variety of sample types is based on the challenges associated with false positive quenching signals.

Keywords: SARS-CoV-2, SNP genotyping, Multiplex assay Liquid Array Diagnostics (LAD), Fluorescence quenching.

1. Introduction

The emergence of the novel coronavirus disease (COVID-19) resulting from severe acute respiratory syndrome coronavirus 2 (SARS-CoV-2) has presented an unparalleled worldwide health challenge. Coronaviruses are a group of enveloped RNA viruses that have a positive-strand genetic material and primarily infect vertebrates. They are classified within the family *Coronaviridae* and the order *Nidovirales* (Yin, 2020). Since its initial appearance late in 2019, the virus has swiftly crossed international borders, resulting in millions of cases of illness and fatalities throughout the globe. In order to prevent and control outbreaks and to discover effective treatments and vaccinations, there was a massive international effort to understand more about the virus, its mode of transmission, and the disease it causes (Harper et al., 2021).

On January 5, 2020, the first complete genome of SARS-CoV-2 was published. Its genome is 29.99 kb in size and encodes for a wide variety of proteins, both structural and non-structural. SARS-CoV-2 has evolved into several variants, all of which have a common set of mutations (Wang et al., 2020). To proficiently handle the pandemic and formulate precise public health strategies, there exists a pressing requirement for dependable and streamlined diagnostic technologies that possess the capability to identify and classify these SARS-CoV-2 variants. The most efficient method for researching the genomic epidemiology of COVID-19 is through SNP genotyping of SARS-CoV-2, which also provides the molecular basis for developing region-specific SARS-CoV-2 diagnostics and therapeutic development. The most prevalent mutations can guide the development of a variety of shell-based vaccinations (Yin, 2020).

1.1 Structural Arrangement of the SARS-CoV-2 Genome

The morphology of SARS-CoV-2 virions is spherical, with an enveloped structure and a diameter that usually ranges between 80 to 120 nm. Figures 1 and 2 depict the genomic structure of SARS-CoV-2, highlighting key regions such as the spike protein gene, non-structural protein genes, and structural protein genes. The virions display multiple homotrimeric spike (S) proteins that protrude outward, resembling club-like structures. These proteins are glycosylated. The unique arrangement of the virus gives it a remarkable resemblance to a solar corona, which is why it is commonly referred to as Coronaviruses (CoVs). The lipid bilayer envelope of the virion contains helically arranged nucleocapsids. The nucleocapsids are made up of an intricate arrangement of single-stranded positive-sense RNA (+ssRNA) and capsid proteins, emphasizing a symmetrical helical structure. The viral

genome contains genes that encode four important structural proteins: spike (S), membrane (M), envelope (E), and nucleocapsid (N) proteins. These proteins are located in the region before the 3' end of the genome. Furthermore, there are several non-structural and/or accessory proteins that are crucial for the virus's structural and functional features (Yadav et al., 2021).

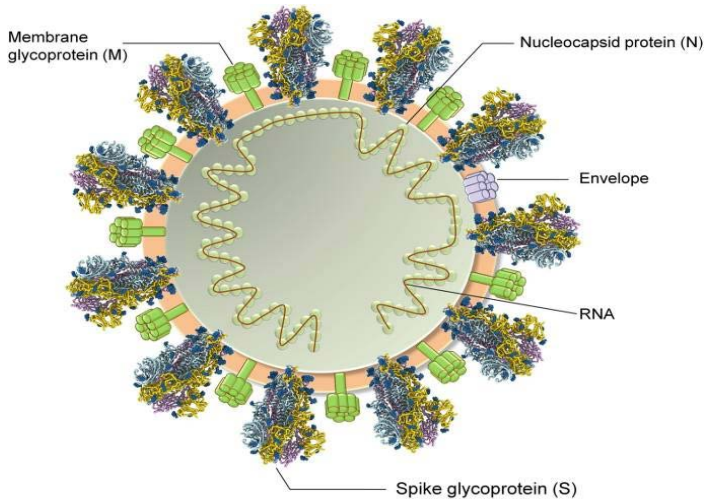

Figure 1: ***SARS-CoV-2: A Structural Perspective****. The spike glycoprotein (S) found on the surface of SARS-CoV-2 plays a crucial role in interacting with the ACE2 receptor on the cellular surface. In addition, the viral membrane glycoprotein (M) and envelope protein (E) are embedded in a lipid bilayer that originates from the host membrane. This bilayer surrounds the helical nucleocapsid, which contains viral RNA(Kumar et al., 2020).*

The replicase gene, known as Open Reading Frame 1a and 1b (ORF1a and ORF1b), is in the initial 20 kilobases (kb) downstream from the 5' end of the viral genomic tract, which constitutes two-thirds of the region. These areas possess the capability to encode the NSPs as polyproteins, specifically pp1a and pp1ab, respectively. The pp1a polyprotein consists of NSP1 to NSP11, while the pp1ab polyprotein includes NSP12 to NSP16. In the genomic region preceding the 3' end, the final 10 kilobases (kb) contain a variety of structural proteins, including the four most significant ones. In addition, this region also contains nine accessory proteins encoded by the structural genes, specifically ORF3a, ORF3d, ORF6, ORF7a, ORF7b, ORF8, ORF9b, ORF14, and ORF10 genes. The genomic region adjacent to the 5' end of the coronavirus genome contains crucial components, including a leader sequence and an untranslated region (UTR). Viral genome replication and transcription require the formation

of numerous stem-loop structures by these components. Transcriptional regulatory sequences (TRSs) are located before each structural and accessory gene to facilitate their functional expression. The structural part of the 3'-UTR is crucial for viral RNA replication (Yadav et al., 2021).

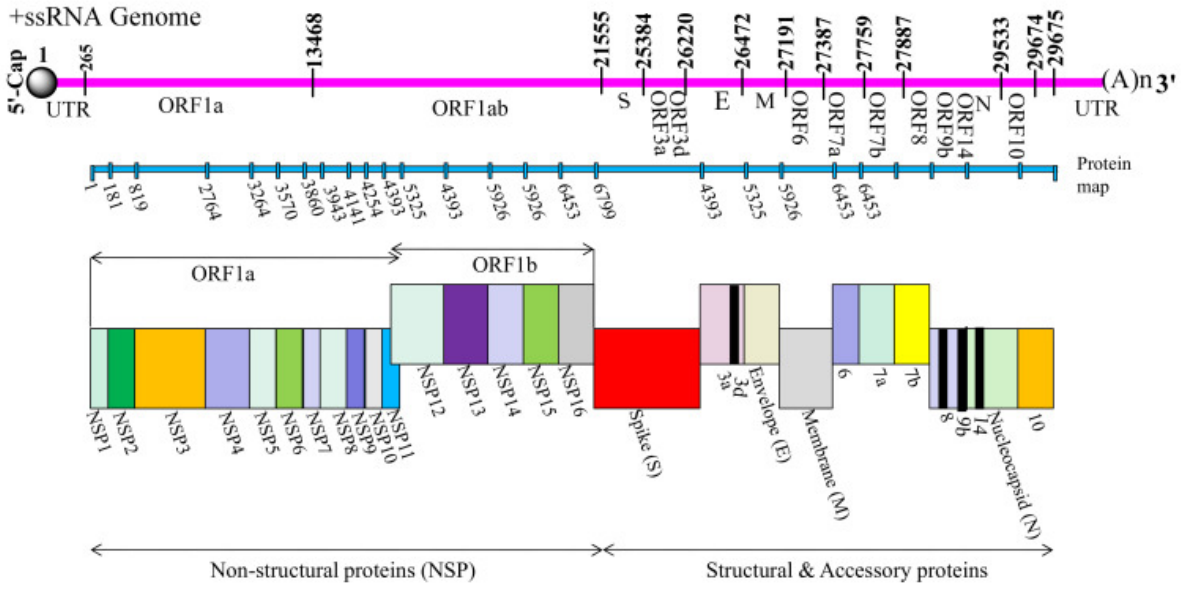

Figure 2: ***Genomic assembly of SARS-CoV-2.*** *The genomic structure of SARS-CoV-2 is organized in a sequential manner, with non-structural, structural, and accessory genes arranged in a certain order. This arrangement starts with the 5'-cap-leader-UTR-replicase-S (Spike)-E (Envelope)-M (Membrane)-N (Nucleocapsid)-3'UTR-poly (A) tail structure. Accessory genes, such as 3a, 3d, 6, 7a, 7b, 8, 9b, 14, and 10, are distributed among the structural genes before reaching the 3' end of the viral RNA genome, coinciding with the presence of a poly (A) tail within the 3' untranslated region (Yadav et al., 2021).*

1.2 Regions of Interest for Genotyping SARS-CoV-2

In order to create efficient multiplex SNP-typing techniques for SARS-CoV-2, it is crucial to concentrate on the specific genomic areas where notable mutations take place. These regions not only determine the variants of concern but also influence the virus's characteristics, such as its ability to spread, evade the immune system, and resist vaccines. The spike gene is the primary region for mutation monitoring, as per the Centers for Disease Control and Prevention (CDC). These mutations may be associated with the increased transmissibility of the disease and the potential for reduced therapeutic and vaccine efficacy (WHO, 2021) . It is observed

that the spike (S) protein, which is highly mutable, facilitates viral entry during infection by mediating the virus's attachment to the human cell surface angiotensin-converting enzyme 2 (ACE2) receptor (Zhao et al., 2021). The host tissue infection, disease severity, and viral load in the upper respiratory tract can all be exacerbated by the increase in affinity, resulting in an increased rate of human-to-human transmission (WHO, 2021).

The mutations in the D614G, E484K, N501Y, L452R, P681R, and E484Q are linked to increased transmissibility because they have a higher affinity for the host's ACE2 receptor. The binding affinity of the receptor-binding domain (RBD) for ACE2 is enhanced through deletions Δ69–70 (Zhao et al., 2021). Furthermore, the presence of E484K hinders the effectiveness of antibody neutralization (WHO, 2021). Despite a decrease in RBD affinity for ACE2, the immunological escape is facilitated by K417N/T mutations (Barton et al., 2021).

1.3 SNP Genotyping

A SNP refers to a specific change in a DNA sequence, usually including two possible nucleotide options at a given place. In order to be identified as a SNP in genomic DNA, it is typical for the less common allele to have a frequency of 1% or higher (Vignal et al., 2002). SNPs exist as bi-, tri-, or tetra-allelic variants. However, in ~~h~~humans, tri-allelic and tetra-allelic SNPs are very rare, almost insignificant. As a result, it is typical to identify SNPs primarily as bi-allelic markers (Brookes, 1999). SNPs are commonly found in noncoding regions of the genome rather than coding regions. They play a significant role as markers in comparative and evolutionary genomics. SNPs within regulatory sites can have an impact on transcription rates and protein production. On the other hand, SNPs occurring in coding regions can lead to changes in protein structure and function. This, in turn, can potentially play a role in the development of diseases or variations in drug response (Kim & Misra, 2007).

Discovering SNPs and genotyping SNPs (also called SNP scoring) are the two primary types of SNP analysis approaches. While SNP genotyping includes finding particular alleles within known polymorphisms, SNP discovery involves finding new polymorphisms. SNP genotyping typically employs three main approaches to differentiate between alleles: hybridization/annealing (with or without further enzymatic activities), primer extension, and enzyme cleavage. The technical platform utilized can range from homogeneous (occurring in a solution) to heterogeneous (containing both liquid-phase and solid-phase components, such as microarrays), depending on the specific methodology. Certain assays necessitate the

amplification of the genomic target prior to analysis, while others have the capability to directly analyze genomic DNA with high sensitivity. Numerous signal detection platforms are available, with the majority involving monitoring the trajectory of a label either continuously in real time or upon reaching the conclusion of the assay (Twyman & Primrose, 2003).

1.3.1 Primer Extension

Primer extension assays can utilize a shared primer to detect both alleles or employ specific primers to detect each individual allele. Using a DNA template and nucleotides in a primer extension process, these techniques exploit enzyme specificity to distinguish between alleles. During a conventional common primer extension (CPE) process, a primer is specifically designed to attach to the 3' end of a SNP site and is then extended with nucleotides by a polymerase enzyme. The SNP genotype is determined by analyzing either the fluorescence or mass of the resulting base identity (Kim & Misra, 2007).

1.3.1 Allele-specific extension

KASP (Kompetitive Allele-Specific PCR) is a genotyping technology that is renowned for its high accuracy and flexibility. It employs competitive allele-specific PCR and fluorescence-based reporting to identify SNPs and indels. It is extensively employed in the fields of human, animal, and plant genetics and is capable of adapting to a variety of microtiter plate formats. A common reverse primer, two FRET cassettes containing fluorescently labeled oligonucleotides (one labeled with HEX and one with FAM) and their corresponding quenchers, and two allele-specific forward primers with unique 5′ tail sequences are the fundamental components of the method. An allele-specific forward primer binds to the DNA template's complementary sequence close to the SNP site in the first step of PCR, whereas a common reverse primer binds downstream. During the PCR process, the allele-specific primer is elongated, resulting in the amplification of the target sequence in addition to the common reverse primer. In the next PCR cycles, the reverse primer amplifies the 5′ tail sequence of the allele-specific primer, resulting in an increased number of tail copies in the reaction (He et al., 2014).

An essential part of KASP is the production of fluorescence signals. Upon annealing to the amplified tail sequence, the fluorescently tagged strand of a FRET cassette is integrated into subsequent PCR products. By incorporating the fluorescent label, the quencher is released, resulting in the emission of a signal that is related to the SNP variant. In the case of a homozygous genotype, just a single fluorescence signal (either FAM or HEX) is produced.

However, in the case of a heterozygous genotype, both fluorescent signals are generated (He et al., 2014).

1.3.2 Hybridization

Assays based on hybridization require two carefully developed allele-specific probes that, in the event of perfect complementarity, will exclusively hybridize with the target sequence. Even under well-designed assay settings, a single base mismatch can greatly affect the hybridization process stability, making it nearly impossible for the allelic probe to anneal with the target sequence. Allelic discrimination is achieved through hybridization, which is a straightforward technique for genotyping as it does not require the involvement of enzymes. Hybridization can be observed by detecting the label after unbound targets have been washed away, which occurs when allele-specific probes are anchored on a solid platform and labeled target DNA samples are captured. The target DNA sample's genotype can be inferred by knowing where the probe sequences are on the solid support. Several sophisticated homogenous genotyping tests also rely on allele-specific hybridization. The reporting of the hybridization event varies among these experiments (Kwok, 2001).

1.3.2.1 TaqMan Assay

The TaqMan SNP genotyping technique, also referred to as the '5'-nuclease allelic discrimination assay', employs forward and reverse PCR primers along with two TaqMan minor groove binder (MGB) probes bearing distinct labels, enabling allele-specific identification through the use of dye-labeled probes alongside the amplification of the polymorphic sequence of interest by forward and reverse primers. One probe at the 5' site is labelled with VIC® dye to identify the "Allele 1" sequence, and the other with 6FAM™ dye (6' -carboxyfluorescein), to detect the "Allele 2" sequence. Both VIC® and 6FAM^{TM} are often referred to as reporter dyes. Nonfluorescent quenchers (NFQs) are attached to the probes at the 3' site in accordance with the principle of fluorescence resonance energy transfer. When both the dyes and the probe are in close contact, the NFQ will absorb the energy of the reporter dyes. In addition, the 3' end of TaqMan® probes has an MGB.

To enhance hybridization-based assays, the MGB molecule (e.g., dihydrocyclopyrroloindole tripeptide [DPI3]) attaches to the minor groove of the DNA helix and stabilizes the probe/template combination. The melting points and specificity of MGB probes are higher than those of unmodified DNA. *Taq* polymerase initiates strand synthesis after template denaturation and annealing of probe and assay components. While the reaction is underway,

the polymerase comes into contact with the annealed probe, which causes the appropriate probe's to 5'-bound fluorescent dye to be separated due to the 5' → 3' exonuclease activity of the *Taq* enzyme. Since the fluorescence signal has been quenched, laser excitation can now be used to detect it. The TaqMan assay can identify individuals with homozygous genotypes, where the SNP is present in one of the alleles, or heterozygotes, who carry SNPs on both alleles, based on their genotype (Schleinitz et al., 2011).

1.3.2.2 Molecular Beacon Assay

Molecular beacons are oligonucleotide probes consisting of a single strand that exhibit fluorescence upon binding to nucleic acids that are a perfect complement. Due to their lack of fluorescence in the absence of binding to their target, these probes can be utilized in hybridization procedures without the need to separate the probe-target hybrids from the unbound probes. Structurally, molecular beacons are stem-and-loop entities. A fluorophore and a quencher are covalently attached to opposite ends of the molecule. The hairpin stem prevents fluorescence when the fluorophore is not attached to the target by bringing it close enough to the quencher. The quencher receives the energy that the fluorophore has absorbed and then releases it as heat. Nevertheless, the hairpin stem is forced to unwind by the probe-target hybrid's rigidity as the loop's probe sequence anneals to its target sequence. This separation of the fluorophore and quencher allows the fluorescence to be restored. Figure 3 depicts the detailed process. Due to the fact that molecular beacons can be tagged with a wide range of fluorophores, it is possible to discriminate between numerous targets in a single solution by employing multiple molecular beacons, each tailored to detect a distinct target (Marras et al., 2002).

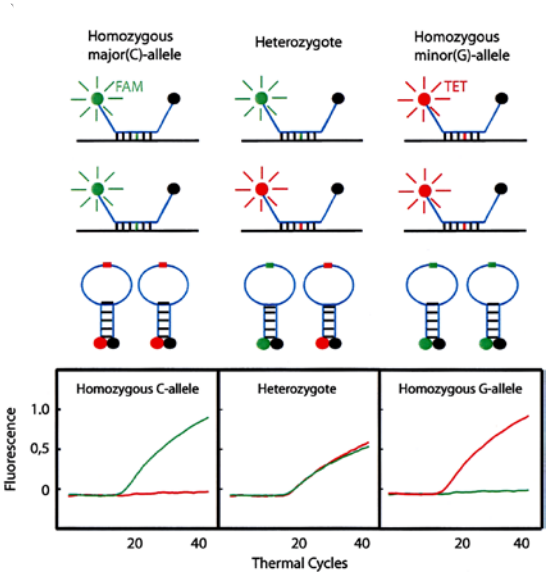

Figure 3: ***Method of spectral genotyping using PCR with SNP detection as an example.*** *The FAM-labeled molecular beacon becomes fluorescent when it hybridizes with the amplicons in individuals who are homozygous for the major (C) allele, whereas the TET-labeled molecular beacon stays closed. Only the TET-labeled molecular beacon is fluorescent in individuals who are homozygous for the minor(G)-allele. Although the total amount of target is theoretically the same in heterozygote individuals, the levels of fluorescence from both fluorophores are decreased compared to when a homozygous sample is present, even when both molecular beacons hybridize to the amplicons (Mhlanga & Malmberg, 2001).*

A duplex labeling scheme offers the advantage of having a greater number of distinct combinations of precisely two colors compared to the number of colors that may be discerned. For example, fifteen separate molecular beacon pairs, one for each target amplicon, can be labeled using PCR tools that can differentiate between six different fluorescent colors. This labeling method provides a code that clearly identifies the current target by labeling one part of the amplicons from that target one color and another part of the amplicons from the same target another color. When there is just one target sequence anticipated in the sample, this approach is useful for homogenous real-time PCR screening tests (Marras et al., 2019).

1.4 Multiplexed SNP Genotyping

The process of detecting and analysing several SNPs in a single reaction is referred to as multiplexed SNP genotyping. Instead of genotyping each SNP separately, this method enables high-throughput genotyping of many SNPs, which is more efficient and saves both time and funds. In the broader context of SNP genotyping technologies, companies such as Affymetrix and Illumina provide large microarray platforms, including chips, plates, and bead-chips, that are capable of genotyping between 50,000 and 600,000 SNPs in a single cycle. For example, the Affymetrix GeneChip and the Illumina's Infinium BeadChips offer high-throughput genotyping, making these technologies crucial for genetic research and whole-genome association (WGA) studies (Ragoussis, 2009). However, a wide variety of methodologies, including the SNPlex Genotyping System, multiplex SNaPshot assay, and liquid array diagnostic (LAD), have been developed for the targeted genotyping of tens to hundreds of SNPs. These methods facilitate the analysis of numerous SNP markers in a single reaction by employing specified platform parameters.

Adaptable to multiplex formats, nucleic acid-based assays use either signal amplification or target amplification approaches. Initial PCR amplification of a disease marker is the first step in target amplification. Then, a hybridization of a labeled detection probe is performed, and finally, the bound probe is detected. To keep the original target concentration, signal amplification detects the signal event first, then amplifies the signal probe (Deshpande & White, 2012). The efficiency and throughput of multiplex SNP genotyping assays have been enhanced by the development of several multiplexing approaches.

1.4.1 Real Time Multiplex PCR in multiplex SNP genotyping

Multiplexing PCR by utilizing hybridization probes with distinct emission spectra enhances real-time analysis for quantification and allele typing, by distinguishing probe color and Tm. Employing spectra of pure dyes, the spectral overlap between dyes can be rectified. Because of their reversible fluorescence and relative ease of synthesis and purification, single-labeled probes are preferable. A virtual two-dimensional array is generated by multiplexing by color and Tm ; this array can be used to detect amplification products by analyzing their melting points and fluorescence spectra (Wittwer et al., 2001). Nevertheless, only a limited number of systems have demonstrated the ability to provide a high-throughput and cost-effective solution for mid-plex analysis, often involving 10 to 50 targets.

The 2D label was used in a 16-plex assay for genotyping 15 high-risk human papillomaviruses and a 96-plex assay for genotyping 48 forensic SNPs. Both assays demonstrated its universality in detecting the existence of one or multiple targets or simultaneous targets in one reaction. A reporter fluorogenic probe was used to hybridize the target with an artificial sequence that had a unique Tm in the initial hybridization with a pair of ligation oligonucleotides. A melting curve analysis approach was used to denature the ligated products after they had been amplified using a universal primer pair. In each fluorescence detection channel, the targets were located according to their Tm values. (Liao et al., 2013).

1.4.1.1 Enhancements to qPCR Multiplexing using PlexProbes

Modern probe technology, called PlexProbes, doubles the number of targets that PCR devices can detect and discriminate by allowing multiple targets to be detected and discriminated in a single fluorescence channel. PlexPCR is a quantitative polymerase chain reaction (qPCR) technique that employs target-specific catalytic nucleic acids called PlexZymes to cleave universal PCR probes, resulting in the production of fluorescence. Primers are used to increase the amount of target sequences by producing amplicons, which are then used to produce

PlexZymes. PlexZyme enzymes that are in an active state attach to and break down universal probes, resulting in the production of fluorescence. Utilizing PlexZymes in conjunction with self-quenching fluorescent probes called PlexProbes allows for the construction of extremely sensitive and specific multiplex reactions (Mokany et al., 2013; Tan et al., 2017)

PlexProbes emit fluorescent light that can be "turned on" or "turned off" in response to a target by adjusting the temperature. In real-time and at endpoint, PlexProbes can discriminate two targets per channel, allowing multiplex qPCR detection of six targets in three fluorescence channels (Hasick et al., 2022).

1.4.2 Multiplexed minisequencing and Fluorescence-Based Genotyping Techniques

A wide range of formats, including homogeneous reaction and detection, solid-phase detection, and solid-phase-mediated reactions, are implementing CPE techniques that utilize fluorescence-based detection. These techniques involve the single-base extension of primers with fluorescently tagged ddNTPs (Kim & Misra, 2007).

The leading method for SNP detection, Life Technologies' SNaPshot kit (ABI PRISM® SNaPshot™ Multiplex Kit, hereafter referred to as SNaPshot), utilizes a homogeneous reaction and detection procedure that includes a single-base extension (SBE) reaction, followed by the identification of the resulting dye-labeled SBE products using capillary electrophoresis. A dideoxynucleotide (ddNTP) is used to elongate the primers in the SBE process, which begins with the hybridization of oligonucleotide primers that are designed to complementarily bind to the nucleotide sequence immediately preceding the target SNP. Consequently, solely the specific nucleotide that matches the target SNP site is included in the primer. To identify the variant alleles, present at the SNP locus, it is necessary to specifically identify the ddNTPs that are incorporated into the primer. The SNaPshot SBE reaction does this by utilizing a unique fluorescent dye that is linked to each of the four ddNTPs. To distinguish the SNaPshot primer extension products, an automated CE sequencer records the fragment's electrophoretic mobility and the wavelength of its fluorescent signal by detecting fluorescence at timed intervals. With the use of nonhuman DNA sequences that change mobility, this method allows for extensive multiplexing possibilities; for example, it can differentiate numerous primers that are extended at the same time within a single extension experiment (Fondevila et al., 2017).

1.4.3 Multiplex ligase-dependent probe amplification

The detection techniques that have been used in signal amplification assays are usually based on sequencing or hybridization. One of the most well-known approaches in this field is MLPA, which stands for Multiplex Ligation-dependent Probe Amplification. This method relies on hybridizing two probes that are next to each other on a target sequence, then ligating them in the presence of a ligase. This produces a signal, which is a single-stranded stretch, and it can be amplified by universal PCR with labeled PCR primers. A single reaction tube can be used to ligate and uniformly amplify many pairs of probes. Gel electrophoresis or microarrays are used to detect the amplified result. Assays that target unique sequences (signatures), SNPs, indels, and some repeats are also made possible by multiplexed ligation because the assay chemistry only needs that the target-specific regions of the probe pairs identify a target and be effectively ligated (Deshpande & White, 2012).

1.4.4 Multiplex Oligonucleotide Ligation PCR Assay (MOL-PCR)

An enhanced version of the original OLA assay format, the multiplex oligonucleotide ligation PCR assay permits ligation prior PCR amplification. A detection probe is comprised of a sequence that is complementary to the target sequence, as well as an extension that is composed of the TAG sequence and a primer binding site. The second probe has a resemblance to the first probe, with the exception that it does not possess the TAG sequence. All pairings share the same primer sequence, but each probe is specific for a different target sequence. Essentially, for a molecule to become a template for single-stranded DNA, these modular detecting probes must anneal to a target sequence and ligate into a complex molecule of single-stranded DNA. Furthermore, because the lengths of all the ligation products are quite close to one another (about 100 bp to 120 bp), it is very possible to amplify numerous small fragments at once using a universal primer pair during PCR. MOL-PCR exhibits persistence against amplification bias and necessitates only a small amount of target material. The system has capabilities for detecting sequences, identifying SNPs, detecting insertions and deletions (indels), screening for pathogens, and determining antibiotic resistance. It has the potential to substitute MLPA or QPCR in regular diagnostic applications (Reslova et al., 2017).

Additionally, the SNPlex™ Genotyping System is a high-throughput, scalable tool for genotyping SNPs, using pre-optimized kits and SNP-specific probes to perform up to 48-plex levels. This technique requires only three unlabeled probes per SNP, minimal gDNA, high multiplexing, and CE equipment. By utilizing the oligonucleotide ligation/PCR assay

(OLA/PCR), it employs a systematic workflow consisting of eight steps for SNP genotyping. The steps involved in this process are as follows: (1) Phosphorylation is used to activate the ligation probes and linkers. (2) The linkers and probes are ligated onto the genomic DNA target. (3) Exonucleases are used to remove any unligated or incompletely ligated oligonucleotides and genomic DNA. (4) PCR is used to simultaneously amplify the ligation products, using a set of universal primers. (5) The biotinylated amplicons are captured on streptavidin-coated plates, and the unbound strand is removed. (6) The universal set of ZipChute probes is hybridized to the complementary ZipCode product sequence on the captured PCR strand. (7) Specifically hybridized ZipChute probes are released. (8) The fluorescent ZipChute probes are detected using CE (Vega et al., 2005).

1.5 Liquid Array Diagnostics (LAD)

LAD is an innovative genotyping method that utilizes single nucleotide primer extension and incorporates high-resolution melting (HRM) on a liquid array platform (Hiseni et al., 2019). Using only commonly accessible equipment, specifically a qPCR machine, it can detect several targets in a single tube in a single working day.

The LAD assay consists of four major steps (figure 4). The assay begins with PCR amplification of the target DNA to create the template for further labeling. Then, using Exonclease and phosphatase, the PCR primers and deoxyribonucleotide triphosphates are degraded. In the subsequent stage, the process involves the addition of LPs, quenchers labelled ddNTPs (ddNTP-Q), and a polymerase like thermosequenase to the reaction. This reaction is then subjected to 5-20 cycles of labelling. The polymerase combines the complementary quencher labelled ddNTPs under ideal conditions since LPs are made to hybridize with the template DNA close to the 5' end of the SNP site. Ensuring a successful labeling process requires that the quencher-labelled ddNTP type used in the reaction be complementary to the base located downstream from the 3'end of the LP, as well as right across from it. During the last stage, the sodium dodecyl sulphate (SDS) reagent is introduced into the process to deactivate the polymerase before the addition of the 5' fluorescently labeled RPs. The RPs undergo hybridization with their complementary LPs. These duplexes are intentionally designed to have distinct Tms. In multiplex reactions, they exhibit distinctive quenching responses from one another. When quenching occurs, the assay shows a drop in fluorescence

intensity at certain temperatures and detecting channels, which is represented as negative peaks (Hiseni et al., 2019).

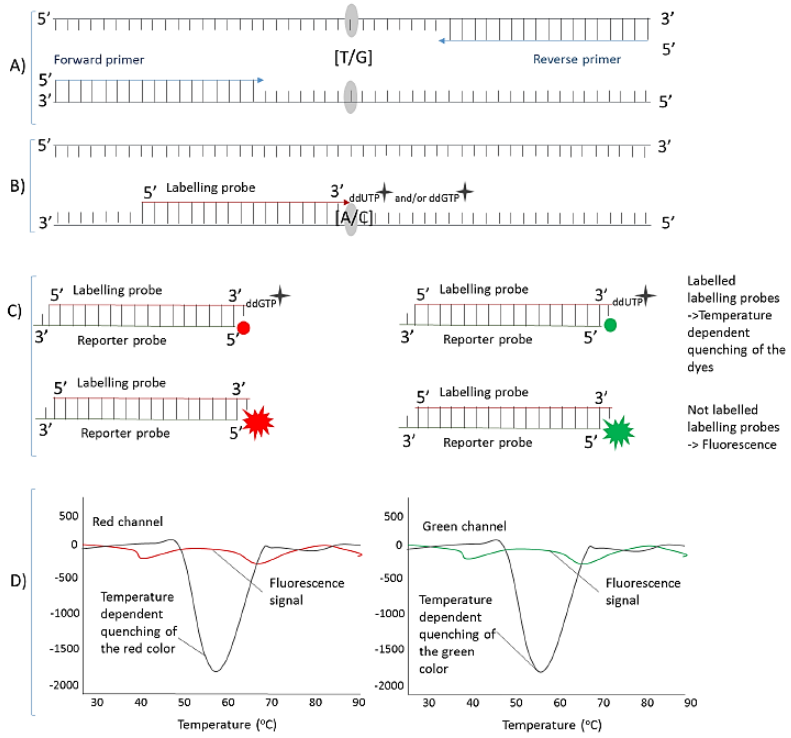

Figure 4: ***Illustration of Liquid Array Diagnostics SNP genotyping****. (A) In the presence of DNA polymerase and dNTPs, PCR involves the amplification of genomic DNA, which generates a sufficient template for the subsequent labelling LPs. Treatment of PCR reaction with phosphatase (degrades dNTPs) and exonuclease I (degrades PCR primers). Phosphatase and exonuclease enzymes inactivated by incubation at 85 °C. (B) The labelling reaction is demonstrated by introducing a labeled probe, quencher labelled ddNTPs, and polymerase. In a homozygous sample, just one ddNTP is labeled, whereas in a heterozygous sample, two ddNTPs are labeled. (C) Proteinase K treatment is performed prior to the insertion of the 5`fluorescently labelled reporter probe. (D) An analysis of melting curves and the detection of fluorescence. The color of the quenched channel indicates whether the SNP genotypes are homozygous or heterozygous (Hiseni, 2016).*

The LAD assay can be applied to create a multiplex test that can identify all SARS-CoV-2 variants on the current GISAID monitoring list by refining the multiplex SNP/indel genotyping approach. By using the single-tube multiplex reaction, nine SNP/indel underlying

18 allele variants can be detected, which can distinguish between all viral variants and the "wild type."

1.6 Rapid genotyping of SARS-CoV-2 variants

Whole-genome sequencing (WGS) of positive SARS-CoV-2 samples has revealed the lineages of the virus by identifying new emerging variants and any alterations to viral genomes (Korber et al., 2020; Paul et al., 2021). It is widely regarded as the most reliable and accurate technology for detecting novel circulating SARS-CoV-2 variants on a global scale. Nevertheless, the restricted accessibility rendered it impractical to promptly identify variants for public health measures like contact tracing and assessing the prevalence of concerning variants within the community (Lind et al., 2021). The widespread adoption of WGS in numerous laboratories worldwide is complicated by the necessity of technical proficiency, costly apparatus, and a significant amount of time. Due to the difficulties involved in implementing WGS, it is crucial to have additional surveillance methods that can quickly screen for specific viral strains associated with increased transmission, severe disease, or resistance to vaccines. One example of a rapid genotyping approach is the TaqMan SARS-CoV-2 mutation panel, which combines TaqMan SNP genotyping with one-step real-time PCR to quickly identify SARS-CoV-2 mutations and speed up viral variant screening and monitoring. Sequence-specific forward and reverse primers are employed in the TaqMan SNP genotyping assays to amplify target regions. To detect mutation sequences, FAM dye-labeled probes are employed, and VIC dye-labeled probes are employed to detect reference sequences. TaqMan minor groove binder (MGB) probes with nonfluorescent quenchers (NFQ) are also incorporated into the procedure (Neopane et al., 2021).

This technique identified common SARS-CoV-2 variants including B.1.526, B.1.525, B.1.617, P.1, B.1.1.7, and B.1.351 by targeting Spike (S) and ORF8 gene SNPs. The mutation panel was used to test validation controls and SARS-CoV-2-positive patient samples. The precision of each SNP assay was ensured by conducting triple tests on different days. The allelic discrimination plots generated by this technique exhibited distinct differences between wild-type and mutant samples (Neopane et al., 2021).

A different study evaluates multiplexed real-time reverse transcription-PCR (RT-PCR) tests designed to quickly detect specific mutations in the spike protein of SARS-CoV-2, ensuring precise and sensitive identification of variants of concern (VOC) and variants being monitored

(VBM). By utilizing PlexPrime® and PlexZyme® technology, these assays enable the simultaneous detection of SARS-CoV-2 through the RdRp gene and specific spike protein mutations. Additionally, SpeeDx Pty Ltd's PlexPrime variant assays allow for the concurrent identification of SARS-CoV-2 and specific mutations associated with VOCs. The evaluated assays consist of PlexPrime® SARS-CoV-2 Alpha/Beta/Gamma, which targets the E484K, N501Y, and S982A mutations. Additionally, there is PlexPrime® SARS-CoV-2 Alpha/Beta/Gamma+, which includes an extra N501Y probe to detect the Omicron variant. Another assay, PlexPrime® SARS-CoV-2 P681R Delta, focuses on the P681R mutation found in the Delta variant. Lastly, there is PlexPrime® SARS-CoV-2 L452Q Lambda, which detects the L452Q mutation specific to the Lambda variant. The assays involve mixing nucleic acid extract with a reaction mix and performing RT-PCR on an ABI 7500 FAST Dx Instrument using optimal conditions, following established methods for sample extraction and RT-PCR setup using the MagNA Pure 96 instrument. Acquiring and analyzing fluorescence data for each mutation and the RdRp gene enables the precise measurement of quantification cycles between channels. This ensures the accurate and rapid identification of specific mutations, hence enabling efficient genomic surveillance of SARS-CoV-2 variations (Borillo et al., 2022).

1.7 Aim of the study

The aim of this study was to develop a multiplex test capable of identifying all SARS-CoV-2 variants currently listed on the GISAID monitoring list by creating the multiplex SNP/indel genotyping approach. To find nine SNP/indel markers, which together covered 18 allele variants, this method utilized four-tube multiplex PCR reaction. These markers were capable of differentiating between different viral variants and the wild type. The method employed short DNA duplexes, consisting of one oligonucleotide labelled with a fluorophore and the other with a quencher, to demonstrate the existence of target DNA by means of fluorescence quenching, in turn dependent on single nucleotide primer extension with a specific, quencher-coupled dideoxynucleotide. This novel method utilized various duplex melting profiles and numerous detection channels on qPCR equipment to identify multiple targets simultaneously by using four reaction tubes.

In order to accomplish this objective, the study was subdivided into the subsequent sub goals:

- **Identification of unique Single Nucleotide Polymorphism sites**: Distinguishing unique SNP locations that can be utilized for discriminating between different SARS-CoV-2 variants.
- **Designing of Labelling Probes**: Creating labeling probes for nine SNP/indel markers, covering 18 allele variants, to enable accurate genotyping.
- **Designing of Reporter Probes**: Developing fluorescently labelled reporter probes complementary to the labelling probes to facilitate the detection process.
- **Detection of LP-RP Duplexes in a Single-Tube Reaction**: Implementing the detection of LP-RP duplexes inside four-tubes reaction setup to effectively identify SNPs in different variants.

2. Material and Methods

2.1 Study Design and ethics

The study was authorized by the Data Protection Officer at Innlandet Hospital Trust, under project code 26168642. It was conducted following the experimental workflow as illustrated in Figure 5.

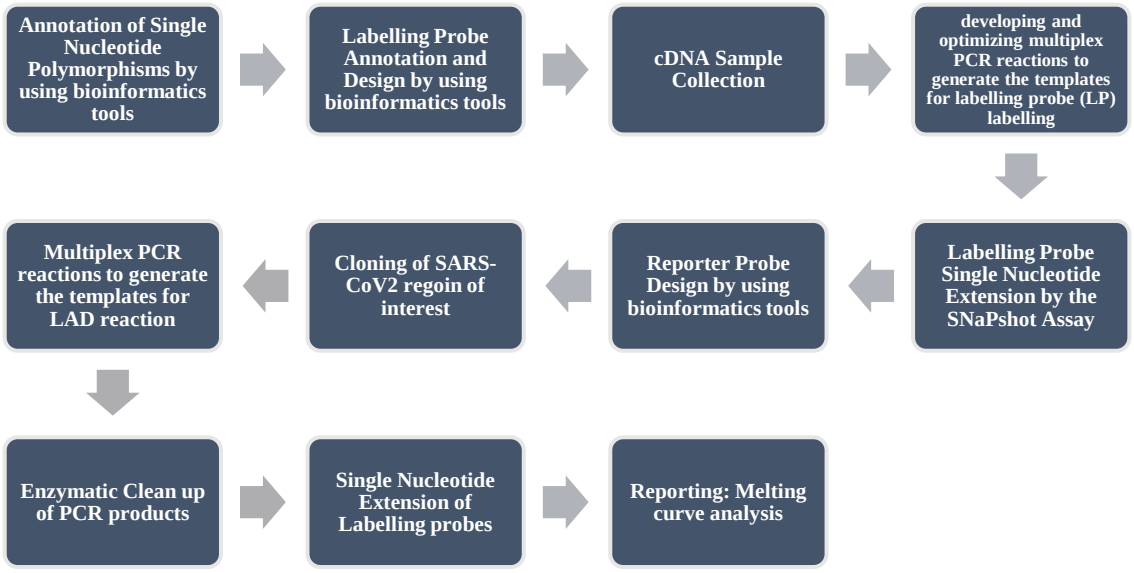

*Figure 5**: Flowchart of the study:** Experimental workflow for LAD on SARS-CoV-2 variant detection.*

2.2 Annotation of Single Nucleotide Polymorphisms

Initially, SNPs found within 13 specific variants of SARS-CoV-2, as documented on the Global Initiative on Sharing All Influenza Data (GISAID) monitoring platform, were systematically annotated using CLC Main Workbench version 7.9.3 (QIAGEN, Aarhus, Denmark). These variants were selected based on their prevalence and significance in the global spread of SARS-CoV-2, as documented on the GISAID monitoring platform up to August 2022, and their recognition by global health organizations due to their impact on transmissibility, virulence, and potential for vaccine escape. The selected variants are:

- 20I (Alpha, V1) (B.1.1.7)
- 20H (Beta, V2) (B.1.351)
- 20J (Gamma, V3) (P.1)
- 21A (Delta) (B.1.617.2)
- 21B (Kappa) (B.1.617.1)
- 21K (Omicron) (BA.1)
- 21L (Omicron) (BA.2)
- 22A & 22B (Omicron) (BA.4 & BA.5)
- 22C (Omicron) (BA.2.12.1)
- 22D (Omicron) (BA.2.75)
- 21D (Eta) (B.1.525)
- 21G (Lambda) (C.37)
- 21H (Mu) (B.1.621)

The polymorphic sites analysed are located in the Spike protein gene of SARS-CoV-2. To differentiate between the 13 viral variants and the 'wild type' (Wuhan-Hu-1, NC045512), 9 SNPs and insertion/deletion (indel) sites encompassing 18 allelic variations were selected. These nine polymorphic sites provide sufficient allelic diversity to effectively distinguish among the 13 variants. Detailed information regarding the selection of these SNPs is provided in Appendix section 1 figure 1.

2.3 Labelling Probe Annotation and Design

LPs were annotated to align with the nine SNPs of interest by using CLC Main Workbench version 7.9.3 (QIAGEN, Aarhus, Denmark). The Tm and homodimer/hairpin attributes were checked using Oligoanalyzer tool 3.1 from Integrated DNA Technologies (IDT, USA) with parameter settings Mg++ concentration 1 mM, dNTP concentration 0.0008 mM, oligo concentration 0.1 μM and Na+ concentration 50 mM with Tm around 70 ℃. In order to amplify particular genomic regions containing the targeted SNP(s) connected to the mutation

of interest (Table A 1), these LPs were used as PCR primers. The list of designed probes is included in Appendix Table A 2. The genomic region of interest for the Liquid Array Diagnostic (LAD) experiment was covered by these primers. Primer Set 1:

Forward primer: CoV2_H69&V70:-_tA

Reverse primer: CoV2_F157-_tB(rev)_LB

Primer Set 2:

Forward primer: CoV2_K417N_tA(for)_LK

Reverse primer: CoV2_P681H_tB(rev)_LK,

The PCR products generated from these primer sets encompass the entire genomic segment containing the 9 SNP sites. Appendix figure A 5 contains a detailed map generated by the CLC Main Workbench 7.9.3 software that shows the genomic area of SARS-CoV-2 intended for the LAD experiment and indicates the coverage by these primers.

2.4 Sample Collection

Initially cDNA samples were retrieved from The Norwegian Institute of Public Health (NIPH). Subsequent to obtaining approval from the Data Protection Officer at Innlandet Hospital Trust, cDNA samples were collected from Innlandet Hospital for the comprehensive execution of the project.

2.5 Single Base Extension by SNapShot Assay

2.5.1 PCR template generation

PCR setup 1(without Universal Primer A and B):

A 15 µl reaction volume was set up comprising 5µl cDNA samples (from NIPH) (1:10 dil) and H_2O (as non-template control) 0.2 U/µl HOT FIREPol® DNA polymerase, 1X Buffer B1, 2.5 mM $MgCl_2$ (all from Solis Biodyne, Estonia), 0.2 mM dNTPs, 0.05 µM A-tailed forward primer(s), and 0.05 µM B-tailed reverse primer(s). Both multiplex and singleplex setups were used, with primer set CoV2_H69&V70:-_tA(for) and CoV2_F157-_tB(rev)_LB and another

primer set CoV2_K417N_tA(for)_LK and CoV2_P681H_tB(rev)_LK being utilized for both configurations. PCR amplification with initiation period of 12 minutes at 95 ℃ as the activation step to activate the DNA polymerase, followed by a step of 40 cycles consisting of 10 seconds denaturation at 95 ℃, 10 seconds annealing at 68 °C with 50% ramp rate and 1 minute extension at 72 ℃ was performed using an Applied Biosystems Veriti™ Thermal Cycler (Life Technologies, USA). A final extension step of 1 cycle 7 minutes at 72 ℃ and 10 ℃ hold until retrieval was also included.

PCR setup 2 (with Universal Primer A and B):

A 15 µl reaction volume was set up comprising 5µl cDNA samples (from NIPH) (1:10 dil) and H_2O (as non-template control) 0.2 U/µl HOT FIREPol® DNA polymerase, 1X Buffer B1, 2.5 mM $MgCl_2$ (all from Solis Biodyne, Estonia), 0.2 mM dNTPs, 0.2 µM Universal A-tail, 0.2 µM Universal B-tail (Thermo Fisher Scientific, MA, USA), 0.05 µM A-tailed forward primer(s), and 0.05 µM B-tailed reverse primer(s). Both multiplex and singleplex setups were used, with primer set CoV2_H69&V70:-_tA(for) and CoV2_F157-_tB(rev)_LB and another primer set CoV2_K417N_tA(for)_LK and CoV2_P681H_tB(rev)_LK being utilized for both configurations. The PCR amplification was conducted using the following temperature sequence: The DNA polymerase is activated by pre-incubating at 95 ℃ for 12 minutes. This is followed by 5 cycles of denaturation at 95 ℃ for 10 seconds and then annealing the A- and B-tailed sequence specific forward and reverse primers at a specific temperature of 68 ℃ and a ramp rate of 50% for 10 seconds, followed by a temperature of 72 ℃ for 1 minute. This is followed by 35 cycles of a temperature of 95 ℃ for 10 seconds, a particular annealing temperature of 59 ℃ for 10 seconds for the universal A- and B tails, and a temperature of 72 ℃ for 1 minute. Finally, there is a final extension step at a temperature of 72 ℃ for 7 minutes. The procedure for the reaction was conducted using the Applied Biosystems® Veriti® 96-Well Thermal Cycler (Life Technologies, CA, USA).

2.5.2 Fragment Analysis by Gel Electrophoresis

Gel electrophoresis was conducted using a 1% agarose gel in 1X TAE buffer supplemented with 6X loading dye to assess the fragment lengths of PCR-generated products. The sizes of the fragments were evaluated by comparison with a 100-base pair (bp) DNA ladder obtained from New England Biolabs (NEB; Ipswich, MA., USA). A volume of 5 µL of PCR products was loaded into the gel for visualization.

2.5.3 Enzymatic PCR Cleanup by FastAP alkaline phosphatase and ExoI exonuclease

For the remaining 10 µL of each reaction, 1.34 U Exonuclease I (from Thermo Scientific, MA, USA) was added, along with 3.33 U Fast alkaline phosphatase (from Thermo Scientific, MA, USA). The reaction mixture was then incubated at 37 °C for a duration of 60 minutes, followed by enzyme inactivation at 85 °C for 15 minutes using the Applied Biosystems® Veriti® 96-Well Thermal Cycler from Life Technologies, USA.

2.5.4 SNaPshot Multiplex and Singleplex reaction

Single Base Extension reactions consisted of a final volume of 3 µL containing 1 µL enzymatically treated PCR product and H_2O (as non-template control), 1.5 µL SNaPshot ready reaction mix (Applied Biosystems, Foster City, CA., USA), and 0.5 µL labelling primer mix (1 µM concentration for each LP) for multiplex reactions. For the singleplex reaction, the configuration was set up in a similar manner, using a labelling primer concentration of 1 µM. The omission of the non-template control was due to the limited availability of SNaPshot ready reaction mix, which can only accommodate 100 reactions. Thermocycling of the SBE reactions was performed in Applied Biosystems Veriti™ Thermal Cycler (Life Technologies, USA) with the following conditions: 96 °C for 10 seconds, 68 °C for 1 min followed by 25 cycles. SBE products were forwarded to the post-extension treatment to purify the products by adding 1 U FastAP alkaline phosphatase (Thermo Scientific, MA, USA) to the reaction solution and incubating it at 37 °C for 60 min.

2.5.5 Single Nucleotide Extension detection by Capillary Electrophoresis

CE was conducted utilizing ABI PRISM 3130xl Genetic Analyzer (Applied Biosystems), equipped with a 36 cm length capillary and POP-7™ polymer, employing a customized run module. The electrophoretic separation was achieved by combining 8.925 µL of HiDi™ Formamide with 0.075 µL of GeneScan™ 120 LIZ™ size standard (Applied Biosystems, ThermoFisher Scientific), followed by the addition of 1 µL of SNaPshot products mixture. Samples were denatured at 95 °C for 2 min before subjected to ABI PRISM 3130*xl* Genetic Analyzer (Applied Biosystems). Data were visualized using GeneMapper v.5 (Applied Biosystems). PCR primers included and fragment sizes are listed in Appendix Table A 2.

2.6 Reporter Probe Annotation and Design

A series of RP were designed to be complementary to, and thus form duplexes with, the LPs, characterized by a specific predetermined Tm. The Tm was calculated utilizing the OligoAnalyzer 3.1 web-based bioinformatics tool (Integrated DNA Technologies), with parameter settings including a Mg^{+2} concentration of 5 mM, dNTP concentration of 0.0008 mM, RP oligo concentration of 0.01 μM, and Na+ concentration of 50 mM. RP were 5'-labelled with FAM or ROX fluorophores. The excitation and emission wavelengths of each fluorophore, along with the quenching ranges of the quencher molecules, were chosen to enable effective quenching during dissociation. Hairpin homo- and hetero-dimer formations of RPs and LPs were evaluated by the AutoDimer v1 software. The list of designed RPs is included in Appendix Table A 3 and Table A 4.

2.7 Cloning of SARS-CoV2 genome

After obtaining clinical samples from the Innlandet Hospital, it was decided to utilize cloning technology because there were limitations in the availability of clinical specimens to carry out the entire experiment. The TOPO TA cloning technology was employed to clone amplicons generated from the SARS-CoV2 genome.

2.7.1 TOPO® TA Cloning® reaction

PCR templates were derived from the clinical samples (Sample 1 variant BN.1.3.1, Sample 2 variant BA.5.1.5 and Sample 3 variant BQ.1), following the procedural guidelines outlined in section 2.5.1 (PCR setup 1) with precision. After successful amplification, as confirmed through gel electrophoresis analysis, the TOPO® TA Cloning® reaction was executed on variant BA 5.1.5 and BQ.1, followed by the protocol of TOPO® TA Cloning® Kit for Sequencing (Invitrogen, USA). The gel electrophoresis image is displayed in appendix figure A 7. To make separately a total reaction volume of 7.5 μL: 0.5 μL of amplified PCR products by using the CoV2_H69&V70:-_tA forward primer and CoV2_F157-_tB(rev)_LB reverse primer were combined with 1 μL of the pCR™4-TOPO® vector for one reaction. Simultaneously, another 0.5 μL of amplified PCR products by using the CoV2_K417N_tA(for)_LK forward primer and CoV2_P681H_tB(rev)_LK reverse primer were combined with 1 μL of the pCR™4-TOPO® vector for a separate reaction. Following

this, 1 μL of a salt solution containing 0.08 M NaCl and 0.004 M MgCl2 was added to each reaction mixture and the remaining volume was then supplemented with PCR-grade water. This process resulted in the initiation of four TOPO-TA cloning reactions, with two reactions initiated for each variant (BA 5.1.5 and BQ.1), corresponding to each set of PCR products. Following a gentle mixing, the reaction mixture was allowed to stand at room temperature for five minutes.

2.7.2 Transformation of cloning reaction into TOP10 *E. coli* cells

Two μL of the individual TOPO® cloning reactions (from section 2.7.1) were added separately to a vial containing One Shot® chemically competent *E. coli* cells, and then mixed gently. Afterwards, the reaction was placed on ice and incubated for a duration of 5 minutes. The cells were subjected to a heat-shock treatment at 42 °C for 30 seconds, without any movement or stirring. Right after that, the tube was moved back to ice for further processing. Each of the four reaction tubes then received 250 μL of room temperature S.O.C. media. After being tightly sealed, the tubes were shaken horizontally at 37°C for an hour at 200 rpm. At the final step, 25 μL and 50 μL aliquots of each sample type were evenly spread onto Luria-Bertani agar plates supplemented with 50 mg/ml of Kanamycin. A final overnight incubation at 37 °C was performed on the plates. Colony growth was monitored the following day on the plates. The LB agar media composition is detailed in Appendix section 8.

2.7.3 Tube culture of bacterial cells containing SARS-COV-2 genes

The effective transformation of the plasmid vectors, each containing a distinct set of PCR products with SARS-CoV-2 variant BA.5.1.5 and variant BQ.1 sequences, into E. coli cells was confirmed by the appearance of colonies produced on LB agar plates. Subsequently, individual colonies from each insert were carefully transferred into separate test tubes containing LB media for further cultivation. Appendix section 9 contains the ingredients for LB media. Overnight, the tubes were placed in an incubator set at 37 °C. The following day, the tubes were examined for cell growth in liquid medium.

2.7.4 Isolation of plasmid DNA using the PureYieldTM miniprep kit

The presence of cloudiness in the LB media signified the rapid proliferation of *E. coli* cells harboring specific plasmids with unique inserts. Plasmid 1 contained the CoV2_H69&V70:-_tA and CoV2_F157-_tB(rev)_LB amplified product from clinical sample variant BA.5.1.5, along with the CoV2_K417N_tA(for)_LK and CoV2_P681H_tB(rev)_LK amplified product

from the same variant. Similarly, Plasmid 2 carried the CoV2_H69&V70:-_tA and CoV2_F157-_tB(rev)_LB amplified product from clinical sample variant BQ.1, as well as the CoV2_K417N_tA(for)_LK and CoV2_P681H_tB(rev)_LK amplified product from the same variant. The PureYield™ miniprep equipment from Promega Corporation, USA, was employed to isolate the plasmid. The manufacturer's instructions, available at www.promega.com/tbs, were followed. In this process, 30 µL of plasmid DNA was eluted from a 3 ml liquid culture. The Nanodrop instruments were used to determine the concentration of the eluted plasmid DNA, which was then kept at -20 ℃.

2.7.5 NANODROP instrument for measuring DNA concentration

Following the plasmid isolation, the concentration of the isolated plasmid DNA, which contained each pair of inserts of SARS-CoV2, was measured using Nanodrop Instrumentation by Thermo Scientific. Plasmid DNA concentration, listed in appendix Table A 5, was determined by comparing the absorbance at 260 nm and 280 nm levels.

2.7.6 Double digestion with PmeI and NotI-HF

A reaction volume of 10 µL, which included 8 µL of plasmid DNA and PCR-grade water, was treated with 1 µL of rCut Smart Buffer and 0.5 µL of PmeI and NotI-HF enzymes, respectively. Following this, the mixture underwent incubation at 37℃ for 60 minutes, succeeded by additional incubation at 65 ℃ for 20 minutes, with a hold at 10 ℃ until retrieval. The fragments were visualized by gel electrophoresis.

2.7.7 Sequencing reaction of SARS-CoV2 gene

The Sanger sequencing method was used to sequence the SARS-CoV2 gene. The **Step** technique was used for sequencing purposes (Platt et al., 2007). For this, 10 µL were added to an Eppendorf tube which included 5 µL of plasmid DNA (equivalent to around 200 ng of plasmid DNA concentration), 2 µL of 5x sequencing buffer, 2 µL of 1.7 µM T7 forward primer and T3 sequencing primer, 0.5 µL of BD v 3.1, and the remaining volume was PCR-grade water. The contents were thoroughly mixed. The PCR machine was used to run the **Step** program in the following manner: The protocol consists of a single cycle at 96 ℃ for 1 minute, followed by 15 cycles at 96 ℃ for 10 seconds, 15 cycles at 50 ℃ for 5 seconds, and 15 cycles at 60 ℃ for 1 minute and 15 seconds. This is followed by 5 cycles at 96 ℃ for 10 seconds, 5 cycles at 50 ℃ for 5 seconds, and 5 cycles at 60 ℃ for 1 minute and 30 seconds. Finally, there

are 5 cycles at 96 ℃ for 10 seconds, 5 cycles at 50 ℃ for 5 seconds, and 5 cycles at 60 ℃ for 2 minutes. The protocol concludes with a single cycle at 10 ℃, with hold until retrieval.

2.7.8 Cleanup of sequencing reaction

Following the completion of the Step procedure, a NaOAc/EDTA/EtOH selective precipitation was employed to carry out to concentrate the extension products while eliminating unincorporated nucleotides prior to CE. Each sample from the reaction phase was transferred into a 1.5 ml Eppendorf tube. In a sequential manner, 10 μL of PCR-grade water, followed by 2 μL of 125 mM EDTA, 2 μL of 3 M NaOAc (pH 5.2), and 52 μL of 96% ethanol were added. The contents were thoroughly mixed and then incubated at room temperature for 15 minutes. Subsequently, the mixture was subjected to centrifugation at maximum speed in a microcentrifuge at 4 °C for 30 minutes, with careful consideration given to the positioning of the tubes. The supernatant was meticulously removed from the oriented tube using a micropipette. Subsequently, 70 μL of 70% ethanol was added, followed by centrifugation at room temperature for 15 minutes, with attention to tube orientation. The supernatant was again delicately withdrawn from the orientated tube. After that, the tubes were left to air dry in a fume hood for half an hour. Following that, 10 μL of deionized formamide was used to resuspend each pellet. Capillary electrophoresis and data extraction were carried out using the ABI 3130xl Genetic Analyzer. The samples were carefully added to adjacent wells of a 96-well microtiter plate in accordance with the instructions.

2.8 PCR template generation and ezymatic treatment for LAD experiment

Following confirmation through sequencing analysis (refer to the Appendix section 11), the individual plasmid DNA containing specific region of interest of SARS-CoV2 variant BA.5.1.5 and BQ.1 (plasmid DNA detailed information in section 2.7.4) was diluted to the specified concentrations of 1:10, 1:100, 1:500, and 1:1000. A 50 μL PCR product was generated following the procedure described in section 2.5.1(PCR setup 1). Considering the procedure outlined in section 2.5.3, enzymatic treatment was subsequently conducted. The PCR amplification template included plasmid DNA (diluted 1:100) with specific inserts from both variants. The primer sets used were CoV2_H69&V70_tA forward primer with

CoV2_F157_tB(rev)_LB reverse primer, and CoV2_K417N_tA(for)_LK forward primer with CoV2_P681H_tB(rev)_LK reverse primer.

2.9 Single Nucleotide Extension of Labelling probes

Four multiplex labelling reactions were used to identify SNPs. Each reaction included a distinct quencher-labeled ddNTP (ddNTPQ) and three unlabeled ddNTPs to prevent extension of the labeling primer with a non-complementary quencher-labeled nucleotide. PCR products treated with ExoI/FastAP (10 µL) were utilized as templates in the labeling reaction, resulting in a final reaction volume of 20 µL. The reaction mixture comprised 0.1 µM of labeling primers (LPs) along with either 0.8 µM ddUTP-ATTO540Q or 0.8 µM ddCTP-ATTO612Q or 0.8 µM ddGTP-DYQ660 or 0.8 µM ddATP-ATTO540Q (sourced from Jena Biosciences, Ulm, Germany). Additionally, 40 µM ddTTP, ddCTP, ddGTP, and ddATP (Thermo Scientific, MA, USA) were added, except in the case of the corresponding labelled nucleotide. The reaction buffer C (1X), 1 mM $MgCl_2$, and 0.375 U of HOT TERMIPol® DNA Polymerase (all obtained from Solis Biodyne, Estonia) were also added. The labeling reaction was performed using a thermocycler (Applied Biosystems® Veriti® 96-Well Thermal Cycler), with initial denaturation at 95 °C for 12 minutes, followed by 40 cycles consisting of denaturation at 96 °C for 20 seconds and annealing/elongation at 68 °C for 40 seconds.

2.10 Dissociation Curve analysis

An analysis of the dissociation curve was conducted using a 7500 Fast qPCR instrument from Applied Biosystems, USA. The reaction volumes were set at 15 µL. Every reaction contained 10 µL of the labeling reaction, 0.01 µM of a 5'-fluorescently labelled RP, 5 mM of $MgCl_2$ (sourced from Solis Biodyne, Estonia), and SDS at a concentration of 1%. The dissociation parameters were as outlined: initial exposure at 95 °C for 15 seconds, followed by incubation at 30 °C for 1 minute, another exposure at 95 °C for 15 seconds, and a subsequent incubation at 60 °C for 15 seconds. Fluorescence measurements were taken at 0.1 °C intervals and plotted as the derivative of fluorescence versus temperature (-dF/dT) against temperature (T). This analytical approach yielded derivative dissociation curves featuring negative peaks indicative of duplexes containing a quencher-labelled labelling primer. Detailed information regarding

RP sequences, as well as the excitation and emission wavelengths of fluorophores, is available in the accompanying Table A 3 and Table A 4 in the appendix.

2.11 Designing of new Labelling Probe and Reporter Probe

GISAID data from the most recent round revealed that variation BA 2.86 carries the F157S mutation. New probes were subsequently developed for this SNP, namely the LP (CoV2_F157S-tA(for)_LY) and the RP (CoV2_F157S-tA(for)_RY) with FAM labelled at the 5' end of the RP. LP sequence details had been provided in Table A 10 and RP sequence details in Table A 11.

3. Results

This section presents a thorough review of the experimental results produced by several molecular techniques employed in the present study. The initial step is describing the optimization process of the multiplex PCR procedure, which is crucial for improving the efficiency and specificity of amplification across multiple loci. The subsequent section provides a comprehensive description of the verification process for single nucleotide extension in labeling probes using the SNaPshot assay. The validation of the multiplex PCR results through CE is emphasized, particularly the importance of confirming that the LPs were correctly labelled. Initially, the expected and observed fragment lengths were verified as a preliminary step. However, the primary objective was to determine which nucleotide was labeled with which labeling probe. By utilizing the relative migration methods during CE, a distinct indication of the correct labeling was obtained by comparing the relative positions of the fragments.

Additionally, the detection of labeling probe signals for specific SARS-CoV-2 variants using plasmid clones is examined. This encompasses a comprehensive examination of the dissociation reactions and the challenges encountered, such as the formation of secondary structures in probes and the impact of FastAP treatment. Lastly, the assessment of the genotyping accuracy of the LAD technology in detecting various SARS-CoV-2 variants and the detection of wild type sequences are addressed, providing insights into the performance and reliability of the developed assays. Each subsection is supported by relevant figures and tables to elucidate the experimental findings comprehensively.

3.1 Optimization of the multiplex PCR protocol

A crucial step towards enhancing amplification efficiency for various loci was optimizing the PCR primer annealing temperature. The determination of primer annealing temperatures was estimated using the OligoAnalyzer tool 3.1 from Integrated DNA Technologies (IDT, USA). This was explained in section 2.3 of the Materials and Methods. The results indicated that both the sequence-specific forward and reverse primers had Tm of around 70°C and the universal tail-A and B primers had a Tm of around 59°C. To optimize the overall efficiency of multiplex PCR, the most effective technique was to initially assess the PCR settings (refer to method section 2.5.1), including annealing temperature, primer concentration, and cycle number, for efficient amplification of targets in singleplex reactions. By executing gradient PCR

experiments with different annealing temperatures, it was found that using a temperature of 68 °C and a ramp rate of 50% during the annealing step of the PCR protocol resulted in increased amplification rates, reduced non-specific primer binding, and no signal in the No Template Control (NTC). These PCR experiments were performed with the dsDNA fluorescent dye EvaGreen in the reaction mix to facilitate amplicon detection in real-time and based on a post-PCR dissociation curve analysis. Figure 6 illustrates the successful PCR amplification of the targeted template region using primer set (CoV2_H69&V70:-_tA forward primer and CoV2_F157-_tB(rev)_LB reverse primer) and the primer set (CoV2_K417N_tA(for)_LK forward primer and CoV2_P681H_tB(rev)_LK reverse primer) in both singleplex and multiplex reactions.

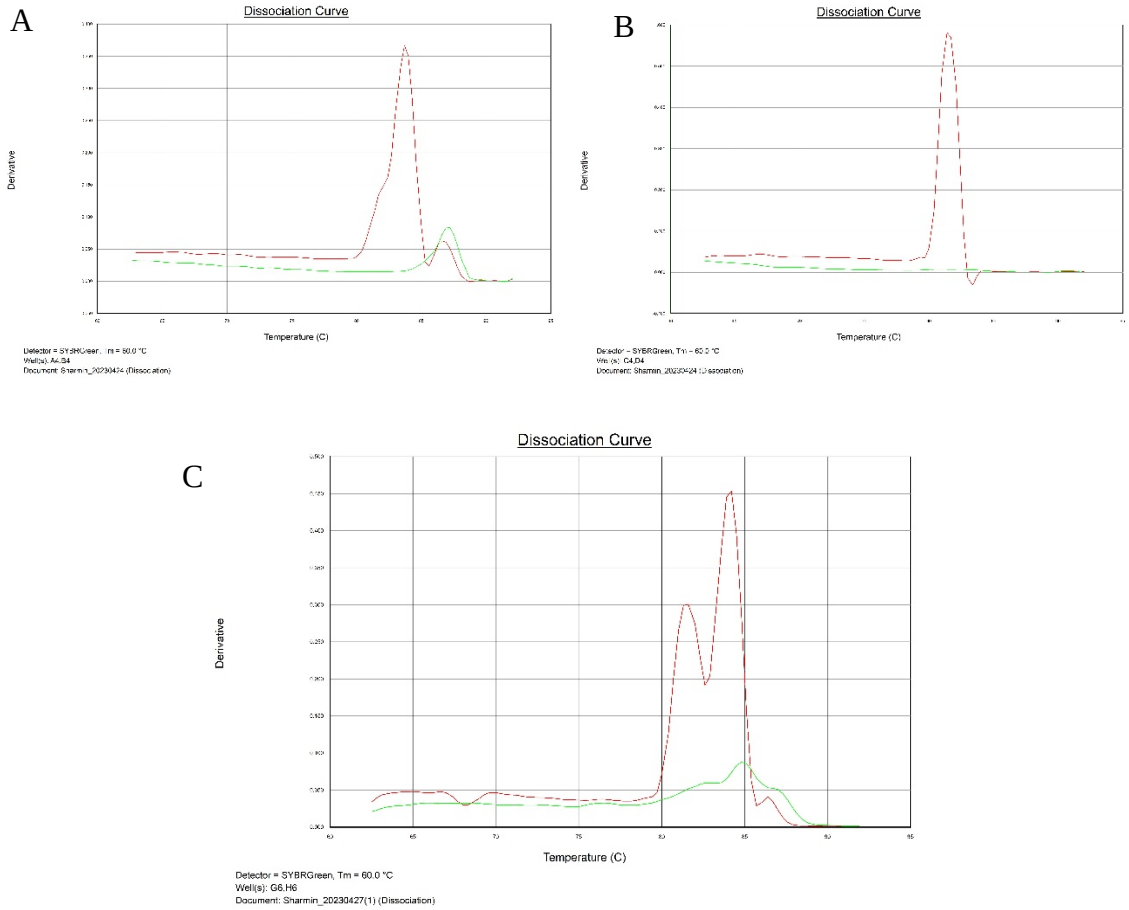

Figure 6: ***Single plex and multiplex PCR amplification by use of primer set (CoV2_H69&V70:-_tA(for) and CoV2_F157-_tB(rev)_LB) and the primer set (CoV2_K417N_tA(for)_LK and CoV2_P681H_tB(rev)_LK).*** *The red curves show the fluorescence signals of EvaGreen dsDNA-specific dye for PCR-amplified target DNA sequences, whereas the green curves indicate the "no-template" controls (NTCs). Panel (A) demonstrates the amplification of the template containing primer*

set (CoV2_H69&V70:-_tA forward primer and CoV2_F157-_tB(rev)_LB reverse primer) in a singleplex reaction. Panel (B) depicts the amplification of the template containing primer set (CoV2_K417N_tA(for)_LK forward primer and CoV2_P681H_tB(rev)_LK reverse primer) in a singleplex reaction. Panel (C) represents the amplification of the template containing primer set (CoV2_H69&V70:-_tA forward primer and CoV2_F157-_tB(rev)_LB reverse primer) and the primer set (CoV2_K417N_tA(for)_LK forward primer and CoV2_P681H_tB(rev)_LK reverse primer) in a multiplex reaction.

3.2 Confirmation of Labelling Probe Single Nucleotide Extension by the SNaPshot Assay

After successfully visualized PCR-amplified target DNA sequences using gel electrophoresis in both singleplex and multiplex procedures (followed from method section 2.5.1), SNaPshot test was performed for LPs extension. Figure A 6 in the appendix displays the DNA fragments obtained using gel electrophoresis. The SNaPshot assay utilizes a single base primer extension technique where the amplified DNA fragments serve as templates for the extension reaction. The SNaPshot assay used four ddNTPs, each labelled with a unique fluorophore: green for nucleotide adenine (A), black for nucleotide cytosine (C), blue for nucleotide guanine (G), and red for nucleotide thymine (T). Table A demonstrates the color and size of the electropherograms produced for each LP in the Singleplex SNaPshot. The results of the SNaPshot analysis are illustrated in Figure 7.

Table 1 Summary of Snapshot results: Detection of Labelled LPs by Singleplex SNaPshot assay. The data was extracted from GeneMapper v.5 (Applied Biosystems).

Labelling Probe	Length (bp)	Wild Type	Mutation	Expected Peak Color	Observed Peak Color	Observed Peak Size	Height
CoV2_H69&V70:-_tB(rev)_LY	52	A(TACATG)T	A()T	Green/Red	Red	62	2005
CoV2_G142D_-_tA(for)_LD	70	G, G(GTG)T	A,G()T	Green/Blue/Red	Green	75.54	1494
CoV2_F157-_tB(rev)_LB	63	C, G(TTC)A	A, G()A	Green/Yellow/Blue	Blue	66.04	3615
CoV2_K417N_tA(for)_LK	46	G	T	Blue/Red	Red	52.90	678
Cov2_L452R_tB(rev)_LH	70	T	G/A	Green/Blue/Red	Yellow	73.35	560
CoV2_F486V_tB(rev)_LM	65	T	G, C	Red/Blue/Yellow	Yellow	69.71	316

Cov2_H655Y_tA(for)_LY	45	C	T	Yellow/Red	Red	49.04	1822
CoV2_P681H_tB(rev)_LK	42	C	A/T	Yellow/Green/Red	Red	53.49	786

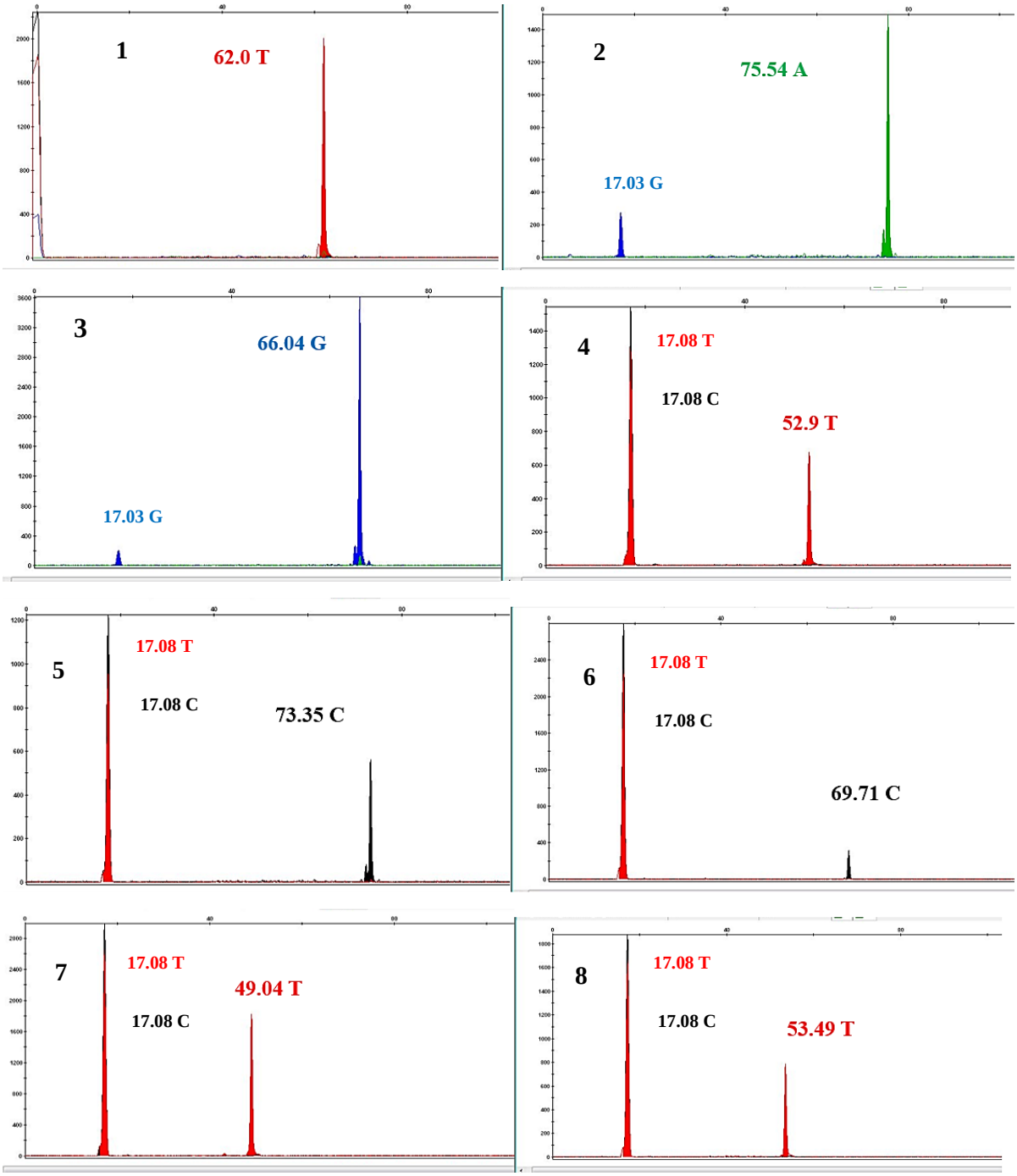

*Figure 7**: Electropherograms obtained from the Singleplex SNaPshot assay.** The ABI 3130 Genetic Analyzer was used to perform capillary electrophoresis of SNaPshot products. Panel 1 showed a red peak with a size of 62.0 nucleotides was observed, a green peak was observed with a size of 75.54 nt in panel 2, in panel 3, a*

66.04 nt sized blue peak was visible; panel 4 displays 52.90 sized red peak. Panel 5 exhibited a 73.35 nt sized black peak, panel 6 a 69.71 nt sized black peak, while panel 7 and 8 harbored a 49.04 nt sized red peak and a 53.49 nt sized red peak, respectfully. Blue peaks observed with sizes of 17.03 nt in panels 2 and 3 were likely artifacts, indicating nonspecific extensions during the SNaPshot assay. In addition, panels 4-8 showed overlapping red and black peaks with size of 17.08 nt, which also indicated nonspecific extensions. The following colors are used to symbolize nucleotides: A = green, C = black, G = blue, and T = red.

Although seven LPs were located in the singleplex SNaPshot analysis according to their predicted colour peaks, the observed sizes, measured in nucleotides, were higher than the theoretical limits. From figure 7, The red peak with a size of 62.0 nucleotides was observed, expected oligo size of LP CoV2_H69&V70:-_tB(rev)_LY which was 52 nucleotides. Additionally, a green peak with a size of 75.54 nucleotides closely matched the expected oligo size of LP CoV2_G142D:_tA(for)_LD, which was 74 nucleotides. A blue peak with a size of 66.04 nucleotides was visible, corresponding to the expected oligo size of LP CoV2_F157:_tB(rev)_LB, which was 63 nucleotides. Furthermore, a red peak with a size of 52.90 nucleotides closely related to the expected oligo size of LP CoV2_K417N:_tA(for)_LK, which was 53 nucleotides. The black peak at 69.71 nucleotides was associated with the expected oligo size of LP CoV2_F486V:_tB(rev)_LM, which was 69 nucleotides. Another red peak at 49.04 nucleotides corresponded to the expected oligo size of LP CoV2_H655Y:_tA(for)_LY, which was 49 nucleotides. Lastly, a red peak at 53.49 nucleotides was identified, corresponding to the expected oligo size of LP CoV2_P681H:_tB(rev)_LK, which was 54 nucleotides. However, the LP CoV2_L452R_tB(rev)_LH unexpectedly yielded a peak with a Yellow/Black coloration at size 73.35 nt, indicating it was labelled with C, deviating from the anticipated label of G with length of 70 nucleotides.

Table A 6 in the appendix represents the color and size of the electropherograms produced for each LP in the Multiplex SNaPshot assay. Figure 8 and 9 contained the illustration of Detection of Labelled LPs by Multiplex SNaPshot assay. They exceeded the expected oligo sizes and are considered artifacts, indicative of nonspecific extensions during the SNaPshot assay.

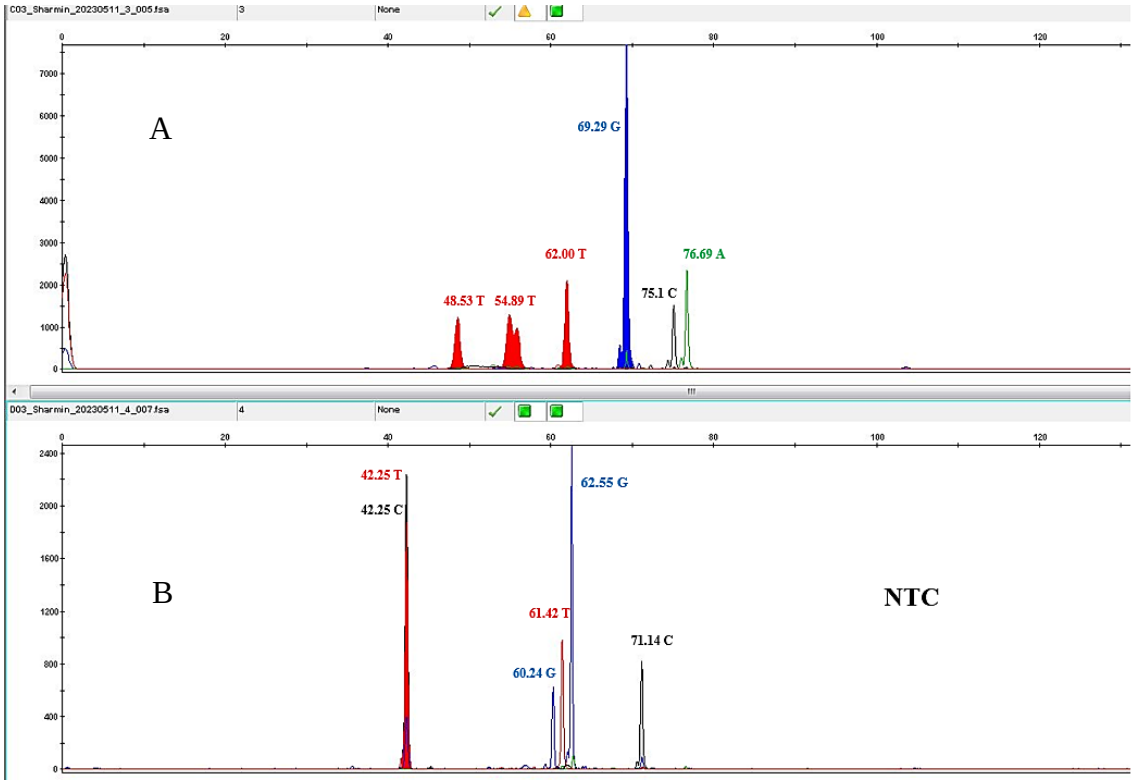

*Figure 8**: Electropherograms obtained from the multiplex SNaPshot assay.** In this analysis, the universal tail A and tail B primers were used during the multiplex PCR. Panel A: Three red peaks, measuring 48.53 nts, 54.89 nts, and 62.00 nts, were observed in the SNaPshot data. Double blue peaks, measuring 69.29 nts, was also visible. Additionally, a black peak at 75.10 nts and a green peak at 76.69 nts were detected. Panel B: In the non-template control, a double peak in red and black at 42.25 nts was observed. Additional peaks were noted at 60.24 nts (blue), 61.42 nts (red), 62.55 nts (blue), and 71.14 nts (black). The following colors are used to symbolize nucleotides: A = green, C = black, G = blue, and T = red.*

From figure 8, three red peaks were observed in the SNaPshot data, measuring 48.53 nts, 54.89 nts, and 62.00 nts. These peaks corresponded to the oligo sizes of LP CoV2_K417N_tA(for)_LK, LP CoV2_H69&V70_tB(rev)_LY, and LP CoV2_F486V_tB(rev)_LM, respectively. Additionally, double blue peaks, measuring 69.29 nts, were also visible which was related to the oligo sizes of LP CoV2_G142D_-_tA(for)_LD and Cov2_L452R_tB(rev)_LH. Furthermore, a black peak at 75.10 nts and a green peak at 76.69 nts were detected, both exceeding the expected oligo sizes and considered to result from artifacts, indicative of nonspecific extensions during the SNaPshot assay. A blue peak with a size of 62.55 nucleotides was observed, closely corresponding to the expected oligo size of

LP CoV2_F157:_tB(rev)_LB, which was anticipated to be 63 nucleotides. Additionally, a black peak with a size of 42.25 nts was detected, associated with the expected oligo size of LP CoV2_P681H:_tB(rev)_LK, which was anticipated to be 42 nucleotides, in the non-template control. Moreover, there were instances of artifacts, indicative of nonspecific extensions beyond the anticipated length range of the labelling primers. The illustrative data from figure 9 has been incorporated into Table A 6.

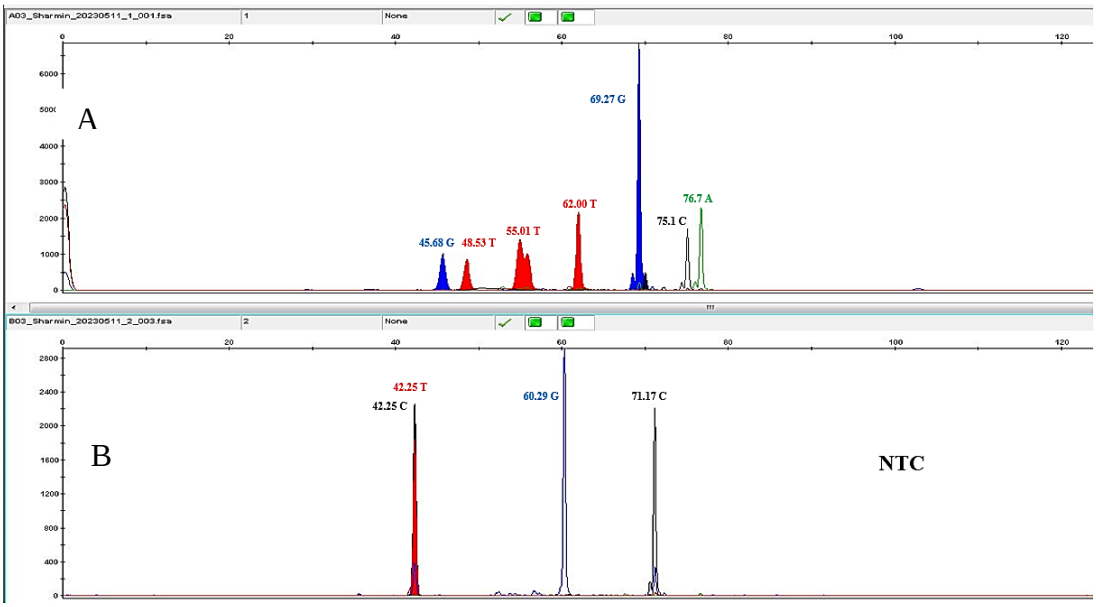

Figure 9. ***Results of the multiplex SNaPshot analysis for both the template and non-template control samples.*** *In this analysis, the universal tail A and tail B primers were not used during the multiplex PCR. Panel A: The SNaPshot data revealed several peaks, including three red peaks measuring 48.53 nts, 55.01 nts, and 62.00 nts, and two blue peaks measuring 45.68 nts and 69.27 nts. Additionally, a black peak at 75.10 nts and a green peak at 76.70 nts were observed. Panel B: In the non-template control, peaks were observed at 60.29 nts (blue) and 71.17 nts (black). Additionally, a double peak in red and black at 42.25 nts was visible. The following colors are used to symbolize nucleotides: A = green, C = black, G = blue, and T = red.*

3.3 Confirmation of multiplex PCR by capillary electrophoresis

Multiplex PCR tests were performed (followed from method section 2.5.1 PCR setup 1) using a FAM-labeled universal 15 bp primer A and an unlabeled universal 15bp primer B with the

primers listed in Table A 7. Afterwards, the study of fragment length was conducted by using CE. For the multiplex PCR reactions, templates comprised plasmid clones containing specific amplicons from clinical sample variant BA.5.1.5. These included CoV2_H69&V70:-_tA and CoV2_F157-_tB(rev)_LB amplicons, as well as another clone containing CoV2_K417N_tA(for)_LK and CoV2_P681H_tB(rev)_LK amplicons. Figure 10 illustrates the electropherograms that were obtained by using CE and displays the sizes of the observed DNA fragments. These observed fragment sizes were then compared to the expected sizes based on the target sequences amplified during the multiplex PCR, which are referred to as amplicon sizes (bp) (detail in Table A 7).

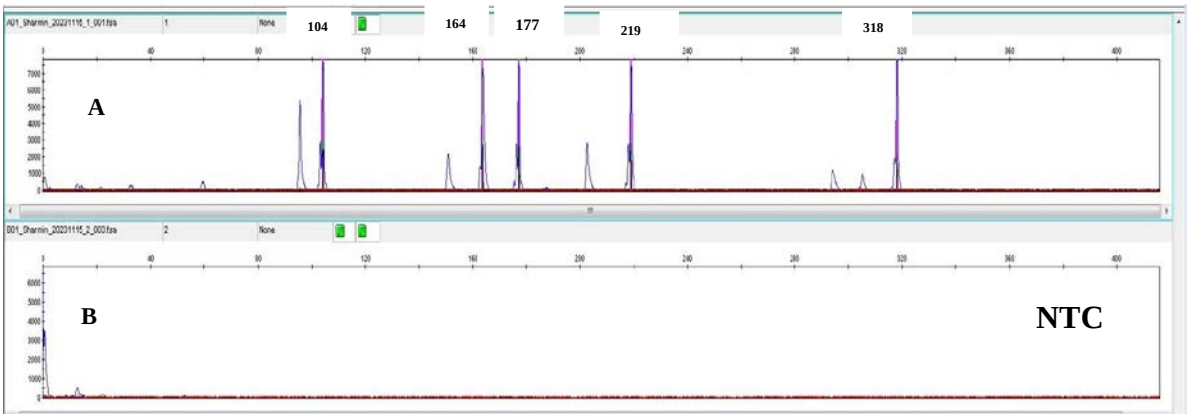

Figure 10: ***Fragment length analysis of FAM labelled multiplex PCR products.*** *Only the nearest bases electropherograms are marked here, which closely correspond to the lengths of the LPs' bases. The upper panel (A) shows the detected several signal peaks appeared at 104, 177, 219, 318 and 164. No signals were detected in the "non-template control," as shown in the lower panel (B), which indicates the absence of amplification. The multiplex PCR reaction was facilitated by a universal primer labeled with a fluorescent dye known as FAM dye in the presence of GeneScan™ 500 LIZ™, potentially resulting in the generation of minor signals preceding the actual PCR outcome due to primer dimer formation. Raw data generated by 3130xl Genetic Analyzer software.*

3.4 Sequence Validation and SNP Confirmation

After performing Sanger sequencing (refer to method 2.7.7) on the plasmids containing the inserted PCR products, the sequences were compared with the reference sequences SNP sites which were obtained from GISAID monitoring list for SARS-CoV-2 variants BA 5.1.5 and BQ.1 to validate the presence of the correct SNP alleles targeted during the amplification and

cloning processes. Appendix section 10 contains the detailed sequence information. These sequences corresponded to the PCR products containing the CoV2_H69&V70:-_tA and CoV2_F157-_tB(rev)_LB regions, inserted into plasmids for variants BA 5.1.5 and BQ.1, as well as the CoV2_K417N_tA(for)_LK and CoV2_P681H_tB(rev)_LK regions, similarly inserted into the plasmids for both variants. Appendix Section 11 contains the SNP validation, displaying the nucleotide alterations corresponding to the specific SNPs characteristic of variants BA 5.1.5 and BQ.1. Table 2 shows the comparison of SNP alleles between reference sequences and cloned sequences.

Table 2 Variants BA 5.1.5 and BQ.1: A Comparison of Reference and Cloned Sequences for SNP Alleles

SNP sites	Reference sequence nucleotides (variant BA 5.1.5)	Cloned sequences nucleotides	Reference sequence nucleotides (variant BQ.1)	Cloned sequences nucleotides
SNP site 1 and 2"H69/V70"	AT	AT	AT	AT
SNP site 3 "G142D"	A	A	A	A
SNP site 4 "F157-"	C	C	C	C
SNP site 5 "K417N"	T	T	T	T
SNP site 6 "L452R"	G	G	G	G
SNP site 7 "F486V"	G	G	G	G
SNP site 8 "H655Y"	T	T	T	T
SNP site 9 "P681H"	A	A	A	A

3.5 Detection of LAD Signals in Multiplex Reaction for SARS-CoV-2 Variants BA.5.1.5 and BQ.1 Using Plasmid Clones Containing Specific Amplicons

The purpose of this experiment was to evaluate the LAD method on SARS-CoV-2 Variants BA.5.1.5 and BQ.1 using plasmid clones containing specific amplicons, wherein 8 LPs were

specifically designed to incorporate ddATP-Q, ddCTP-Q, ddGTP-Q, or ddUTP-Q when hybridized to templates containing nine distinct SNPs spanning different variants, subsequently exhibiting a quenching response within predetermined ranges of Tm when paired in duplexes with their corresponding FAM- or ROX-labelled RPs.

After completing a successful PCR reaction, which was performed according to the procedure outlined in Method Section 2.5.1 PCR setup 1, a labelling reaction was conducted following the procedure described in Section 2.9. The templates used for the multiplex PCR reactions consisted of plasmid clones containing specific amplicons derived from clinical sample variants BA.5.1.5 and BQ.1. These templates included the CoV2_H69&V70:-_tA and CoV2_F157-_tB(rev)_LB amplicons, as well as another clone containing the CoV2_K417N_tA(for)_LK and CoV2_P681H_tB(rev)_LK amplicons. The dissociation reaction consisted of 10 µl of individual labeling reaction, 0.01 µM of a 5'-fluorescently labeled RP, 5 mM of MgCl2, and a 1% SDS solution. Dissociation parameters were as follows: initial exposure at 95 °C for 15 seconds, followed by incubation at 30 °C for 1 minute, another exposure at 95 °C for 15 seconds, and subsequent incubation at 60 °C for 15 seconds (refer to method 2.10). Figure 11 represents the first LAD signals appeared in multiplex reaction for both the FAM and ROX channels for plasmid clones containing CoV2_H69&V70:-_tA and CoV2_F157-_tB(rev)_LB amplicons and CoV2_K417N_tA(for)_LK and CoV2_P681H_tB(rev)_LK amplicons from clinical sample variants BA.5.1.5. False positive (FP) quenching signals were observed for both channels. The confirmed SNP sites from the results in Section 3.4 served as control validations, ensuring the accuracy of LAD signals generated in these experiments. Plasmid clones containing specific regions from variant BA 5.1.5, dissociation curve analysis results are included in Appendix Table A 8.

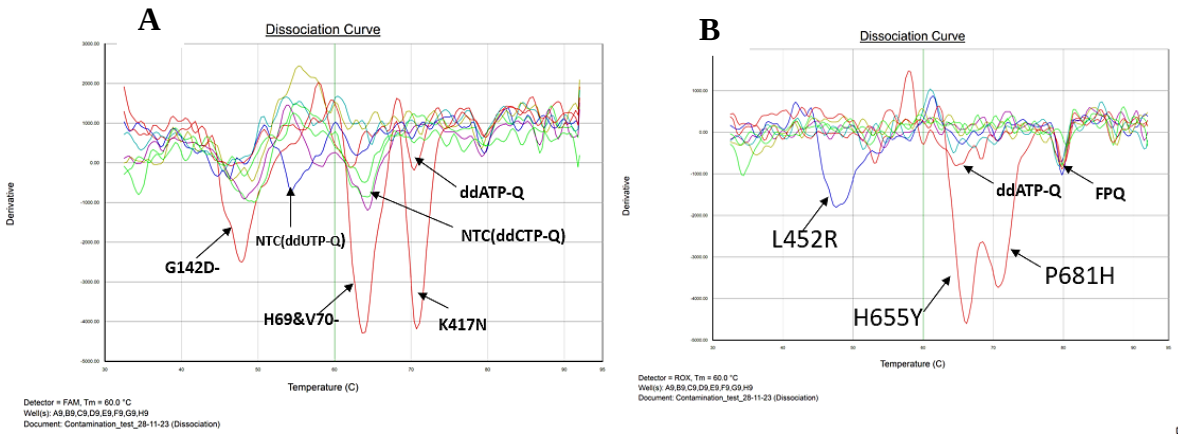

Figure 11: ***Detection of Variant BA 5.1.5 (using plasmid clones) through LP-RP duplex melting curve analysis****.* ***(A) FAM channel detection****: The H69/V70 SNP site 1 and 2 were detected through a quenching signal labelled with ddUTP-Q at a melting temperature (Tm) of 64 °C. Another quenching signal labelled with ddUTP-quencher at a Tm of 71 °C was detected for the K417N SNP site 5. Similarly, the G142D SNP site 3 was detected by a quenching signal for the ddATP-Q labelling reaction at Tm 48 °C. False positive quenching signal was observed for ddATP-Q at Tm 71 °C. Non-template control reaction showed quenching signal for ddUTP-Q reaction at 53 °C and ddCTP-Q reaction at 61 °C. SNP site 4, F157-, was expected to be labelled with ddGTP-Q at 50.6 °C but remained unlabelled.* ***(B) ROX channel detection:*** *SNP site 6 L452R was detected by a quenching signal labelled with ddCTP-Q at Tm 48 °C. SNP site 8 ("H655Y") and SNP site 9 ("P681H") were detected by a quenching signal labelled with ddUTP-Q at Tm of 66 °C and 71 °C, respectively. False positive quenching signal was also detected for ddATP-Q at Tm 65 °C. The SNP site 7, F486V, was supposed to be labelled with ddCTP-Q at a Tm of 49.6 °C, however it remained unlabeled.*

During the dissociation reaction, LP-RP Tm duplex formation facilitated the detection of seven out of nine SNP sites, including two deletion sites located at positions S:H69--(T21765-) and S:V70-(A21768-)(details in appendix section 2 table A 1). Despite the observed Tm values exceeding the expected values, they were interpreted as indicative of a labelled quenching response. During the dissociation reaction, SNP site 4 (F157-) and SNP site 7 (F486V) were not detected for both variants. Instead of true quenching signals, a false positive quenching signal was detected with a Tm of 61°C in the ddCTP-Q labelling reaction plasmid clones containing (Variant BA 5.1.5) and 55°C plasmid clones containing (Variant BQ.1) in the non-template control. The dissociation curve analysis results for plasmid clones from clinical sample variant BQ.1 was mentioned in Appendix Table A 9.

3.6 Secondary structure formation of LP CoV2_F157-_tB(rev)_LB

An inaccurate quenching event was observed in multiplex reactions where the labelling probe LP CoV2_F157-_tB(rev)_LB and RP CoV2_F157-_tB(rev)_RB were tested in “non- template control” (Appendix figure A 12). LP CoV2_F157-_tB(rev)_LB was designed to become labelled with ddGTP-Q when annealed to a template harbouring the SNP site 4 "F157-". Thus

labelled, this LP would generate a quenching response in the range of 50.6 ºC Tm when in duplex with FAM-labelled RP CoV2_F157-_tB(rev)_RB. It appeared that this LP was being labelled with ddCTP-Q without a template since a quenching response was observed in the "non-template" control within the 61 °C Tm range (see Figure A 12).

Figure A 13 in the appendix demonstrates that the bioinformatic analysis of the CoV2_F157-_tB(rev)_LB labelling probe sequence suggested that secondary structures of the probe allowed labelling with ddCTP-Q opposite to a G located in the third position from the 5'-end. That was as a consequence of either self-dimerization of the probe which had a calculated delta of G -4.77kcal/mol or its hairpin structure with a delta G of -6.65.

To alleviate the quenching signal from the non-template control, a mismatch was introduced in the labeling probe. Specifically, the A at the fourth position from the 5' end was replaced with a C (Appendix figure A 14). Furthermore, it was anticipated to be labelled with ddGTP-Q upon annealing to a template containing the SNP site 4 "F157-". However, no quenching response (figure 12) was observed at this site.

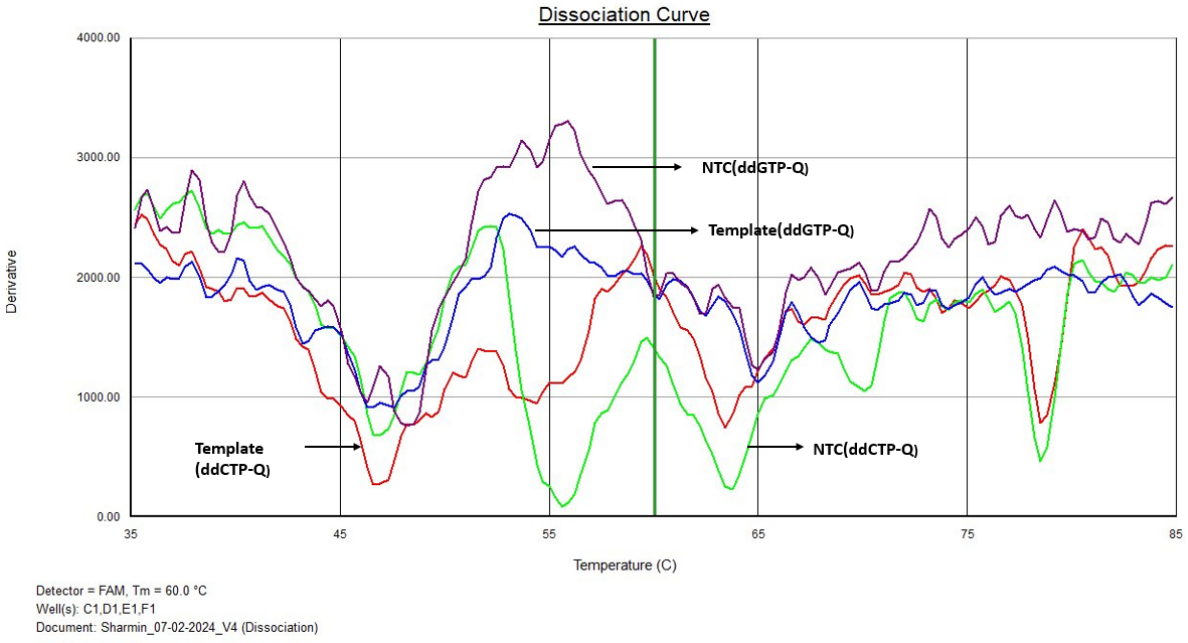

Figure 12: ***Dissociation curves of the reactions comprised of the labelling probe LP CoV2_F157-_tB(rev)_newLB and the reporter probe CoV2_F157-_tB(rev)_RB****. No quenching signal was observed, as quenching events typically manifest as negative peaks.*

3.7 Effects of Fast Alkaline Phosphatase Treatment on Tm Shifts during Dissociation Reactions

It was observed that the theoretical Tm values of all LP-RP duplexes differed from those observed in dissociation curve analyses, even in reactions where the polymerase was supposed to be inactive. A new set of multiplex reactions was developed using the plasmid clones containing CoV2_H69&V70:-_tA and CoV2_F157-_tB(rev)_LB amplicons and CoV2_K417N_tA(for)_LK and CoV2_P681H_tB(rev)_LK amplicons from clinical sample variants BQ.1 as the template, comprising a mixture of all LPs and RPs, to investigate the potential factors that might contribute to the Tm shifts during the dissociation reaction. The labelling reaction was conducted according to the methods described in sections 2.9.

After completing the labelling reaction, two experimental setups were employed: one included Fast alkaline phosphatase (FastAP) treatment to degrade unincorporated dideoxynucleotides, including the ddNTP-Qs followed by heat deactivation of the enzyme, while the other excluded FastAP treatment aimed to not to degrade the unincorporated ddNTPs and ddNTP-Qs in the reaction mixture. 10 µL of the labelling reaction was treated with 3.33U FastAP. The reaction mixture was then incubated at 37 °C for 60 minutes, followed by enzyme inactivation at 85 °C for 15 minutes using the Thermal Cycler. Subsequently, both experiments underwent dissociation curve analysis as outlined in section 2.10. The outcomes of the experiments were effectively depicted in Figure 13 and 14. The experimental data exported from the 7500 Fast qPCR instruments is presented in Appendix section Table A 12.

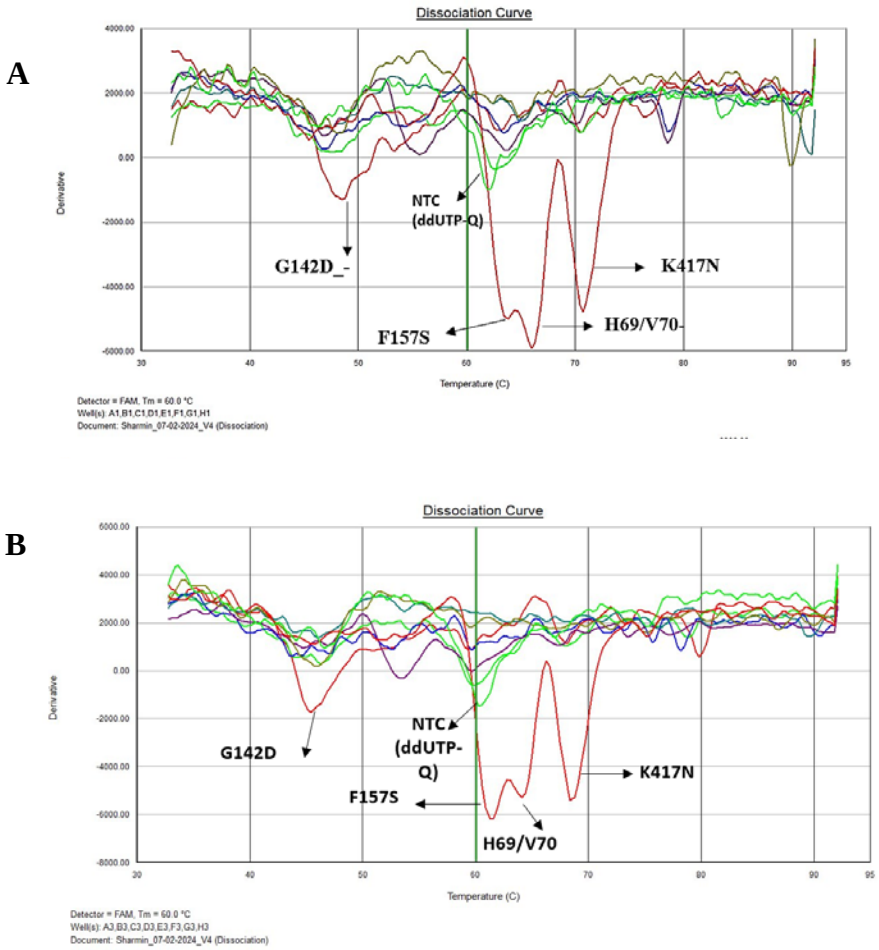

Figure 13: ***FAM channel detection:*** *Panel A shows the multiplex reaction dissociation curve without applying the FastAP after Labelling reaction. SNP site H69/V70, F157S, K417N, were labelled with ddUTP-Q and the duplex formation at Tm 66 °C, 64 °C and 71 °C respectively. For SNP site G142D, ddATP-Q labelled quenching response was produced at 49°C. Panel B illustrates the multiplex reaction dissociation curve subsequent to the application of FastAP following the Labelling reaction. SNP sites H69/V70, F157S, and K417N were labelled with ddUTP-Q, with duplex formation Tm values recorded at 63 °C, 61 °C, and 69 °C, respectively. A ddATP-Q labelled quenching signal was detected at 45°C which was near to the expected Tm value of SNP site G142D. Both panels contained information regarding a false positive signal, which exhibited quenching at 62 °C (Panel A) and 60 °C (Panel B) and was labelled with ddCTP-Q despite the absence of a template.*

From Figure 13, the ddATP-Q quenching response (approximately ranging from -1700 relative fluorescence units) decreased to -1900 after treating the labelling reaction with FastAP. A similar response was observed for the ddUTP-Q labelled quenching reaction where

the signal was decreased approximately ranging from -6000 relative fluorescence units. Furthermore, following treatment with FastAP, all LP-RP duplex formation Tm values exhibited closer alignment with the expected values (see Table A 12).

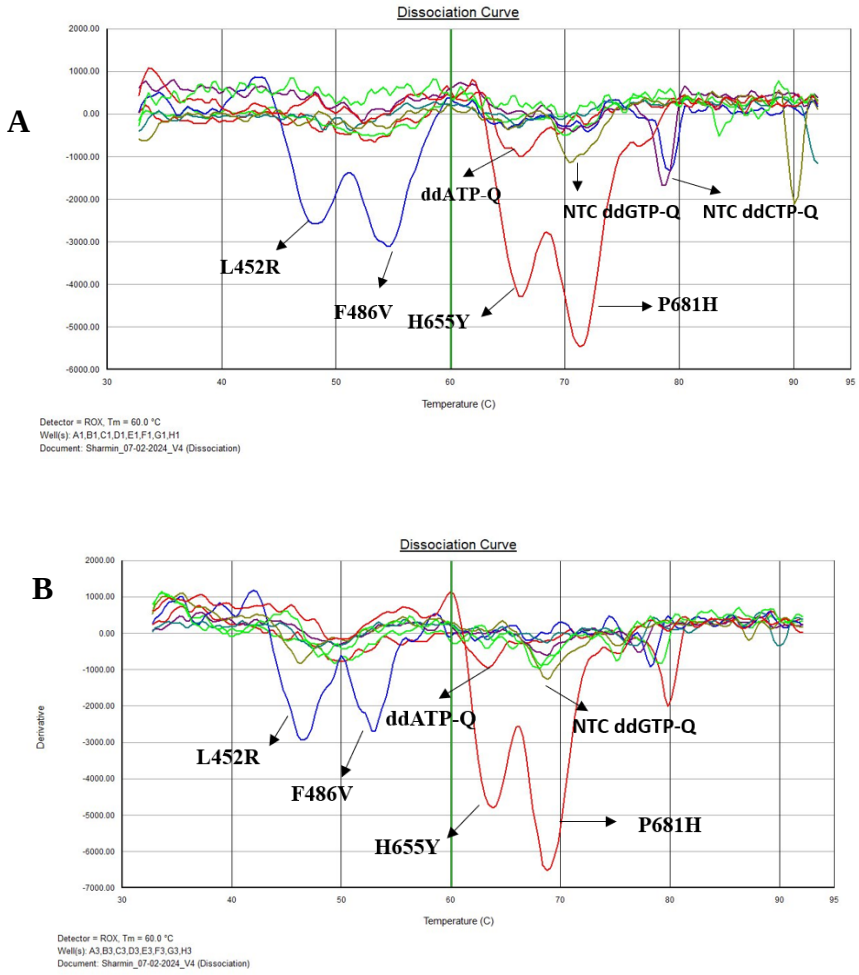

Figure 14: ***ROX channel detection:*** *Panel A depicts the multiplex reaction dissociation curve before the application of FastAP following the Labelling reaction. SNP sites L452R and F486V were labelled with ddCTP-Q, yielding duplex formation Tm values of 49 °C and 55 °C, respectively. ddUTP-Q labelled quenching responses were observed at 71 °C and 67 °C for SNP sites P681H and H655Y, respectively. Panel B presents the multiplex reaction dissociation curve following the application of FastAP subsequent to the Labelling reaction. SNP sites L452R and F486V were labelled with ddCTP-Q, resulting in duplex formation Tm values of 47 °C and 51.5 °C, respectively. Quenching responses labelled with ddUTP-Q were observed at 69 °C and 62 °C for SNP sites P681H and H655Y, respectively. False positive quenching signals were generated by the ddATP-Q labeled quencher reaction, while the ddGTP-Q quencher reaction produced signals in the non-template control.*

The quenching response dropped by around -500 relative fluorescence units for all the labeling reactions, as detected by the ROX channel (figure 14). In addition, after being treated with FastAP, the Tm values for LP-RP duplex formation were more correlated with the anticipated values. It was also notable that the quenching signal from the non-template control was also reduced.

3.8 FastAP Enzyme Activity, SDS Effect, and Polymerase Activity During Dissociation Reaction

To assess FastAP enzyme activity, the effect of SDS, and polymerase activity during the dissociation reaction, only a ddUTP-Q-labelled multiplex labelling reaction was conducted. This experiment focused on LPs intended for labelling with ddUTP-Q, as the LP-RP duplex Tm for the U reaction yielded a higher quenching signal. After completing the labelling reaction, which was followed from the method 2.9, two reaction setups were prepared for this purpose. In Step 1, FastAP was added to the labelling reaction, followed by incubation and heat inactivation. Subsequently, the dissociation reaction (followed from section 2.10) occurred with or without 1% SDS. In Step 2, FastAP was heat-inactivated at 85°C for 15 minutes before being added to the labelling reaction. The reaction then underwent incubation and heat inactivation, followed by the dissociation reaction with or without 1% SDS. In the figure 15 and 16 the red curve represents the procedure of Step 1, while the blue curve represents the procedure of Step 2.

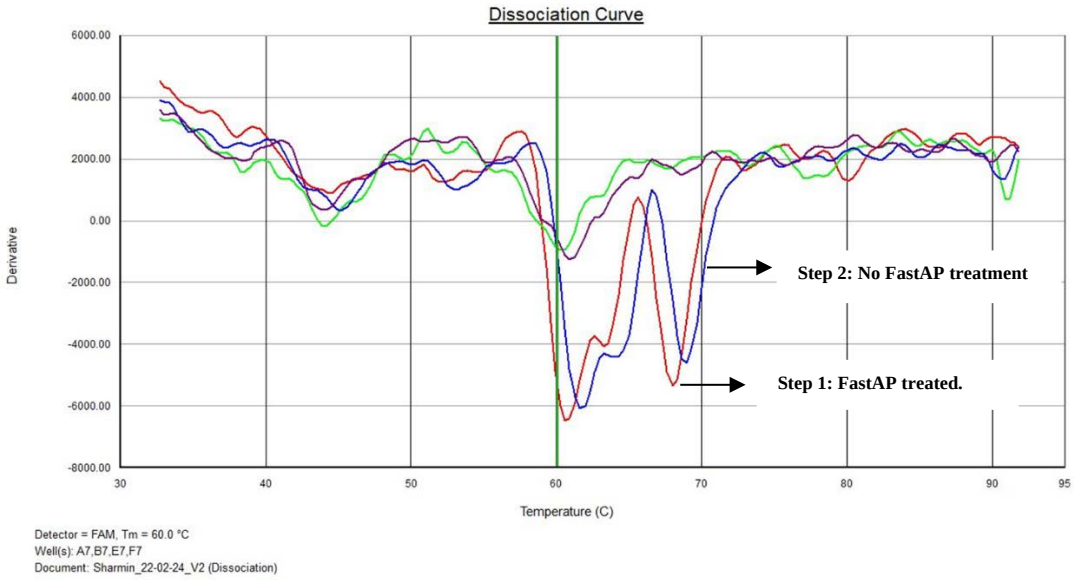

Figure 15: ***Illustration of the ddUTP-Q labelled multiplex dissociation reaction with 1% SDS reagent observed through the FAM channel detector****. The Red curve represents the procedure of step 1 and blue curve represents step 2 where it shows three broad quenching response (approximate range -4000 to -6000 relative fluorescence units) detected SNP site H69&V70, F157S, K417N. It is visible that the Tm for three quenching signals has a shift of approximately 1 °C to 2 °C with a higher intensity signal (approximately -500 relative fluorescence units) after treating the labelling reaction with FastAP. The green and purple curves showed a slight quenching response, despite being non-template control reactions.*

The theoretical Tm values for the FAM-labelled RPs CoV2_H69&V70:-_tB(rev)_RY, CoV2_F157S-tA(for)_RY, and CoV2_K417N_tA(for)_RK were calculated as 59.8 °C, 53 °C, and 69.8 °C, respectively. Following a ddUTP-Q labelled labelling reaction, the LP-RP duplex dissociation curve analysis revealed higher Tm values than the expected theoretical Tm values. CoV2_H69&V70:-_tB(rev)_LY-CoV2_H69&V70:-_tB(rev)_RY duplex exhibited a quenching response at Tm 64.5 °C, CoV2_F157S-tA(for)_LY-CoV2_F157S-tA(for)_RY duplex at Tm 61.5 °C, and CoV2_K417N_tA(for)_LK -CoV2_K417N_tA(for)_RK at 69.9 °C. However, after the FastAP treatment of the labelling reaction, Tm shifts closer to the expected values were observed and enhanced the signal intensity (figure 15).

Similar observations were made through the ROX channel reactions. The theoretical Tm values for the ROX-labelled RPs CoV2_H655Y_tA(for)_RY and CoV2_P681H_tB(rev)_RK

were 61.7 °C and 68.3 °C. Following a ddUTP-Q labelled labelling reaction, the LP-RP duplex dissociation curve analysis revealed higher Tm values than the expected theoretical Tm values, 64 °C and 69.9 °C, respectively. Moreover, after the FastAP treatment of the labelling reaction, Tm shifts closer to the expected values, 61.7 °C and 68.3 °C and it also enhanced the signal intensity (figure 16).

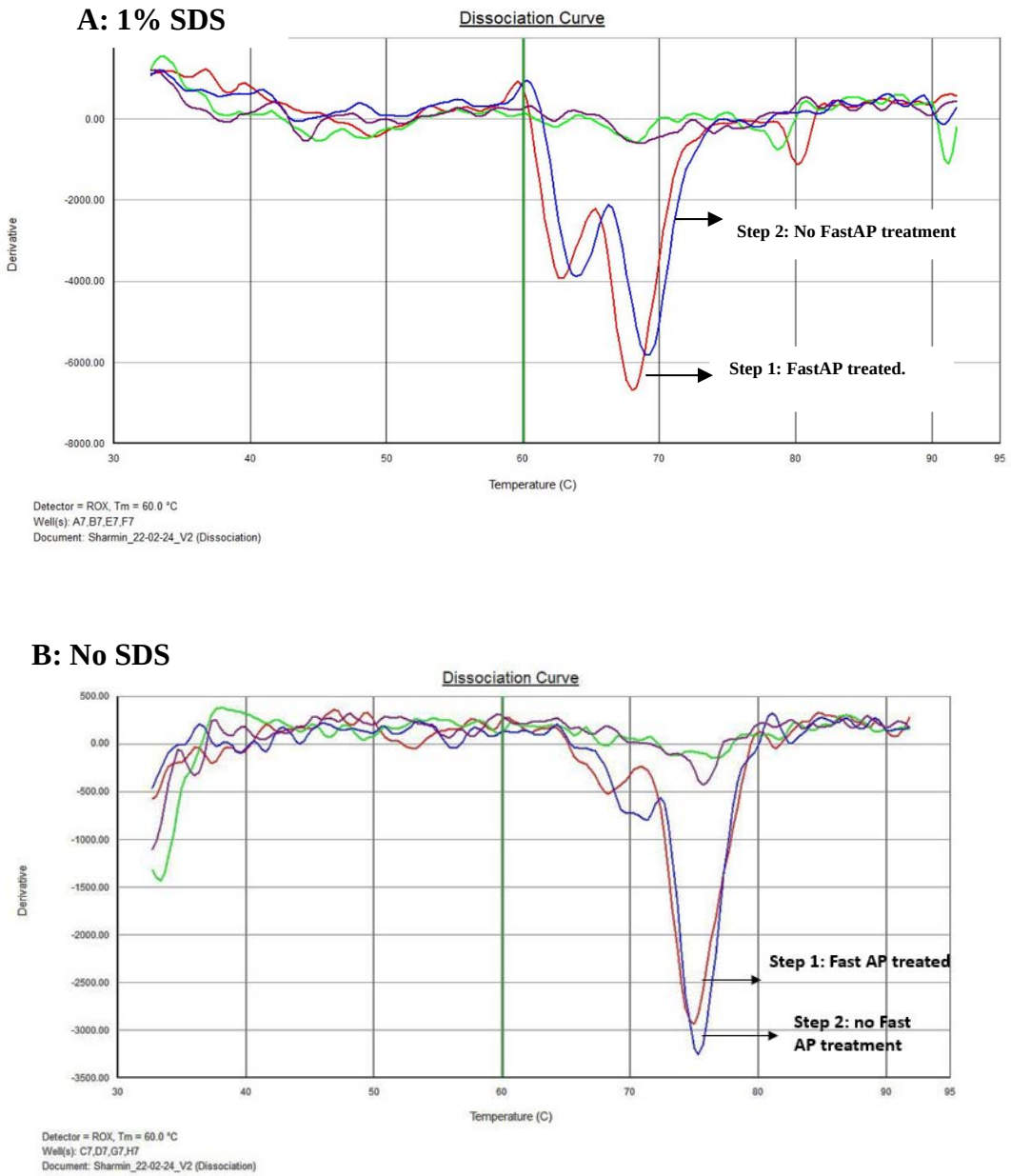

Figure 16: ***Illustration of the ddUTP-Q labelled multiplex dissociation reaction with and without 1% SDS reagent, each with and without post-labelling FastAP treatment, observed through the ROX channel detector****. Red curves represent the procedure of step 1 and blue curves represent step 2. Panel A (with 1% SDS) shows*

two broad quenching response (approximate range -4000 to -8000 relative fluorescence units) detected SNP site H655Y and P681H. A Tm shift was visualized for both quenching signals, with FastAP treatment yielding the lower Tm. The green and purple curve which represents "non template control" had no quenching response. Panel B shows one quenching response near about -3500 fluorescence units.

Although the reaction setups in Panel A and Panel B were identical in figure 16, with the only difference being the absence of SDS reagent in the dissociation reaction of Panel B, the quenching response in Panel B was noticeably reduced compared to Panel A. Additionally, Panel B shows only one quenching response near about -3500 units fluorescence units whereas Panel A displays two quenching response (approximate range -4000 to -8000 relative fluorescence units).

3.9 Genotyping and detecting of SARS-CoV2 Variants Using Multiplex LAD Technology: Triplicate Analysis

Following the acquisition of the LAD quenching response from the plasmid clones containing CoV2_H69&V70:-_tA and CoV2_F157-_tB(rev)_LB amplicons and CoV2_K417N_tA(for)_LK and CoV2_P681H_tB(rev)_LK amplicons from clinical sample variants BQ.1, as illustrated in Figures 13 and 14, a final multiplex reaction was established for the purpose of genotyping and detecting SARS-CoV-2 variants. In this experiment, six clinical samples and plasmid clones containing CoV2_H69&V70:-_tA and CoV2_F157-_tB(rev)_LB amplicons and CoV2_K417N_tA(for)_LK and CoV2_P681H_tB(rev)_LK amplicons from clinical sample variants BQ.1 were analyzed in triplicates. Clinical cDNA samples were collected from Innlandet Hospital with the variant list. Among these variants, six were chosen for analysis, characterized by the highest variability across the nine selected SNP sites (appendix table A 1). The variants and GenBank accession number details are provided in Appendix Table A 13 while Table 14 contains information regarding mutations and labelling.

The results obtained from this experiment are summarized in Table 3 (FAM-channel detection) and Table 4 (ROX-channel detection).

Table 3: LP-RP Melting Curve analysis for SARS-CoV-2 Variants from FAM Channel Detector of 7500 qPCR Machine.

Labelling Probe	Reporter Probe	Theoretical Tm value	Variants							LAD comments
			CH1.1	BE.1.1	BF.7	XBB1.5	CJ.1	BA.4.6.3	BQ.1	
CoV2_H69&V70:-_tB(rev)_LY	CoV2_H69&V70:-_tB(rev)_LY	59.8 ºC	ddCTP-Q quenching signal was detected at 56 ºC	ddUTP-Q quenching signal was detected at 62 ºC	ddUTP-Q quenching signal was detected at 62 ºC	ddCTP-Q quenching signal was detected at 48,62ºC and ddUTP-Q at 62 ºC	ddCTP-Q quenching signal was detected at 62.5 ºC and ddUTP-Q 56, 62 and 71 ºC	ddUTP-Q quenching signal was detected at 64 ºC	ddUTP-Q quenching signal was detected at 67 ºC	double quenching signal ddCTP-Q and ddUTP-Q was observed for variant XBB1.5 and CJ.1.
CoV2_G142D_-_tA(for)_LD	CoV2_G142D_-_tA(for)_LD	41.5ºC	ddATP-Q quenching signal was detected at 49 ºC	ddATP-Q quenching signal was detected at 49,61,70 ºC	ddATP-Q quenching signal was detected at 49,61 ºC	ddATP-Q quenching signal was detected at 49,61 ºC	ddATP-Q quenching signal was detected at 49,61,70 ºC	ddATP-Q quenching signal was detected at 49,61,70 ºC	ddATP-Q quenching signal was detected at 50 ºC	ddATP-Q quenching signal was observed at different Tms. However, at 49-50 ºC it was consistent to all the variants

CoV2_F157S-tA(for)_LY	CoV2_F157S-tA(for)_RY	53 ºC	ddUTP-Q and ddGTP-Q quenching signal was detected at 61 ºC and 55 ºC	ddUTP-Q quenching signal was detected at 62 ºC	ddUTP-Q quenching signal was detected at 62 ºC	ddUTP-Q quenching signal was detected at 61 ºC	ddUTP-Q quenching signal was detected at 62 ºC	ddUTP-Q quenching signal was detected at 62 ºC and ddCTP-Q 55 ºC	ddUTP-Q quenching signal was detected at 62 ºC	ddUTP-Q,ddGTP-Q and ddCTP-Q quenching signals were observed at different Tms. However, at ddUTP-Q 62 ºC it was consistent to all the variants
CoV2_F157-_tB(rev)_newLB	CoV2_F157-_tB(rev)_RB	50.6 ºC	ddUTP-Q quenching signal was detected at 62 ºC	ddGTP-Q quenching signal was detected at 58,70 ºC	ddGTP-Q quenching signal was detected at 58,70 ºC	ddGTP-Q quenching signal was detected at 58 ºC	ddGTP-Q quenching signal was detected at 58 ºC and ddUTP-Q at 62 ºC	ddGTP-Q quenching signal was detected at 58 ºC	ddGTP-Q quenching signal was detected at 58 ºC	Only for variant CJ.1 extra ddGTP-Q quenching signal was observed
CoV2_K417N_tA(for)_LK	CoV2_K417N_tA(for)_LK	69.8 ºC	ddUTP-Q quenching signal was detected at 70 ºC	ddUTP-Q quenching signal was detected at 70 ºC	ddUTP-Q quenching signal was detected at 70 ºC	ddUTP-Q quenching signal was detected at 71 ºC	ddUTP-Q quenching signal was detected at 71 ºC	ddUTP-Q quenching signal was detected at 71ºC and ddGTP-Q 71 ºC	ddUTP-Q quenching signal was detected at 71 ºC	Only for variant BA .4.6.3 extra ddGTP-Q quenching signal was observed

Table 4: LP-RP Melting Curve Duplex Results for SARS-CoV-2 Variants from ROX Channel Detector of 7500 qPCR Machine.

Labelling Probe	Reporter Probe	Theoretical Tm value	Variants							LAD comments
			CH1.1	BE.1.1	BF.7	XBB1.5	CJ.1	BA.4.6.3	BQ.1	
Cov2_H655Y_tA(for)_LY	Cov2_H655Y_tA(for)_LY	61.7 ºC	ddUTPQ quenching signal was detected at 66 ºC	ddUTPQ quenching signal was detected at 66 ºC	ddUTPQ quenching signal was detected at 66 ºC	ddUTPQ quenching signal was detected at 66 ºC	ddUTPQ quenching signal was detected at 66 ºC	ddUTPQ quenching signal was detected at 66 ºC	ddUTPQ quenching signal was detected at 66 ºC	Signal detection was precise for all the variants.
CoV2_P681H_tB(rev)_LK	CoV2_P681H_tB(rev)_LK	68.3 ºC	ddUTPQ quenching signal was detected at 71 ºC	ddUTPQ and ddGTPQ quenching signal was detected at 71 ºC and 72 ºC	ddUTPQ and ddGTPQ quenching signal was detected at 71 ºC and 72 ºC	ddUTPQ quenching signal was detected at 71 ºC	ddUTPQ quenching signal was detected at 71 ºC	ddUTPQ quenching signal was detected at 71 ºC and ddGTPQ 71 ºC	ddUTPQ quenching signal was detected at 71 ºC	extra ddGTP-Q quenching signal was detected at 72 ºC for variant BE 1.1, BF.7 and BA 4.6.3

CoV2_F486V_tB(rev)_LM	CoV2_F486V_tB(rev)_LM	49.6 ºC	No desired signal detected	ddCTPQ quenching signal was detected at 55 ºC	ddCTPQ quenching signal was detected at 55 ºC	ddATPQ quenching signal was detected at 50 ºC	ddATPQ quenching signal was detected at 49 ºC	No desired signal detected	ddCTPQ quenching signal was detected at 55 ºC	No desired signal was detected for vaiant CH 1.1 and BA 4.6.3
Cov2_L452R_tB(rev)_LH	Cov2_L452R_tB(rev)_LH	39.9 ºC	ddCTPQ quenching signal was detected at 54 ºC	ddCTPQ quenching signal was detected at 49 ºC	ddCTPQ quenching signal was detected at 49 ºC	ddCTPQ quenching signal was detected at 42 ºC	No desired signal detected	No desired signal detected	ddCTPQ quenching signal was detected at 49 ºC	No desired signal was detected for vaiant CJ.1 and BA 4.6.3

Using multiplex LAD technology, plasmid clones containing CoV2_H69&V70:-_tA and CoV2_F157-_tB(rev)_LB amplicons and CoV2_K417N_tA(for)_LK and CoV2_P681H_tB(rev)_LK amplicons from clinical sample variants BQ.1 was accurately genotyped, with successful detection in both the FAM and ROX channels. Figures 17 and 18 present the results obtained from the 7500-qPCR machine for variant BQ.1 in triplicates.

The quenching response, labelled with ddUTP-Q, was detected in the FAM channel at Tm values of 67 °C, 62 °C, and 71 °C. These Tm values closely correspond to the Tm values of the LP-RP duplex (Table 3) for the SNP sites H69/V70, F157S, and K417N, respectively. Throughout this multiplex experiment, the fluorescence signal exhibited a range of -4000 to -6000 relative fluorescence units (figure 17). The SNP sites G142D and F157- were identified using quenchers tagged with ddATP-Q and ddGTP-Q. The measured Tm for the LP-RP duplex were 49 °C and 58 °C, respectively, which closely corresponded to the expected Tm values for these particular reactions (Table 3). The fluorescence signal for the quencher response labelled with ddATP-Q was roughly -4000 relative fluorescence units, whereas the response labelled with ddGTP-Q was around -5000 relative fluorescence units (figure 17).

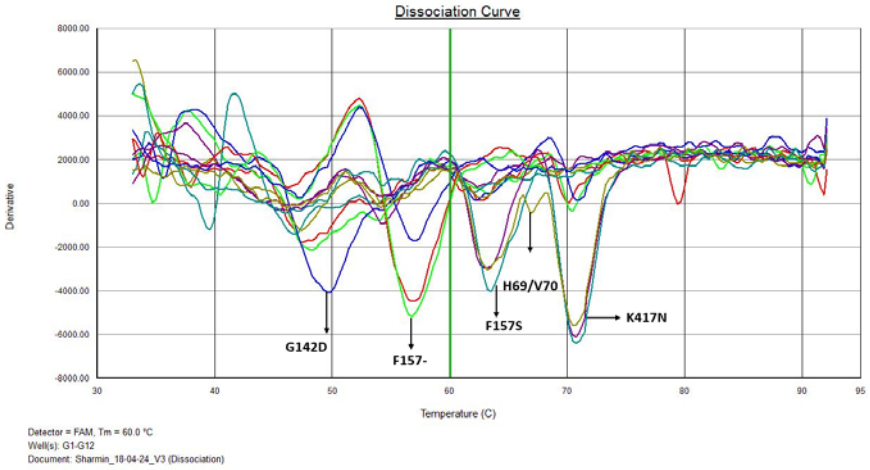

Figure 17: ***Detection of SNP sites in the FAM channel:*** *The multiplex LAD reaction identified five SNP sites H69/V70, G142D, F157-, F157S, and K417N in triplicate samples for plasmid clones containing CoV2_H69&V70:-_tA and CoV2_F157-_tB(rev)_LB amplicons and CoV2_K417N_tA(for)_LK and CoV2_P681H_tB(rev)_LK amplicons from clinical sample variants BQ.1.*

The quenching response, denoted as ddUTP-Q, was detected in the ROX channel at two distinct Tm thresholds of 66 °C and 71 °C during the conducted experiment. Significantly, the

Tm values of the LP-RP duplex (refer to Table 4) at the SNP loci H655Y and P681H correspond to these values. As illustrated in Figure 18, fluorescence signals varied between -6000 and -7000 relative fluorescence units over the course of the multiplex experiment.

Moreover, the SNP sites F486V and L452R- were effectively detected by ddCTP-Q labelled signal. The Tm values obtained for the LP-RP duplex at these locations were 55 °C and 49 °C, respectively, indicating a close concordance with the expected Tm values for these particular reactions (refer to Table 4). The fluorescence signal linked to the quenching response labelled with ddCTP-Q was shown to remain at about -4000 relative fluorescence units, as displayed in Figure 18.

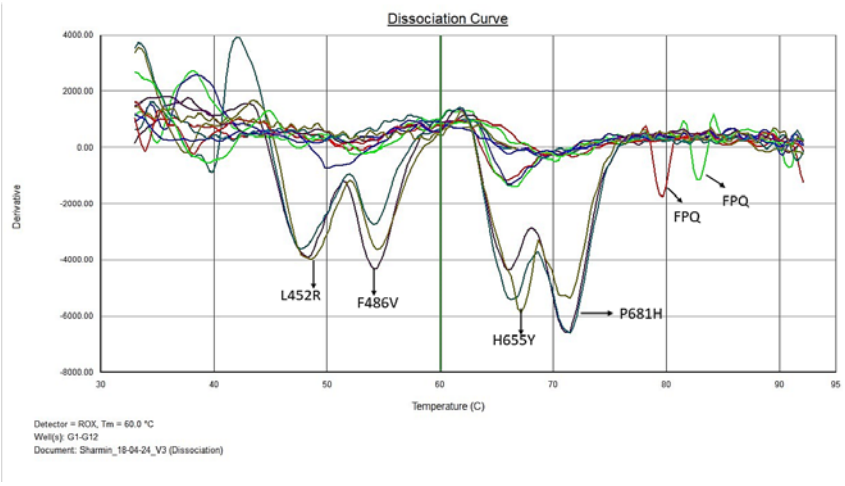

Figure 18: ***Detection of SNP sites in the ROX channel****: The multiplex LAD reaction identified four SNP sites L452R, F486V, H655Y and P681H in triplicate samples for plasmid clones containing CoV2_H69&V70:-_tA and CoV2_F157-_tB(rev)_LB amplicons and CoV2_K417N_tA(for)_LK and CoV2_P681H_tB(rev)_LK amplicons from clinical sample variants BQ.1. Two false positive quenching signals were detected at 80 ºC and 82 ºC.*

Triplicate analysis of non-template control (NTC) samples yielded the mean and standard deviation (SD) of the fluorescence signals. The threshold for distinguishing true positive quenching signals from false positives was established by subtracting 2x SDs from the mean value of the NTC samples. Tables 5 and 6 present the summarized calculations of true and false quenching signals.

Table 5. Calculation of True/False Quenching Signals from FAM channel detection

Quencher Reaction	fluorescence units	Mean	SD	Threshold	Template Signal (fluorescence units)	LAD comment
ddATP-Q	-1100					
ddATP-Q	-1000					
ddATP-Q	-300	-800	435.889894	-1671.77979	-4000	True positive signal
ddCTP-Q	4000					
ddCTP-Q	500					
ddCTP-Q	-3800	233.3333333	3906.83162	-7580.32991	-1000	False Positive signal
ddGTP-Q	1000					
ddGTP-Q	300					
ddGTP-Q	-2500	-400	1852.02592	-4104.05184	-5500	True positive signal
ddUTP-Q	-500					
ddUTP-Q	-500					
ddUTP-Q	-4000	-1666.66667	2020.72594	-5708.11855	-5900	True positive Signal

Table 6 Calculation of True/False Quenching Signals from ROX channel detection

Quencher Reaction	Fluorescence units	Mean	SD	Threshold	Template Signal (fluorescence units)	LAD comment
ddATP-Q	-1000					
ddATP-Q	-800					False positive signal
ddATP-Q	-500	-766.667	251.6611	-1269.99	-1100	
ddCTP-Q	300					
ddCTP-Q	-100					True Positive signal
ddCTP-Q	-400	-66.6667	351.1885	-769.044	-4000	
ddGTP-Q	-100					
ddGTP-Q	-6000					False positive signal
ddGTP-Q	-6200	-4100	3465.545	-11031.1	-6000	
ddUTP-Q	-10					
ddUTP-Q	-900					True positive Signal
ddUTP-Q	-1000	-636.667	545.0076	-1726.68	-6500	

3.10 Detection of Wild Type Sequence in SARS-CoV-2 Variant XBB 1.5 and CJ.1 Using LAD Technology

During the final LAD experiment, which involved genotyping and detecting SARS-CoV-2 variants in six clinical samples with different variants and plasmid clones containing CoV2_H69&V70:-_tA and CoV2_F157-_tB(rev)_LB amplicons and CoV2_K417N_tA(for)_LK and CoV2_P681H_tB(rev)_LK amplicons from clinical sample variants BQ.1), a specific mutation result F486P was noticeable for variants XBB 1.5 and CJ.1(figure 20). This SNP site was expected to be labelled with ddGTP-Q at a Tm of 49.6 ºC. However, the experimental results indicated that the ddATP-Q-labelled reaction occurred at a slightly higher Tm of 50 ºC for both variants (figure 20). Figure 19 displays the F486V mutation site across the variants.

*Figure 19**: F486V mutation site**. The wild type sequence (NC_045512) exhibits a thymine (T) base at position 23018. In contrast, the SARS-CoV-2 variants XBB 1.5 (OY813584.1) and CJ.1 (OY179166.1) possess a mutation at this position, resulting in a cytosine (C) base. Illustration from CLC Main Workbench 7.9.3*

A

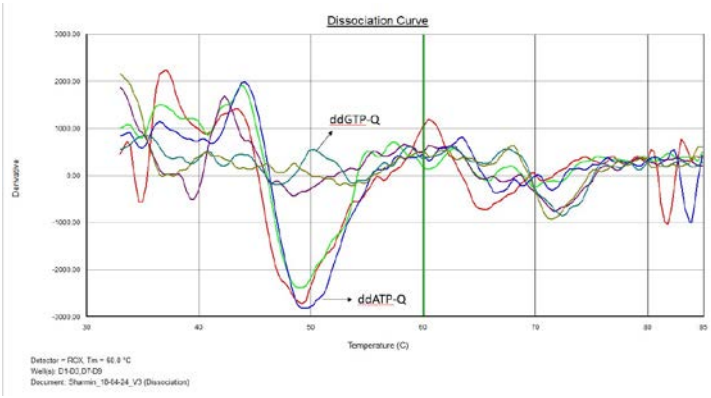

B

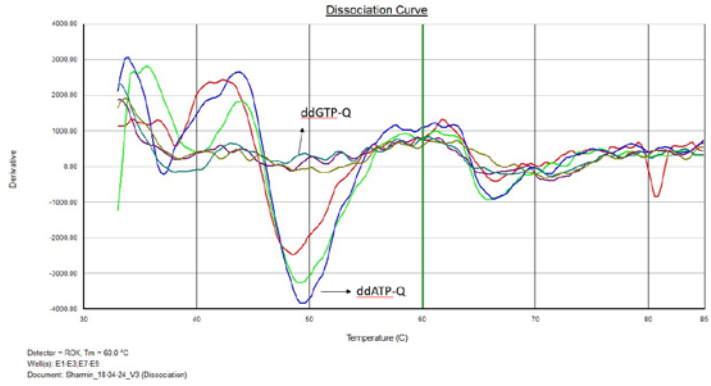

*Figure 20**: Panel A**: ddATP-Q labelled quenching response at Tm 50 ºC (-3000 fluorescence unit) from clinical sample for variant XBB 1.5**. Panel B**: ddATP-Q labeled quenching response at Tm 50 ºC (-4000 fluorescence unit) from clinical sample for variant CJ.1. In contrast to ddATP-Q, the quenching response mediated by ddGTP-Q was not negligible in both panels.*

4. Discussion

The main objective of this study was the application of LAD technology for the detection of SARS-CoV-2 variants. This discussion considers the obtain results, challenges encountered during experimental procedures, including the impact of fluorescent dyes on SNaPshot assay results, the control of false positive quenching signals, the factors that affected Tm values in LAD, the quenching capability of DNA polymerase, strategies for improving signal clarity, potential inhibitors of PCR, and the effectiveness of multiplex LAD reactions. Each subsection focuses on specific challenges, provides insights into the underlying mechanisms, discusses limitations, and suggests potential solutions. Moreover, the discussion clarifies the consequences of the findings in enhancing the comprehension and utilization of these molecular approaches in the field of genotyping and detecting SARS-CoV-2 variations. The purpose of this section is to offer a detailed analysis of the findings, address important research inquiries, and propose ways to improve the methods used in research contexts.

For evaluating diagnostic techniques, it is essential to take into account their ability to perform multiplexing. KASP assays allow for the simultaneous detection of 4-6 loci in a single reaction, while SNPlex assays have the advantage of genotyping a greater number of SNPs, usually ranging from 48 to 96 plex per reaction. Conversely, LAD's potential for high multiplexing enables the simultaneous detection of multiple variants, making it a promising alternative. To maximize its detection capabilities, an 18-plex LAD assay using 4 tubes might be expanded to accommodate a potential of 25-plex per tube. Future developments may necessitate the integration of viral variants beyond SARS-CoV-2, such as those associated with comparable symptomatic profiles, such as influenza and other coronaviruses, in order to fully realize the potential of LAD. This expansion has the capability to substantially improve the utility of LAD in comprehensive variant detection and surveillance efforts.

4.1 Dye effect on SNaPshot assay results

The SNaPshot assay was utilized for the analysis of LPs' fragments. The basis of the SNaPshot reaction is the dideoxy (ddNTP) SBE of an unlabelled oligonucleotide at the 3′-end of the base directly next to the SNP (in the absence of dNTPs in the reaction). Different fluorescent dyes are employed to label each ddNTP, and the internal size marker LIZ120 has been assigned with a fifth colour (Quintáns et al., 2004). Based on the experimental findings of singleplex (result section 3.2) and multiplex reactions (result section 3.2) in the SNaPshot assay, the size

values (measured in nucleotides) of all LP fragments exceeded the anticipated fragment sizes. In the singleplex experiment, the LP CoV2_P681H_tB(rev)_LK, possessing 42 nucleotides, displayed an electropherogram peak at 53.49 nucleotides (figure 7: panel 8), marking the most notable deviation in peak location, which can be ascribed to its relatively shorter fragment length. The potential reason could involve variations in electrophoretic mobility, primarily influenced by factors such as the length, sequence, and dye utilized to mark the extended primer. Additionally, the impact of nucleotide composition tends to be more pronounced in shorter oligonucleotides compared to longer ones (Quintáns et al., 2004).

Depending on the electropherogram (figure 7,8 and 9), different fragments showed varying intensities of fluorescent signal. Among all the ddNTPs, guanines labeled consistently exhibited the highest signal peaks, measuring 3615 in height during the singleplex reaction (results section 3.2 table 1) and 6852 in height for the multiplex reaction (appendix Table A 6). As different fluorescent dyes have different electrophoretic mobilities, the selection of dyes can affect the SNaPshot assay's performance. Electrophoresis migration speeds can vary across dyes with different molecular weights and chemical characteristics, which might impact extension product separation and detection. Potentially impacting the precision and consistency of genotype calling, this can cause changes to the signal intensity and shifting of peaks.

4.2 Covalently incorporating ddNTP-Qs into the labelling probes produces FPQ

During the multiplex SNaPshot analysis, a blue peak with a size of 62.55 nucleotides was observed, closely corresponding to the expected oligo size of LP CoV2_F157:_tB(rev)_LB, which was anticipated to be 63 nucleotides in the non-template control (see 3.2: figure 8) . Conversely, in the LAD experiment, an inaccurate quenching event was observed in multiplex reactions where the labelling probe LP CoV2_F157-_tB(rev)_LB and RP CoV2_F157-_tB(rev)_RB were tested in the "non-template control" condition (Appendix figure A 12). This indicated the presence of false positive quenching signals, which could potentially lead to erroneous interpretation of the results. Upon comparison, it is evident that while both assays exhibited signals in their respective NTC conditions for LP CoV2_F157-_tB(rev)_LB, the nature of these signals differs. In contrast to the SNaPshot assay, which identified a peak that corresponded to the anticipated oligo size, the LAD experiment demonstrated quenching

events that suggest false positive signals. Further investigations should be conducted to examine the elements that contribute to false positive quenching in the LAD assay. This is necessary to ensure that the results are interpreted accurately and to enhance the efficacy of the assay by optimizing its settings.

It is crucial to account for potential intramolecular and intermolecular interactions among probes in a qPCR reaction while designing them (Rodríguez et al., 2015). Labeling probes can create thermodynamically stable secondary structures like hairpin structures, self-dimers, or heterodimers at the reaction's annealing temperature. This can make it possible for complementary ddNTP-Qs to be added to the 3' end. This incorporation, even in the absence of template DNA, can result in false positive quenching (FPQ) signals. Nonspecific interactions between the labeling probes and the complementary ddNTP-Qs lead to these FPQ signals, which cause false signal detection that could resemble real positive signals. Fluorescently labelled RPs produce quenching reactions unrelated to genotype when they form duplexes with tagged LPs in the process. These problems can be resolved by either introducing mismatches to destabilize the secondary structures of the probes or by introducing mismatches to prevent the incorporation of ddNTP-Qs in the reaction by replacing the complementary LP base with a non-complementary one. A specific modification was applied to the LP CoV2_F157-_tB(rev)_LB to prevent false positive quenching in the non-template control. By replacing adenine with cytidine at the fourth position from the 5’ end of the probe (appendix figure A 14), the secondary structure of the labeling probe is altered in such a way that it was not permitted the incorporation of ddCTP-Q opposite this position (figure 12). This modification was aimed at reducing nonspecific binding or incorporation events that could lead to false positive signals.

4.3 Factors Influencing Tm Values in LAD: FastAP Enzyme Activity

It was noted that the Tm values of the LP-RP duplexes exceeded the expected values by approximately 5-9 °C during the execution of the LAD approach on SARS-CoV-2 Variants BA.5.1.5 and BQ.1 using plasmid clones containing specific amplicons derived from clinical sample (Appendix Table A 8 and Table A 9). Significant shifts in Tm values were observed in the LAD signals even in reactions where the polymerase was supposed to be inactivated by the 1% SDS, suggesting that potential factors might influence these results. In order to

investigate this difference, two experimental configurations were created: one included the use of FastAP treatment after the completion of the labelling process to degrade the phosphate groups from any unincorporated ddNTPs and ddNTP-Qs, while the other configuration eliminated FastAP treatment in order to not to degrade the unincorporated ddNTPs and ddNTP-Qs in the reaction mixture. The purpose of this technique was to clarify that Hot Termipol DNA polymerase was not inactivated by using 1% SDS and leading to Tm shifts. After administering FastAP treatment, the Tm values for all the LP-RP duplexes nearly matched the expected values. Figures 13 and 14 illustrate the detailed findings, and Table A 12 in the appendix includes the exported data from the 7500qPCR machine, as presented in Result Section 3.6.

FastAP is frequently employed to dephosphorylate nucleic acid molecules, especially in sequencing processes, to degrade phosphate groups from unincorporated nucleotides and prevent their disruption in downstream reactions. Treating the labelling reaction with FastAP might have degraded any remaining unincorporated nucleotides that could have interfered with the stability of the DNA duplexes during the dissociation reaction. By degrading these interfering components, the dissociation process might have occurred with greater precision, resulting in Tm changes that nearly correspond to the anticipated values. This implies that the existence of remaining nucleotides in the labelling process might have caused variations in the measured Tm values before being treated with FastAP.

Additional investigation of FastAP enzyme activity encompassed two separate stages. The results of both steps were promising, showing Tm shifts that closely matched the expected values and a significant improvement in signal intensity (details result section 3.8 figure 15 and 16). The prior subsequent stages, the direct addition of FastAP to the labeling reaction enabled the degradation of phosphate groups of unincorporated nucleotides. This procedure most likely degrades any remaining unincorporated ddNTPs and ddNTP-Qs, reducing their potential to interfere with the stability of the LP-RP duplex during the dissociation reaction. As a result, the dissociation process occurred with heightened precision, leading to Tm shifts closely resembling the expected values. The decrease in background noise brought about by the degradation of unincorporated nucleotides might also have played a part in the observed signal intensity increase (figure 15 and 16). The process had been slightly modified so that FastAP was heat inactivated before being added to the labelling reaction. By inactivating the enzyme FastAP, this pre-treatment apparently avoided any possible interference in later reaction stages. The results from both stages emphasize the significance of FastAP in

degrading unbound ddNTPs and ddNTP-Qs from the labelling process. This step is essential for obtaining precise Tm values and improving the strength of the signal. The results suggest that incorporating FastAP treatment into the experimental workflow can improve the reliability and sensitivity of the assay, ultimately leading to more precise Tm values.

4.4 DNA Polymerase quenching ability

The LAD technique uses the addition of SDS reagent to inactivate DNA polymerase before administering fluorescently labelled RPs. SDS is recognized as a PCR inhibitor to suppress the activity of DNA polymerase (Schrader et al., 2012), making it an essential element in dissociation operations to prevent undesired polymerase activity that may disrupt following procedures. It was of interest to investigate and elucidate the influence of DNA polymerase activity on the quenching signal observed during dissociation reactions, particularly in the presence and absence of SDS. Figure 17 (Result Section 3.8) provided insights into this phenomenon, indicating that DNA polymerase may act as a quencher, resulting in reduced quenching signals.

Distinct quenching effects were observed when comparing dissociation reactions conducted with and without SDS. In the absence of SDS, the LAD signal displayed a single quenching response, around approximately -3500 units of relative fluorescence. However, when SDS was present, the signal exhibited two extensive quenching reactions covering a range of around -4000 to -8000 relative fluorescence units, particularly at the SNP sites H655Y and P681H (figure 16). These results indicate that the presence of SDS modifies the kinetics of the dissociation reaction, potentially via influencing DNA polymerase activity. The more extensive quenching reactions found with SDS suggest a more intricate interaction between the polymerase, fluorescent probes, and DNA duplexes. Additional research is necessary to comprehensively comprehend the molecular consequences of SDS on polymerase behavior during the LAD test and its subsequent impact on signal interpretation and assay reliability.

4.5 Enhancing LAD Signal Clarity through Iterative Melting Curve Analysis: Consecutive Plate Repeats for Noise Reduction

A significant variation in noise incidence was noted when conducting consecutive melting curve analysis on the same plate, with the most effective results achieved on the third attempt.

The use of this iterative strategy reduced the levels of noise, making it easier to observe the signals that were generated. To address this issue, consecutive runs of melting curve analysis on the same plate following five sequential dissociation reactions were conducted. Significantly, there was a noticeable presence of noise, specifically in the FAM channel detector, at certain temperature ranges (42°C-55°C and 75°C-85°C). This created difficulties in differentiating between the actual signal and the background noise, which might potentially result in false positive results. Possible causes of this noise included changes in incubation duration and temperature after the addition of SDS/RP mix, among other things. An optimization of the reaction conditions was attempted by including a 15-minute initiation step at 95 degrees. However, the noise levels were not significantly reduced by this action. Conducting several melting curve analyses on the same plate finally proven to be useful in decreasing noise and improving the clarity of the signal. Figure A 15 in the appendix section signifies the details.

4.6 PCR Inhibitors may disrupt Quenching response

Technical difficulties with an increasing number of runs and noise that appeared throughout the detection channels (FAM and ROX) led to issues with signal detection. Particularly, the interpretation of the results was made more challenging by the unexpected presence of quenching signals across both channels at the same Tm. As factors such as the 15-minute initiation step at 95 degrees and centrifuging the reaction before melting curve analysis were excluded from causing interference, the source of the interference remains unknown. The observed variations might be attributable to the presence of one or more reaction components. An interfering component that has the potential to disrupt the quenching response is the detergent SDS. It possesses the characteristic of inhibiting PCR reaction (Schrader et al., 2012). SDS inhibits PCR by changing the structure of DNA polymerase and inhibiting its activity, which interferes with the formation of essential complexes. This inhibition persists at low concentrations, such as 0.01% SDS, which significantly inhibits the activity of the polymerase (Rossen et al., 1992). SDS impacts the assembly of the binary complex, in which DNA polymerase attaches to double-stranded DNA with a 3’ recessed end, and potentially hinders the development of the ternary complex. The formation of the ternary complex is crucial since it necessitates the binding of two divalent metal ions (Mg++) prior to the binding of a nucleotide to the binary complex, thus facilitating DNA synthesis. Consequently, these disruptions hinder the DNA polymerase’s ability to efficiently elongate DNA strands during

PCR. Despite the inhibitory effect of 0.01% SDS on PCR, primarily through its impact on polymerase activity, higher concentrations such as 1% SDS might not entirely abolish the interaction between DNA polymerase and double-stranded DNA or nucleotides (Wilson, 2024).

Furthermore, PCR inhibitors can interfere with the quenching mechanism of the fluorescent probes. Fluorescent probes generally consist of a quencher molecule that inhibits fluorescence until the probe attaches to its intended target. Inhibitors have the ability to disrupt this quenching process, which enables the detection of fluorescence even when there is no binding to the target. As a result, the baseline fluorescence is increased (Schrader et al., 2012). Certain inhibitors, such as SDS, can create bubbles in the reaction mixture. During the preparation of the dissociation reaction master mix (method section 2.10) in this experiment, SDS was introduced into the RP mix, resulting in the formation of bubbles. The presence of these bubbles can disrupt the accurate detection of quenching responses by the channel detector during the analysis of melting curves, leading to errors and an elevation in baseline fluorescence levels. Nonetheless, this prospective SDS effect should be investigated further.

4.7 Multiplex LAD reaction setup effectively and efficiently genotypes SNP loci

As mentioned in the results section (3.4: see figures 12), using LAD technology on plasmid clones containing CoV2_H69&V70:-_tA and CoV2_F157-_tB(rev)_LB amplicons and CoV2_K417N_tA(for)_LK and CoV2_P681H_tB(rev)_LK amplicons from clinical sample variants BA.5.1.5 initially generated several false positive quenching responses. Subsequently, in an effort to alleviate these false positives, new PCR primers and probes were meticulously designed and implemented (refer to Appendix figure A 14). However, challenges persisted in detecting the SNP site F157-, which was anticipated to be labelled with ddGTP-Q and exhibit a quenching response at Tm 50.6 ºC, as represented in the results section (3.5: see figure 12).

Nevertheless, the subsequent analysis produced positive results by incorporating triplicate examinations into the multiplex reaction. All SNP sites, including the F157-, were successfully genotyped. The extensive examination, outlined in the results section (3.9: refer to Table 3 and 4 and figure 17 and 18), highlights the strength and effectiveness of the utilized LAD technology, despite the initial challenges addressed. However, persistent false-positive quenching responses still made it complicated to interpret the actual signals. To effectively

distinguish false positives from actual positive LAD signals, the standard deviation (SD) is computed for triplicates in NTC reactions. True positive quenching occurs when the observed signal intensity of the target template sample is significantly lower than that of the non-template control (NTC) by a quantity that exceeds a predetermined threshold. Table 5 and 6 in Result section 3.9 represent the detected LAD signals, as specified by this criterion.

4.8 LAD as Mini-sequencing

The unexpected detection of a ddATP-Q-labelled reaction occurring at a little higher Tm than expected for both variant types XBB 1.5 and CJ.1 prompts the question of whether LAD can serve as a 'mini sequencing' method in this case (figure 20). The LAD technology, which has the capability to genotype and identify specific mutations inside target sequences at the same time, exhibits several resemblances to sequencing methods. However, it diverges in its methodology, depending on quencher labeled detection instead of direct sequencing of nucleotides.

According to the results in Section 3.10, it appeared that LAD and "mini sequencing" had comparable performance. The observed quenching responses, indicating the presence of the wild-type sequence at the mutation site F486P for variants XBB 1.5 and CJ.1, despite the expectation of a specific mutation labelled with ddGTP-Q, suggest that LAD effectively provided information about the nucleotide sequence at this position. Through the detection and analysis of specific mutations in the target sequences, LAD offers valuable information about the genetic composition and variability of the examined samples. Although the observed results deviated from the anticipated outcomes, the ability of LAD to detect the presence or absence of mutations and provide insights into the genetic variants present in the samples aligns with the concept of mini sequencing.

Therefore, despite the unexpected outcomes, the utilization of LAD in this experiment demonstrates its potential as a mini sequencing tool for genotyping and detecting SARS-CoV-2 variants, offering valuable insights into the genetic diversity and composition of the analyzed samples.

4.9 Future Work

The efficacy of LAD Technology for detecting SARS-CoV-2 variants has been demonstrated in this work, suggesting the need for further improvements to boost its reliability and adaptability. One potential approach can be involved by utilizing proteinase K treatment (Hiseni, 2016) subsequent to conducting the labeling reaction of the samples. This treatment necessitates a 30-minute incubation period at 56°C which is then followed by the addition of the RPs. Another way to improve the assay's sensitivity and efficiency is to increase the number of genetic variants utilized and expand the SNP site variations. By integrating a wider spectrum of SNPs obtained from databases, the assay can identify a more extensive variety of genetic markers. To achieve this expansion, it is crucial to carefully construct the probes in order to prevent cross-hybridization. Another crucial aspect for optimization relates to the concentration of DNA polymerase employed in the experiment. To enhance assay accuracy, it is desirable to restrict non-specific amplification and possible artifacts by reducing the quantity of polymerase, especially for Hot FirePol and Hot Termipol. Finally, diversifying the visualization methods beyond the commonly employed FAM and ROX fluorescent dyes can greatly improve the ability of LAD technology to simultaneously detect many targets. By incorporating these improvements, LAD technology can attain higher levels of sensitivity, specificity, and multiplexing capacity, hence enhancing its efficacy as a genetic analysis and diagnostic technique.

5. Conclusion

The precise detection and genotyping of SARS-CoV-2 variants were achieved through the successful development and validation of a multiplex assay utilizing LAD technology in this study. By applying the LAD multiplex reaction to six clinical samples of different variants and one plasmid clone containing specific amplicons from the clinical sample variant BQ.1, the assay's efficacy was confirmed through the detection of the BQ.1 variant in both the FAM and ROX channels. However, further investigation into the quenching mechanisms of the fluorescent probes is needed to optimize assay performance and ensure consistent detection across a variety of samples.

6. References

Barton, M. I., MacGowan, S. A., Kutuzov, M. A., Dushek, O., Barton, G. J., & Van Der Merwe, P. A. (2021). Effects of common mutations in the SARS-CoV-2 Spike RBD and its ligand, the human ACE2 receptor on binding affinity and kinetics. *eLife*, *10*, e70658. https://doi.org/10.7554/eLife.70658

Borillo, G. A., Kagan, R. M., & Marlowe, E. M. (2022). Rapid and Accurate Identification of SARS-CoV-2 Variants Using Real Time PCR Assays. *Frontiers in Cellular and Infection Microbiology*, *12*, 894613. https://doi.org/10.3389/fcimb.2022.894613

Brookes, A. J. (1999). The essence of SNPs. *Gene*, *234*(2), 177–186. https://doi.org/10.1016/S0378-1119(99)00219-X

Deshpande, A., & White, P. S. (2012). Multiplexed nucleic acid-based assays for molecular diagnostics of human disease. *Expert Review of Molecular Diagnostics*, *12*(6), 645–659. https://doi.org/10.1586/erm.12.60

Harper, H., Burridge, A., Winfield, M., Finn, A., Davidson, A., Matthews, D., Hutchings, S., Vipond, B., Jain, N., The COVID-19 Genomics UK (COG-UK) Consortium, Edwards, K., & Barker, G. (2021). Detecting SARS-CoV-2 variants with SNP genotyping. *PLOS ONE*, *16*(2), e0243185. https://doi.org/10.1371/journal.pone.0243185

Hasick, N., Kim, R. R., Xu, Y., Bone, S., Lawrence, A., Gibbs, C., Danckert, N., & Todd, A. (2022). PlexProbes enhance qPCR multiplexing by discriminating multiple targets in each fluorescent channel. *PLOS ONE*, *17*(3), e0263329. https://doi.org/10.1371/journal.pone.0263329

He, C., Holme, J., & Anthony, J. (2014). SNP Genotyping: The KASP Assay. In D. Fleury & R. Whitford (Eds.), *Crop Breeding* (Vol. 1145, pp. 75–86). Springer New York. https://doi.org/10.1007/978-1-4939-0446-4_7

Hiseni. (2016). *Pranvera Hiseni, thesis (final).pdf*.

Hiseni, P., Wilson, R. C., Storrø, O., Johnsen, R., Øien, T., & Rudi, K. (2019). Liquid array diagnostics: A novel method for rapid detection of microbial communities in single-tube multiplex reactions. *BioTechniques*, *66*(3), 143–149. https://doi.org/10.2144/btn-2018-0134

Kim, S., & Misra, A. (2007). SNP Genotyping: Technologies and Biomedical Applications. *Annual Review of Biomedical Engineering*, *9*(1), 289–320. https://doi.org/10.1146/annurev.bioeng.9.060906.152037

Korber, B., Fischer, W. M., Gnanakaran, S., Yoon, H., Theiler, J., Abfalterer, W., Hengartner, N., Giorgi, E. E., Bhattacharya, T., Foley, B., Hastie, K. M., Parker, M. D., Partridge, D. G., Evans, C. M., Freeman, T. M., De Silva, T. I., McDanal, C., Perez, L. G., Tang, H., … Wyles, M. D. (2020). Tracking Changes in SARS-CoV-2 Spike: Evidence that D614G Increases Infectivity of the COVID-19 Virus. *Cell*, *182*(4), 812-827.e19. https://doi.org/10.1016/j.cell.2020.06.043

Kumar, S., Nyodu, R., Maurya, V. K., & Saxena, S. K. (2020). Morphology, Genome Organization, Replication, and Pathogenesis of Severe Acute Respiratory Syndrome Coronavirus 2 (SARS-CoV-2). In S. K. Saxena (Ed.), *Coronavirus Disease 2019 (COVID-19)* (pp. 23–31). Springer Singapore. https://doi.org/10.1007/978-981-15-4814-7_3

Kwok, P.-Y. (2001). Methods for Genotyping Single Nucleotide Polymorphisms. *Annual Review of Genomics and Human Genetics*, *2*(1), 235–258. https://doi.org/10.1146/annurev.genom.2.1.235

Liao, Y., Wang, X., Sha, C., Xia, Z., Huang, Q., & Li, Q. (2013). Combination of fluorescence color and melting temperature as a two-dimensional label for homogeneous multiplex PCR detection. *Nucleic Acids Research*, *41*(7), e76–e76. https://doi.org/10.1093/nar/gkt004

Lind, A., Barlinn, R., Landaas, E. T., Andresen, L. L., Jakobsen, K., Fladeby, C., Nilsen, M., Bjørnstad, P. M., Sundaram, A. Y. M., Ribarska, T., Müller, F., Gilfillan, G. D., & Holberg-Petersen, M. (2021). Rapid SARS-CoV-2 variant monitoring using PCR confirmed by whole genome sequencing in a high-volume diagnostic laboratory. *Journal of Clinical Virology*, *141*, 104906. https://doi.org/10.1016/j.jcv.2021.104906

Marras, S. A. E., Kramer, F. R., & Tyagi, S. (2002). Genotyping SNPs With Molecular Beacons. In P.-Y. Kwok, *Single Nucleotide Polymorphisms* (Vol. 212, pp. 111–128). Humana Press. https://doi.org/10.1385/1-59259-327-5:111

Marras, S. A. E., Tyagi, S., Antson, D.-O., & Kramer, F. R. (2019). Color-coded molecular beacons for multiplex PCR screening assays. *PLOS ONE*, *14*(3), e0213906. https://doi.org/10.1371/journal.pone.0213906

Mhlanga, M. M., & Malmberg, L. (2001). Using Molecular Beacons to Detect Single-Nucleotide Polymorphisms with Real-Time PCR. *Methods*, *25*(4), 463–471. https://doi.org/10.1006/meth.2001.1269

Mokany, E., Tan, Y. L., Bone, S. M., Fuery, C. J., & Todd, A. V. (2013). MNAzyme qPCR with Superior Multiplexing Capacity. *Clinical Chemistry*, *59*(2), 419–426. https://doi.org/10.1373/clinchem.2012.192930

Neopane, P., Nypaver, J., Shrestha, R., & Beqaj, S. S. (2021). SARS-CoV-2 Variants Detection Using TaqMan SARS-CoV-2 Mutation Panel Molecular Genotyping Assays. *Infection and Drug Resistance*, *Volume 14*, 4471–4479. https://doi.org/10.2147/IDR.S335583

Paul, P., France, A. M., Aoki, Y., Batra, D., Biggerstaff, M., Dugan, V., Galloway, S., Hall, A. J., Johansson, M. A., Kondor, R. J., Halpin, A. L., Lee, B., Lee, J. S., Limbago, B., MacNeil, A., MacCannell, D., Paden, C. R., Queen, K., Reese, H. E., … Silk, B. J. (2021). Genomic Surveillance for SARS-CoV-2 Variants Circulating in the United

States, December 2020–May 2021. *MMWR. Morbidity and Mortality Weekly Report*, *70*(23), 846–850. https://doi.org/10.15585/mmwr.mm7023a3

Platt, A. R., Woodhall, R. W., & George, A. L. (2007). Improved DNA sequencing quality and efficiency using an optimized fast cycle sequencing protocol. *BioTechniques*, *43*(1), 58–62. https://doi.org/10.2144/000112499

Quintáns, B., Álvarez-Iglesias, V., Salas, A., Phillips, C., Lareu, M. V., & Carracedo, A. (2004). Typing of mitochondrial DNA coding region SNPs of forensic and anthropological interest using SNaPshot minisequencing. *Forensic Science International*, *140*(2–3), 251–257. https://doi.org/10.1016/j.forsciint.2003.12.005

Ragoussis, J. (2009). Genotyping Technologies for Genetic Research. *Annual Review of Genomics and Human Genetics*, *10*(1), 117–133. https://doi.org/10.1146/annurev-genom-082908-150116

Reslova, N., Michna, V., Kasny, M., Mikel, P., & Kralik, P. (2017). xMAP Technology: Applications in Detection of Pathogens. *Frontiers in Microbiology*, *8*. https://doi.org/10.3389/fmicb.2017.00055

Rodríguez, A., Rodríguez, M., Córdoba, J. J., & Andrade, M. J. (2015). Design of Primers and Probes for Quantitative Real-Time PCR Methods. In C. Basu (Ed.), *PCR Primer Design* (Vol. 1275, pp. 31–56). Springer New York. https://doi.org/10.1007/978-1-4939-2365-6_3

Rossen, L., Nørskov, P., Holmstrøm, K., & Rasmussen, O. F. (1992). Inhibition of PCR by components of food samples, microbial diagnostic assays and DNA-extraction solutions. *International Journal of Food Microbiology*, *17*(1), 37–45. https://doi.org/10.1016/0168-1605(92)90017-W

Schleinitz, D., DiStefano, J. K., & Kovacs, P. (2011). Targeted SNP Genotyping Using the TaqMan® Assay. In J. K. DiStefano (Ed.), *Disease Gene Identification* (Vol. 700, pp. 77–87). Humana Press. https://doi.org/10.1007/978-1-61737-954-3_6

Schrader, C., Schielke, A., Ellerbroek, L., & Johne, R. (2012). PCR inhibitors—Occurrence, properties and removal. *Journal of Applied Microbiology*, *113*(5), 1014–1026. https://doi.org/10.1111/j.1365-2672.2012.05384.x

Tan, L. Y., Walker, S. M., Lonergan, T., Lima, N. E., Todd, A. V., & Mokany, E. (2017). Superior Multiplexing Capacity of PlexPrimers Enables Sensitive and Specific Detection of SNPs and Clustered Mutations in qPCR. *PLOS ONE*, *12*(1), e0170087. https://doi.org/10.1371/journal.pone.0170087

Twyman, R. M., & Primrose, S. B. (2003). Techniques patents for SNP genotyping. *Pharmacogenomics*, *4*(1), 67–79. https://doi.org/10.1517/phgs.4.1.67.22582

Vega, F. M. D. L., Lazaruk, K. D., Rhodes, M. D., & Wenz, M. H. (2005). Assessment of two flexible and compatible SNP genotyping platforms: TaqMan® SNP Genotyping Assays and the SNPlex^{TM} Genotyping System. *Mutation Research/Fundamental and Molecular Mechanisms of Mutagenesis*, *573*(1–2), 111–135. https://doi.org/10.1016/j.mrfmmm.2005.01.008

Vignal, A., Milan, D., SanCristobal, M., & Eggen, A. (2002). A review on SNP and other types of molecular markers and their use in animal genetics. *Genetics Selection Evolution*, *34*(3), 275. https://doi.org/10.1186/1297-9686-34-3-275

Wang, R., Hozumi, Y., Yin, C., & Wei, G.-W. (2020). Decoding SARS-CoV-2 Transmission and Evolution and Ramifications for COVID-19 Diagnosis, Vaccine, and Medicine. *Journal of Chemical Information and Modeling*, *60*(12), 5853–5865. https://doi.org/10.1021/acs.jcim.0c00501

WHO, W. (2021). *WHO-2019-nCoV-surveillance-variants-2021.1-eng_2.pdf*. https://www.who.int/publications/i/item/WHO_2019-nCoV_surveillance_variants

Wilson, R. C. (2024). *Rob Wilson, Personal Communication*.

Wittwer, C. T., Herrmann, M. G., Gundry, C. N., & Elenitoba-Johnson, K. S. J. (2001). Real-Time Multiplex PCR Assays. *Methods*, *25*(4), 430–442. https://doi.org/10.1006/meth.2001.1265

Yadav, R., Chaudhary, J. K., Jain, N., Chaudhary, P. K., Khanra, S., Dhamija, P., Sharma, A., Kumar, A., & Handu, S. (2021). Role of Structural and Non-Structural Proteins and Therapeutic Targets of SARS-CoV-2 for COVID-19. *Cells*, *10*(4), 821. https://doi.org/10.3390/cells10040821

Yin, C. (2020). Genotyping coronavirus SARS-CoV-2: Methods and implications. *Genomics*, *112*(5), 3588–3596. https://doi.org/10.1016/j.ygeno.2020.04.016

Zhao, S., Ran, J., & Han, L. (2021). Exploring the Interaction between E484K and N501Y Substitutions of SARS-CoV-2 in Shaping the Transmission Advantage of COVID-19 in Brazil: A Modeling Study. *The American Journal of Tropical Medicine and Hygiene*, *105*(5), 1247–1254. https://doi.org/10.4269/ajtmh.21-0412

Appendix

1. GISAID monitoring platform for SARS-COV2

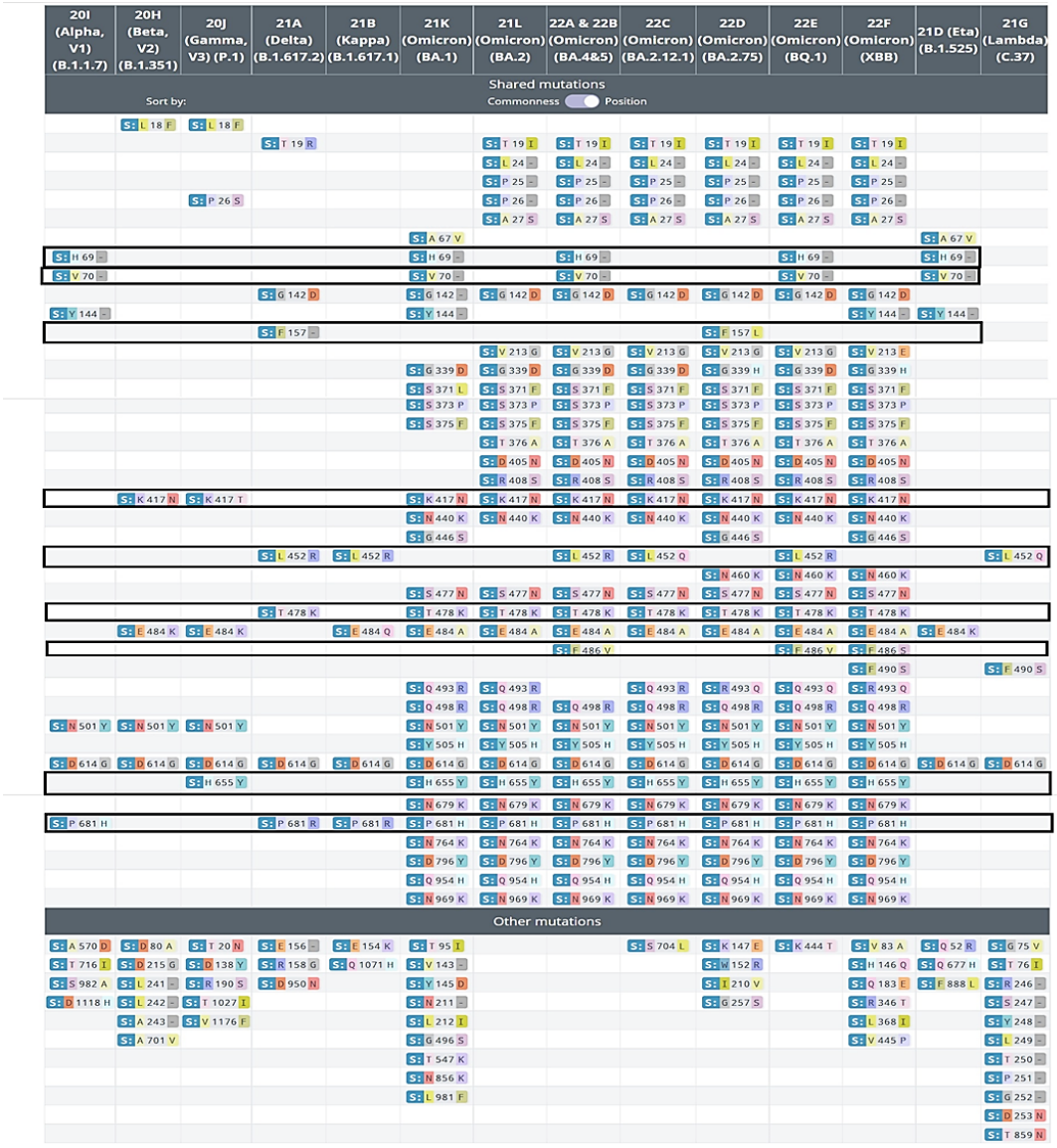

Figure A 1: ***GISAID monitoring platform for SARS-COV2:*** *Black boxes indicates the SNP site has been chosen for LAD experiment.*

2. *Table A 1: 9 SNP sites and their nomenclature.*

SNP site name	Region and mutation
SNP site 1 "H69/V70"	S:H69--(T21765-,"KM")
SNP site 2"H69/V70"	S:V70-(A21768-, "WW")
SNP site 3 "G142D"	S:G142D(G21987A, "RY")
SNP site 4 "F157-"	S:F157-(G 22033 A, "SS")
SNP site 5 "K417N"	S:K417N(G22813T,"KM")
SNP site 6 "L452R"	S:L452R(T22917G,"KM")
SNP site 7 "F486V"	S:F486V(T23018G,"KM")
SNP site 8 "H655Y"	S:H655Y(C 23525 T, "RY")
SNP site 9 "P681H"	S:P681H(C23604A,"KM")

3.

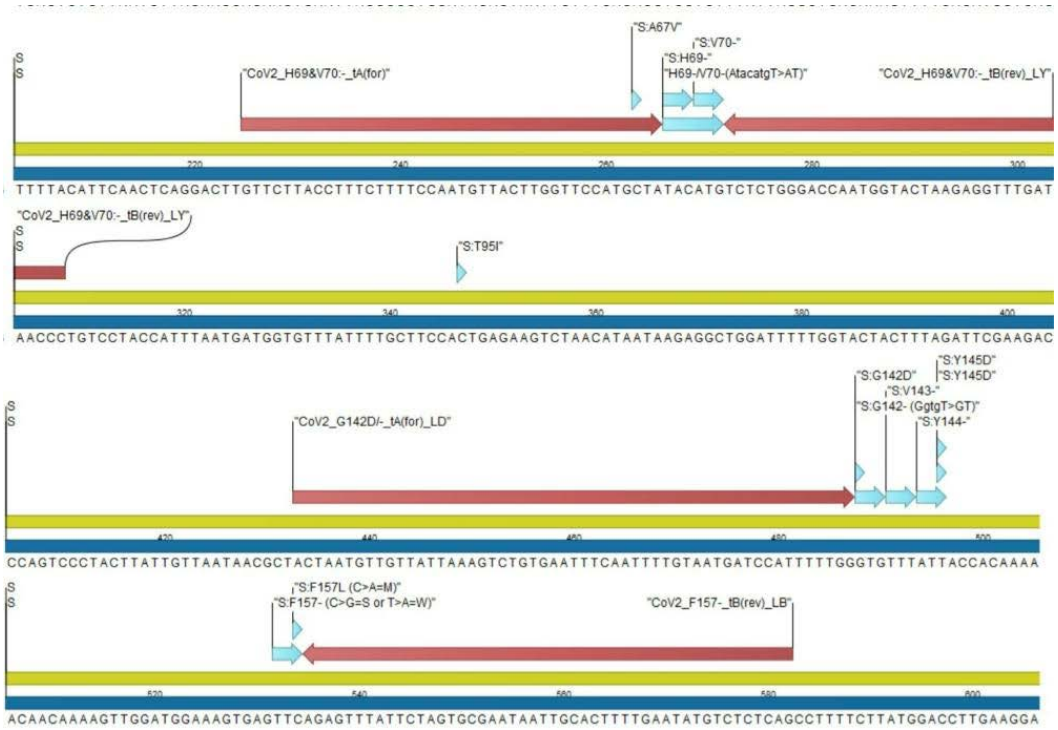

Figure A 2: ***SNPs and LP annotation****: SNP site 1 and 2 "H69/V70", SNP site 3 "G142D" and SNP site 4 "F157-"*

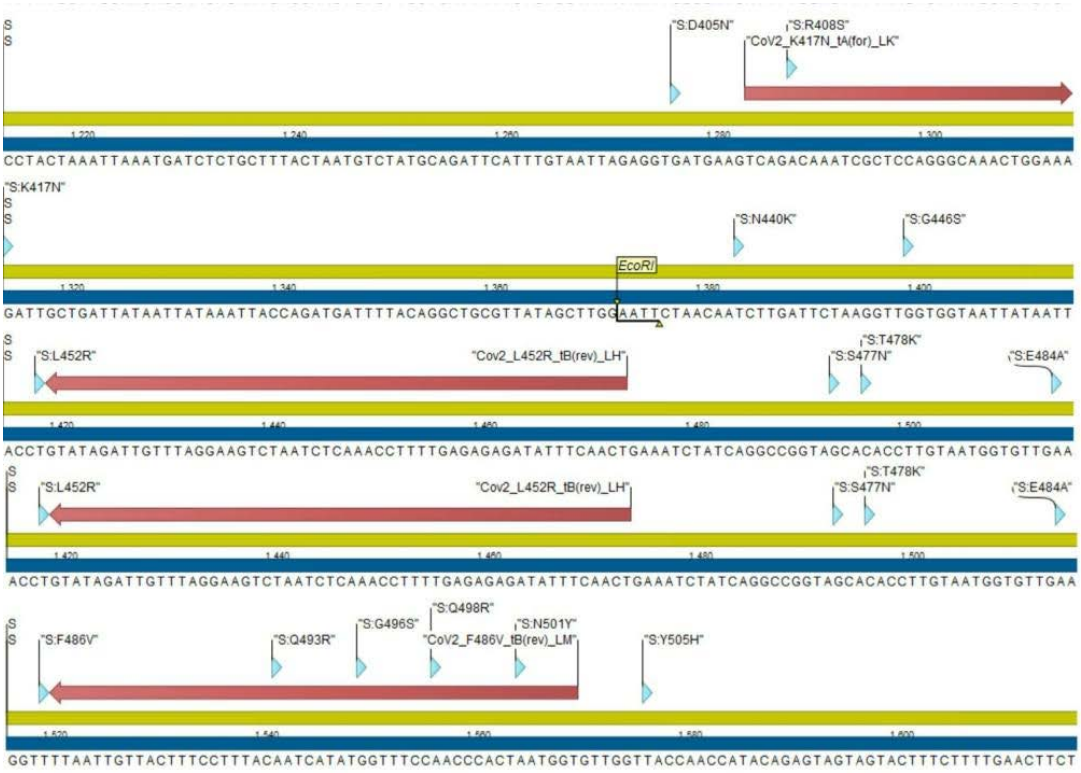

Figure A 3: ***SNPs and LP annotation:*** *SNP site 5 "K417N", SNP site 6 "L452R" and SNP site 7 "F486V"*

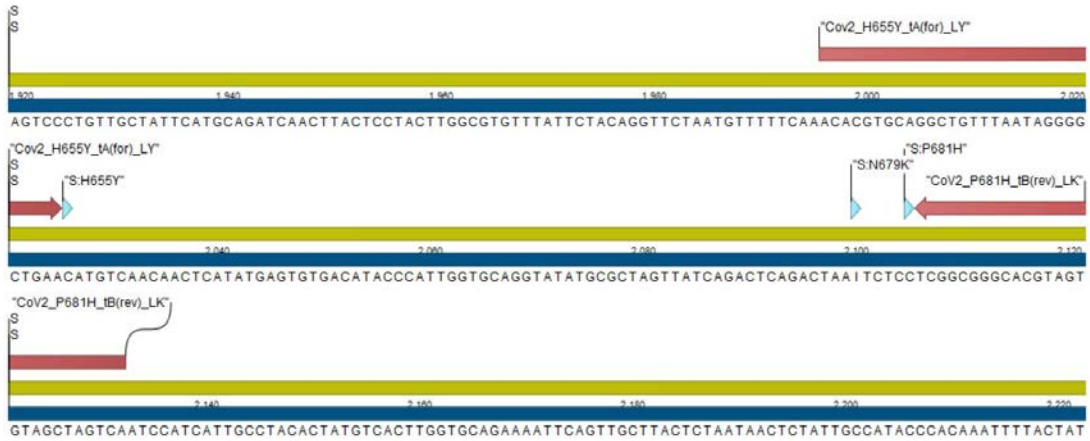

Figure A 4: ***SNPs and LP annotation****: SNP site 8 "H655Y" and SNP site 9 "P681H"*

4. *Table A 2: Labelling Primer List*

Labelling Primer	Labelling Primer with universal tail (5´-3´)	Length
CoV2_H69&V70:-_tA(for)_LY	gcctccctcgcgccaGTTCTTACCTTTCTTTTCCAATGTTACTTGGTTCCATGITA	56
CoV2_H69&V70:-_tB(rev)_LY	gccttgccagcccgcGGGTTATCAAACCTCTTAGTACCATTGGTCCCAGAGA	52
CoV2_G142D_-_tA(for)_LD	gcctccctcgcgccaACTAATGTTGTTATTAAAGTCTGTGAATTTCAATTTTGTAATGATCCATTTTTGG	70
CoV2_F157-_tB(rev)_LB	gccttgccagcccgcCTGAGAGACATATTCAAAAGTGCAATTATTCGCACTAGAATAAACTCT	63
CoV2_K417N_tA(for)_LK	gcctccctcgcgccaTCAGICAAATCGCTCCAGGGCAAACTGGAAA	46
Cov2_H655Y_tA(for)_LY	gcctccctcgcgccaACACGTGCAGGCTGTTTAATAGGGGCTGAA	45
CoV2_P681H_tB(rev)_LK	gccttgccagcccgcTGACTAGCTACACTACGTGCCCGCCGA	42
CoV2_F486V_tB(rev)_LM	gccttgccagcccgcACCATIAGTGGGTIGGAAACIATATGATIGTAAAGGAAAGTAACAATTAA	65
Cov2_L452R_tB(rev)_LH	gccttgccagcccgcAGTTGAAATATCTCTCTCAAAAGGTTTGAGATTAGACTTCCTAAACAATCTATAC	70

5. The genomic area of SARS-CoV-2 intended for the LAD experiment.

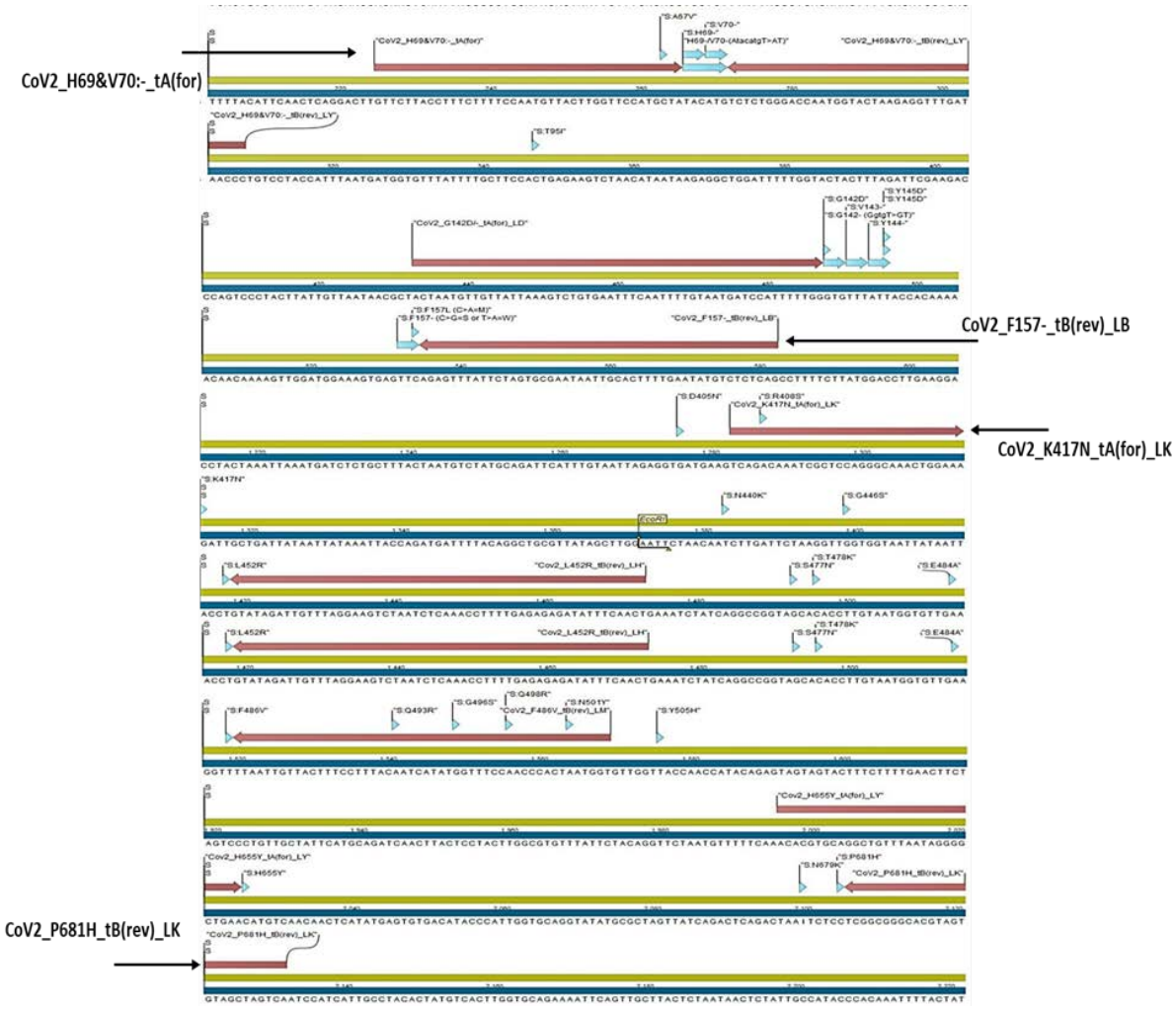

Figure A 5: ***Genomic region of interest****: A comprehensive map displaying the genomic region of SARS-CoV-2 specifically for the LAD experiment. The CLC Main Workbench program has been used to develop the genetic map.*

6. Multiplex PCR was followed from the method in section 2.5.1 and the samples were used as template was taken from FHI Plate 524.

   Primer sets:

   Set 1: CoV2_K417N_tA(for)_LK and CoV2_P681H_tB(rev)_LK (880 bp).

   Set 2: CoV2_H69&V70:-_tA(for) and CoV2_F157-_tB(rev)_LB (388 bp).

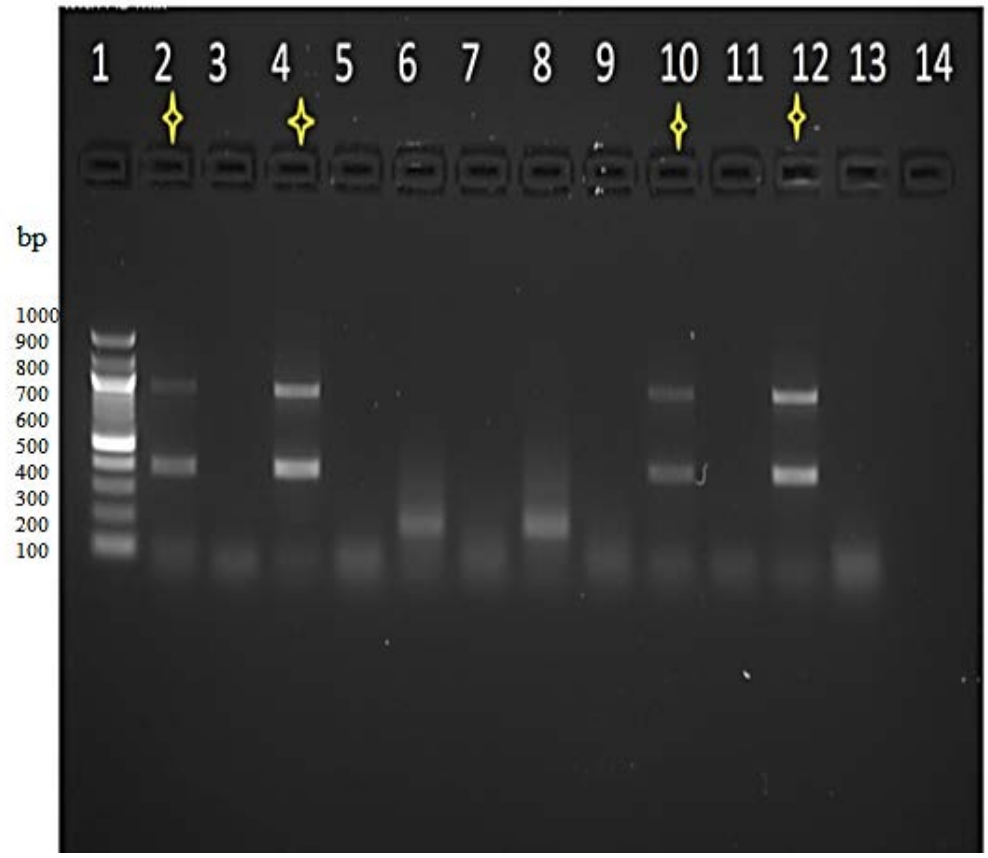

Figure A 6: ***Gel electrophoresis image (1% agarose gel).*** *Lane 1: 100 bp ladder. Lanes 2, 4, 10, 12 indicate amplicon sizes 880 bp and 388 bp (by using primer sets 1 and 2) from samples 1, 2, 5, and 6 with. Lane 6 shows a smeared band lower than 388 bp from sample 3. Lane 8 displays a smeared band lower than 388 bp from Sample 4. Lanes 3, 5, 7, 9, 11, 13 represent No template controls. Lane 14 was blank. Star-marked multiplex PCR products were used for SNaPshot assay.*

7. Reporter Probe list

Table A 3:List of Reporter probe

Reporter Probe	Fluorophore	Sequence 5´-3´	TmValue	Length
CoV2_H69&V70:-_tB(rev)_RY	FAM	TCTCTGGGACCAATGGTACTAAGAG	59.8ºC	25
CoV2_G142D_-_tA(for)_RD	FAM	CCAAAAATGGATCATT	41.5ºC	19
CoV2_F157-_tB(rev)_RB	FAM	tAGAGTTTATTCTAGTGCGAA	50.6ºC	21
CoV2_K417N_tA(for)_RK	FAM	TTTCCAGTTTGCCCTGGAGCGATTTGCCTGA	69.8ºC	31
Cov2_H655Y_tA(for)_RY	ROX	TTCAGCCCCTATTAAACAGCCTGC	61.7ºC	24
CoV2_P681H_tB(rev)_RK	ROX	TCGGCGGGCACGTAGTGTAGCTAGTCA	68.3ºC	27
CoV2_F486V_tB(rev)_RM	ROX	TTAATTGTTACTTTCCTTTACC	49.6ºC	22
Cov2_L452R_tB(rev)_RH	ROX	ttGTATAGATTGTTTAGGA	39.9ºC	19

Table A 4: Fluorophores labelled at 5' reporter probes.

Fluorophore	Excitation (nm)	Emission (nm)
FAM	495	515
ROX	575	605

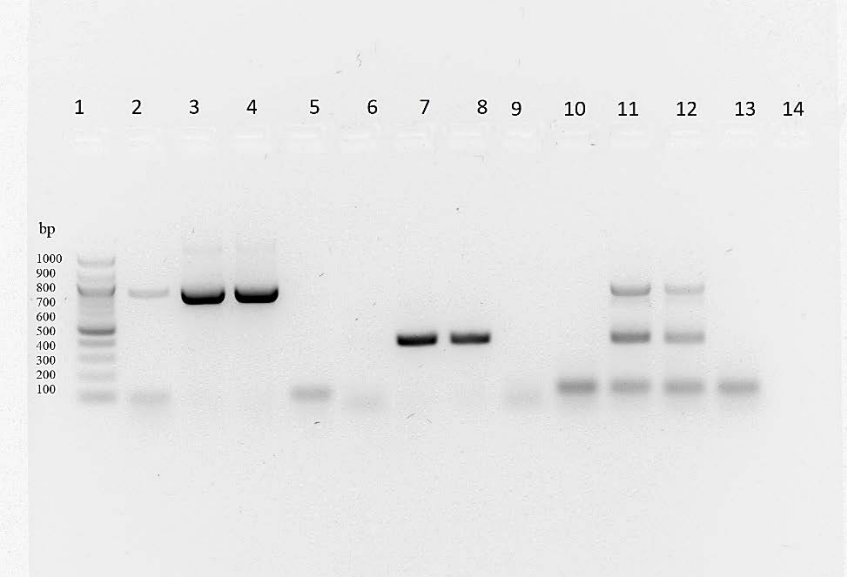

Figure A 7: ***Gel electrophoresis image****. Lane 1 shows the 100 bp ladder. Lanes 2, 3, 4 indicate amplicon size 880 bp from Samples 1, 2, 3. Lanes 6, 7, 8 display amplicon size 388 bp from Samples 1, 2, 3. Lanes 10, 11, 12 show amplicon sizes 880 bp and 388 bp from Samples 1, 2, 3. Lanes 5, 9, 13 represent no template controls. After conducting the method section 2.5.1 PCR reaction with the clinical samples, PCR products were visualized on 1% agarose gel.*

8. LB (Luria-Bertani) agar media preparation:

   LB agar media was prepared by dissolving 6.25g of LB powder and 5g of agar in 250 ml of water. The pH of the solution was checked after sterilization and found to be 6.77. The mixture was autoclaved. After autoclaving, the solution was cooled down at 45°C. Subsequently, 250 microliters of kanamycin solution at a concentration of 50 µg/mL were added to the media. Finally, distribution of the media into plates for further use.

9. LB (Luria-Bertani) media preparation

   LB media was prepared by dissolving 6.25g of LB powder in 250 ml of water. The pH of the solution was checked after sterilization and found to be 6.80. The mixture was autoclaved for 1 hour. After autoclaving, the solution was cooled down. Subsequently, 8 tubes were filled with 30 ml of LB media each. To each tube, 30 microliters of 50 ng/mL kanamycin solution was added to prepare the media.

10. Concentration of isolated plasmid DNA of SARS-CoV2

Table A 5: Concentration determination of isolated plasmid DNA containing specific region of interest of SARS-CoV2 by Nanodrop Spectrophotometer

Plasmid	Clone	ng/µL	260/280 ratio	260/230 ratio
Plasmid 1 (variant BA.5.1.5)	Clone 1(CoV2_H69&V70:-_tA and CoV2_F157-_tB(rev)_LB amplified product)	132.4	1.85	2
	Clone 2 (CoV2_K417N_tA(for)_LK and CoV2_P681H_tB(rev)_LK amplified product)	49.2	1.9	2.28
Plasmid 2 (variant BQ.1)	Clone 1 (CoV2_H69&V70:-_tA and CoV2_F157-_tB(rev)_LB amplified product)	118.4	1.91	2.29
Plasmid	Clone 2 (CoV2_K417N_tA(for)_LK and CoV2_P681H_tB(rev)_LK amplified product)	58.9	1.79	1.36

11. Plasmid Sequences Containing SARS-CoV-2 Inserts:

By using both T7 forward primer and T3 sequencing primer in the sequencing reaction it ensures that both strands of the insert DNA are sequenced bidirectionally.

Variant BA 5.1.5

PCR Product: CoV2_H69&V70:-_tA and CoV2_F157-_tB(rev)_LB (while used T7 forward primer)

- Sequence:

  GGGGGGCGGGGAATCGCCTTGCCTTGCAGCCCGCCTGAGAGACAT
  ATTCAAAAGTGCAATTATTCGCACTAGAATAAACTCTGAACTCACT
  TTCCATCCAACTTTTGTTGTTTTTGTGGTAATAAACATCCAAAAAT
  GGATCATTACAAAATTGAAATTCACAGACTTTAATAACAACATTA
  GTAGCGTTATTAACAATAAGTAGGGACTGGGCCTTCGAATCTAAA
  GTAGTACCAAAAATCCAGCCTCTTATTATGTTAGACTTCTCAGTGG
  AAGCAAAATAAACACCATCATTAAATGGTAGGACAGGGTTATCAA
  ACCTCTTAGTACCATTGGTCCCAGAGATACCATGGAACCAAGTAA
  CATTGGAAAAGAAAGGTAAGAACTGGCGCGAGGGAGGCAAGGGC
  GAATTCGTTTAAACCTGCAGGACTAGTCCCTTTAGTGAGGGTTAAT
  TCTGAGCTTGGCGTAATCATGGTCATAGCTGTTTCCTGTGTGAAAT
  TGTTATCCGCTCACAATTCCACACAACATACGAGCCGGAAGCATA
  AAGTGTAAAGCCTGGGGGTGCCTAATGAGTGAGCTAACTCACATT
  AATTGCGTTGCGCTCACTGCCCGCTTTCCAGTCGGGAAACCTGTCG
  TGCCAGCTGCATTAATGAATCGGCCAACGCGCGGGGAGAGGCGGT
  TTGCGTATTGGCGCTCTTCCGCTTCCTCGCTCACTGACTCGCTGCGC
  TCGGTCGTTCGGCTGCGGCGAGCGGTATCAGCTCACTCAAAGGCG
  GGTAATACGGTTATCCACAGAAATCAGGGGATACGCAGGAAAAG
  AACATGTGAAGCAAAAGGCCAGGCCAAAGCTCCAGGAATCCGTTA
  AAAGGGGCCCGGCTTTTTGGCATG

PCR Product: CoV2_H69&V70:-_tA and CoV2_F157-_tB(rev)_LB (while used T3 sequencing primer)

- Sequence:

  TGAGTAACGCAATTCGCCCTTGCCTCCTCGCGCCAGTTCTTACCTT
  TCTTTTCCAATGTTACTTGGTTCCATGGTATCTCTGGGACCAATGGT
  ACAAAAAGGTTTGATAACCCTGTCCTACCATTTAATGATGGTGTTT
  ATTTTGCTTCCACTGAGAAGTCTAACATAATAAGAGGCTGGATTTT

TGGTACTACTTTAGATTCGAAGGCCCAGTCCCTACTTATTGTTAAT
AACGCTACTAATGTTGTTATTAAAGTCTGTGAATTTCAATTTTGTA
ATGATCCATTTTTGGATGTTTATTACCACAAAAACAACAAAAGTTG
GATGGAAAGTGAGTTCAGAGTTTATTCTAGTGCGAATAATTGCACT
TTTGAATATGTCTCTCAGGCGGGCTGGCAAGGCAAGGGCGAATTC
GCGGCCGCTAAATTCAATTCGCCCTATAGTGAGTCGTATTACAATT
CACTGGCCGT

These sequences represent the PCR product containing the CoV2_H69&V70:-_tA and CoV2_F157-_tB(rev)_LB regions, which were cloned into the plasmid for variant BA 5.1.5.

PCR Product: CoV2_K417N_tA(for)_LK and CoV2_P681H_tB(rev)_LK (while used T7 forward primer)

- Sequence:
  ATAGGCCGGGGGAATTCGCCCTTGCTCCCTCGCGCCATCAGGCAA
  AATCGCTCCAGGGCAAACTGGAAATATTGCTGATTATAATTATAA
  ATTACCAGATAAATATTTACAGGCTGCGTTATAGCTTGGAATTCTA
  ACAAGCTTGATTCTAAGGTTGGTGGTAATTACAATTACCGGTATAG
  ATTGTTTAGGAAGTCTAATCTCAAACCTTTTGAGAGAGATATTTCA
  ACTGAAATCTATCAGGCCGGTAACAAACCTTGTAATGGTGTTGCA
  GGTGTTAATTGTTACTTTCCTTTACAATCATATGGTTTCCGACCCAC
  TTATGGTGTTGGTCACCAACCATACAGAGTAGTAGTACTTTCTTTT
  GAACTTCTACATGCACCAGCAACTGTTTGTGGACCTAAAAAGTCTA
  CTAATTTGGTTAAAAACAAATGTGTCAATTTCAACTTCAATGGTTT
  AACAGGCACAGGTGTTCTTACTGAGTCTAACAAAGAGTTTCTGCCT
  TTCCAACAATTTGGCAGAGACATTGCTGACACTACTGATGCTGTCC
  GTGATCCACAGACACTTGAGATTCTTGACATTACACCATGTTCTTT
  TGGTGGTGTCAGTGTTATAACACCAGGAAACAAATACTTCTAACC
  AGGTTGCTGTTCTTTATCAGGGTGTTAACTGCACAGAAGTCCCTGT
  TGCTATTCATGCAGATCAACTTACTCCTACTTGGCGTGTTTATTCTA
  CAGGTTTCTAATGTTTTTCAAAACACGTGCAGGCTGTTTAATTAGG
  GGCTGATATGTCAACAACTCATATGAGTGTGACATACCCATTTGCT
  GCAGGTATATGCCGCCTAAGTAATCAGACCTCCAGACTTAAGTCTC
  ATCCGCGGCACGGTAATTGTAAGCTTAAGTCCAGCGGGCTGGGCA
  AGGACAGGTCGATATTCCGATTTTTAAACGCTTGTCACGA

PCR Product: CoV2_K417N_tA(for)_LK and CoV2_P681H_tB(rev)_LK (while used T3 sequencing primer)

- Sequence:

  GTATAAGGAAATTTCGCCTTGCCTTGCAAGCCCGCTGACTAGCTAC
  ACTACGTGCCCGCCGATGAGACTTAGTCTGAGTCTGATAACTAGC
  GCATATACCTGCACCAATGGGTATGTCACACTCATATGAGTTGTTG
  ACATATTCAGCCCCTATTAAACAGCCTGCACGTGTTTGAAAAACAT
  TAGAACCTGTAGAATAAACACGCCAAGTAGGAGTAAGTTGATCTG
  CATGAATAGCAACAGGGACTTCTGTGCAGTTAACACCCTGATAAA
  GAACAGCAACCTGGTTAGAAGTATTTGTTCCTGGTGTTATAACACT
  GACACCACCAAAAGAACATGGTGTAATGTCAAGAATCTCAAGTGT
  CTGTGGATCACGGACAGCATCAGTAGTGTCAGCAATGTCTCTGCC
  AAATTGTTGGAAAGGCAGAAACTCTTTGTTAGACTCAGTAAGAAC
  ACCTGTGCCTGTTAAACCATTGAAGTTGAAATTGACACATTTGTTT
  TTAACCAAATTAGTAGACTTTTTAGGTCCACAAACAGTTGCTGGTG
  CATGTAGAAGTTCAAAAGAAAGTACTACTACTCTGTATGGTTGGT
  GACCAACACCATAAGTGGGTCGGAAAACCATATGATTGTAAAGGA
  AAGTAACAATTAACACCTGCAACACCATTACAAGGTTTGTTACCG
  GCCTGATAGATTTCAGTTGAAATATCTCTCTCAAAAAGGTTTGAGA
  TTAGACTTCCCTAAACAATCTATACCGGGTAATTGTAATTTACCCA
  CCCAACCCTTTAGAAATCAAGCTTTGATAGAATTTCCAAGCTATAC
  GCAGCCCTGGTAAAATCATTCTGGTAAATTTTATATTATATTCAAG
  CATATTTCCCAGTTGTCCCTGAGCGATTGGCCGTGAATGGCGCGAA
  GGCTAAGGCCAG

These sequences represent the PCR product containing the CoV2_K417N_tA(for)_LK and CoV2_P681H_tB(rev)_LK regions, which were cloned into the plasmid for variant BA 5.1.5.

Variant BQ.1

PCR Product: CoV2_H69&V70:-_tA and CoV2_F157-_tB(rev)_LB (while used T7 forward primer)

- Sequence:

  GGGGTTAAGGAAATCGCCCTTGCCTCCCTCGCGCCAGTTCTTACCT
  TTCTTTTCCAATGTTACTTGGTTCCATGGTATCTCTGGGACCAATGG
  CACACAAGAGGTTTGATAACCCTGTCCTACCATTTAATGATGGTGT

TTATTTTGCTTCCACTGAGAAGTCTAACATAATAAGAGGCTGGATT
TTTGGTACTACTTTAGATTCGAAGACCCAGTCCCTACTTATTGTTA
ATAACGCTACTAATGTTGTTATTAAAGTCTGTGAATTTCAATTTTG
TAATGATCCATTTTTGGATGTTTATTACCACAAAAACAACAAAAGT
TGGATGGAAAGTGAGTTCAGAGTTTATTCTAGTGCGAATAATTGC
ACTTTTGAATATGTCTCTCAGGCGGGCTGGCAAGGCAAGGGCGAA
TTCGCGGCCGCTAAATTCAATTCGCCCTATAGTGAGTCGTATTACA
ATTCACTGGCCGTCGTTTTACAACGTCGTGACTGGGAAAACCCTG
GCGTTACCCAACTTAATCGCCTTGCAGCACATCCCCCTTTCGCCAG
CTGGCGTAAATAGCGAAAGAGGCCCCGCACCGATCGCCCTTCCCA
ACAGTTTGCGCAAGCCCTATAACGTACCGGCAGTTTAAGGTTTACA
CCCATATAAAAGAGAAGAGCCGTTAATCGTCCTGTTTGTGGGATG
TAAAAAAGTTGAAATATATTGGACA

PCR Product: CoV2_H69&V70:-_tA and CoV2_F157-_tB(rev)_LB (while used T3 sequencing primer)

- Sequence:

  TGGAGCGGGGCGCCGATTCGGCCCCTTGCCTTTGCCAGCCCGCCTG
  AGAGACATATTCAAAAGTGCAATTATTCGCACTAGAATAAACTCT
  GAACTAAAAAAATCCAAAAATTGTTGTTTTTGTGGTAATAAACATC
  CAAAAATGGATCATTACAAAATTGAAATTCACAGACTTTAATAAC
  AACATTAGTAGCGTTATTAACAATAAGTAGGGACTGGGTCTTCGA
  ATCTAAAGTAGTACCAAAAATCCAGCCTCTTATTATGTTAGACTTC
  TCAGTGGAAGCAAAATAAACACCATCATTAAATGGTAGGACAGGG
  TTATCAAACCTCTTAGTACCATTGGTCCCAGAGATACCATGGAACC
  AAGTAACATTGGAAAAGAAAGGTAAGAACTGGCGCGAGGGAGGC
  AAGGGCGAATTCGTTTAAACCTGCAGGACTAGTCCCTTTAGTGAG
  GGTTAATTCTGAGCTTGGCGTAATCATGGTCATAGCTGTTTCCTGT
  GTGAAATTGTTATCCGCTCACAATTCCACACAACATACGAGCCGG
  AAGCATAAAGTGTAAAGCCTGGGGGTGCCTAATGAGTGAGCTAAC
  TCACATTAATTGCGTTGCGCTCACTGCCCGCTTTCCAGTCGGGAAA
  CCTGTCGTGCCAGCTGCATTAATGAATCGGCCAACGCGCGGGGAG
  AGGCGGTTTGCGTATTGGGCGCTCTTCCGCTTCCTCGCTCACTGAC
  TCGCTGCGCTCGGTTCGTTCGGCTGCCGGCGAGCGGTATCAGCTCA
  CTTCAAAGGGCGGTAAATACGGGTTATCCACAGAAATCAGGGGAT

TAACGCCAGGAAGAACCATGTGAGCCAAAGTCAGCAAAGGCCAG
GACCGTAAAGCCGCGATGGCTGGCCGTTTTTCCAATAGGCCTTGCG
ACTC

These sequences represent the PCR product containing the CoV2_H69&V70:-_tA and CoV2_F157-_tB(rev)_LB regions, which were cloned into the plasmid for variant BQ.1.

PCR Product: CoV2_K417N_tA(for)_LK and CoV2_P681H_tB(rev)_LK (while used T7 forward primer)

- Sequence:

  AGGGGGCGGATTCGCCCCTTGCCTCCTCGCGCCATCAGGCAAATC
  GCTCCAGGGCAAACTGGAATATTGCTGATTATAATTATAAATTACC
  AGATGATTTTACAGGCTGCGTTATAGCTTGGAATTCTAACAAGCTT
  GATTCTAAGGTTGGTGGTAATTATAATTACCGGTATAGATTGTTTA
  GGAAGTCTAATCTCAAACCTTTTGAGAGAGATATTTCAACTGAAAT
  CTATCAGGCCGGTAACAAACCTTGTAATGGTGTTGCAGGTGTTAAT
  TGTTACTTTCCTTTACAATCATATGGTTTCCGACCCACTTATGGTGT
  TGGTCACCAACCATACAGAGTAGTAGTACTTTCTTTTGAACTTCTA
  CATGCACCAGCAACTGTTTGTGGACCTAAAAAGTCTACTAATTTGG
  TTAAAAACAAATGTGTCAATTTCAACTTCAATGGTTTAACAGGCAC
  AGGTGTTCTTACTGAGTCTAACAAAAAGTTTCTGCCTTTCCAACAA
  TTTGGCAGAGACATTGCTGACACTACTGATGCTGTCCGTGATCCAC
  AGACACTTGAGATTCTTGACATTACACCATGTTCTTTTGGTGGTGT
  CAGTGTTATAACACCAGGAACAAATACTTCTAACCAGGTTGCTGTT
  CTTTATCAGGGTGTTAACTGCACAGAAGTCCCTGTTGCTATTCATG
  CAGATCAACTTACTCCTACTTGGCGTGTTTATTCTACAGGTTCTAA
  TGTTTTTCAAACACGTGCAGGCTGTTTAATAGGGGCTGAATATGTC
  AACAACTCATATGAGTGTGACATACCCATTGGTGCAGGTATATGC
  GCTAGTTATTCAGACTCAGACTAAGGTCTCCATCGGGCGGGCACG
  TAGTGTAGGCTAGTTCAAGCGGGCCTGGCCAAGCAAAGGGCCGAA
  ATTTCCGGATTTTTA

PCR Product: CoV2_K417N_tA(for)_LK and CoV2_P681H_tB(rev)_LK (while used T3 sequencing primer)

- Sequence:

  GGTTAAGGAAATTCGCCTTGCCTTGCAGCCCGCTGACTAGCTACAC

TACGGTGCCCGCCGATGAGACTTAGTCTGAGTCTGATAACTAGCG
CATAAACCTGCACCAATGGGTATGTCACACTCATATGAGTTGTTGA
CATATTCAGCCCCTATTAAACAGCCTGCACGTGTTTGAAAAACATT
AGAACCTGTAGAATAAACACGCCAAGTAGGAGTAAGTTGATCTGC
ATGAATAGCAACAGGGACTTCTGTGCAGTTAACACCCTGATAAAG
AACAGCAACCTGGTTAGAAGTATTTGTTCCTGGTGTTATAACACTG
ACACCACCAAAAGAACATGGTGTAATGTCAAGAATCTCAAGTGTC
TGTGGATCACGGACAGCATCAGTAGTGTCAGCAATGTCTCTGCCA
AATTGTTGGAAAGGCAGAAACTTTTTGTTAGACTCAGTAAGAACA
CCTGTGCCTGTTAAACCATTGAAGTTGAAATTGACACATTTGTTTT
TAACCAAATTAGTAGACTTTTTAGGTCCACAAACAGTTGCTGGTGC
ATGTAGAAGTTCAAAAGAAAGTACTACTACTCTGTATGGTTGGTG
ACCAACACCATAAGTGGGTCGGAAACCATATGATTGTAAAGGAAA
GTAACAATTAACACCTGCAACACCATTACAAGGTTTGTTACCGGCC
TGATAGATTTCAGTTGAAATATCTCTCTCAAAAGGTTTGAGATTAG
ACTTCCCTAAACAATCTATACCGGGTAATTTATAATTTACCCACCC
AACCCTTAGAATCAAAGCTTGTTAGAATTTCCAAGCTATAACGCA
GCCTGTAAAATTCATCCTGGTAAATTTATACTTTATAATCCAGCCA
TATTTCAAGGTTTGCCCTGAGCGATTGCCTTGATGGCGCGAGGAAG
CTAAGGGGCGAATTTCGCG

These sequences represent the PCR product containing the CoV2_K417N_tA(for)_LK and CoV2_P681H_tB(rev)_LK regions, which were cloned into the plasmid for variant BQ.1.

12. SNP Validation for SARS-CoV2 variant BA 5.1.5 and BQ.1:

Variant BA 5.1.5

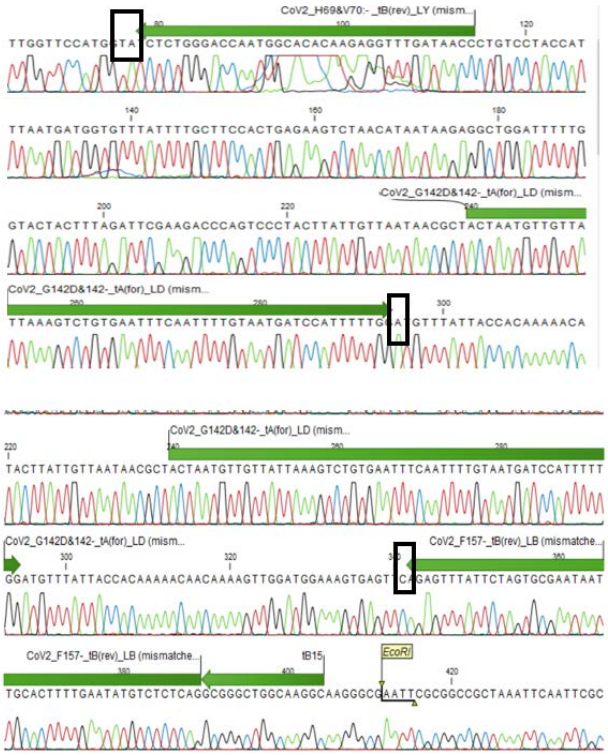

Figure A 8 This figure shows the binding sites of the primers CoV2_H69&V70:-_tB(rev)LY, CoV2_G142D-_tA(for)_LD, and CoV2_F157-_tB(rev)_LB in the sequenced PCR product for variant BA 5.1.5. The black boxes indicate the nucleotide alterations that correspond to the specific SNPs characteristic of variant BA 5.1.5

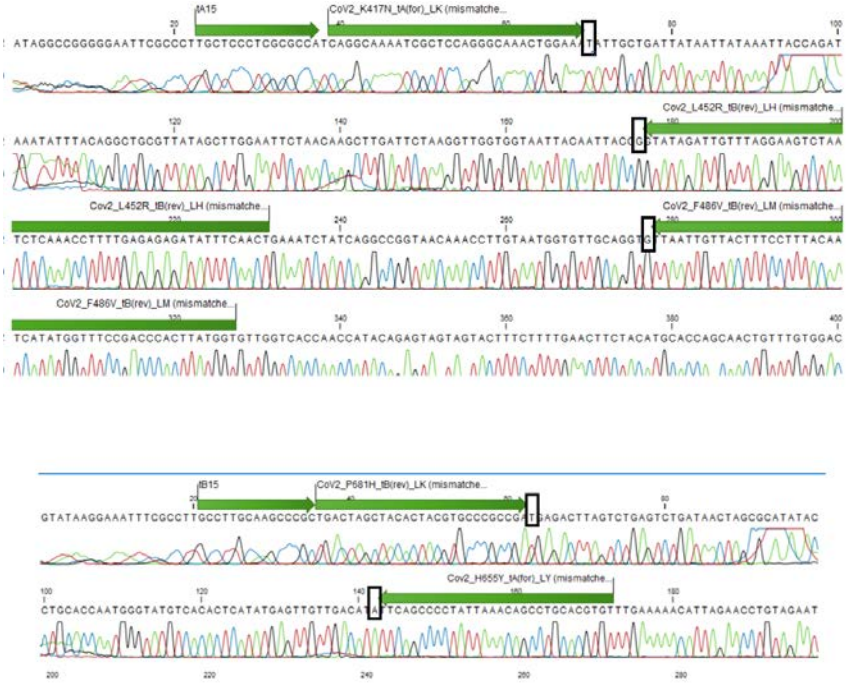

Figure A 9 This figure shows the binding sites of the primers CoV2_K417N_tA(for)_LK, CoV2_F486V_tB(rev)_LM, Cov2_L452R_tB(rev)_LH, Cov2_H655Y_tA(for)_LY, CoV2_P681H_tB(rev)_LK in the sequenced PCR product for variant BA 5.1.5. The black boxes indicate the nucleotide alterations that correspond to the specific SNPs characteristic of variant BA 5.1.5

Variant BQ.1

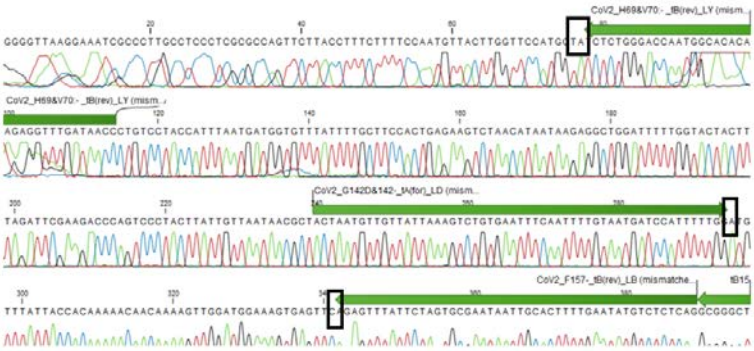

Figure A 10 This figure shows the binding sites of the primers CoV2_H69&V70:-_tB(rev)LY, CoV2_G142D-_tA(for)_LD, and CoV2_F157-_tB(rev)_LB in the sequenced PCR product for variant BQ.1. The black boxes indicate the nucleotide alterations that correspond to the specific SNPs characteristic of variant BQ.1

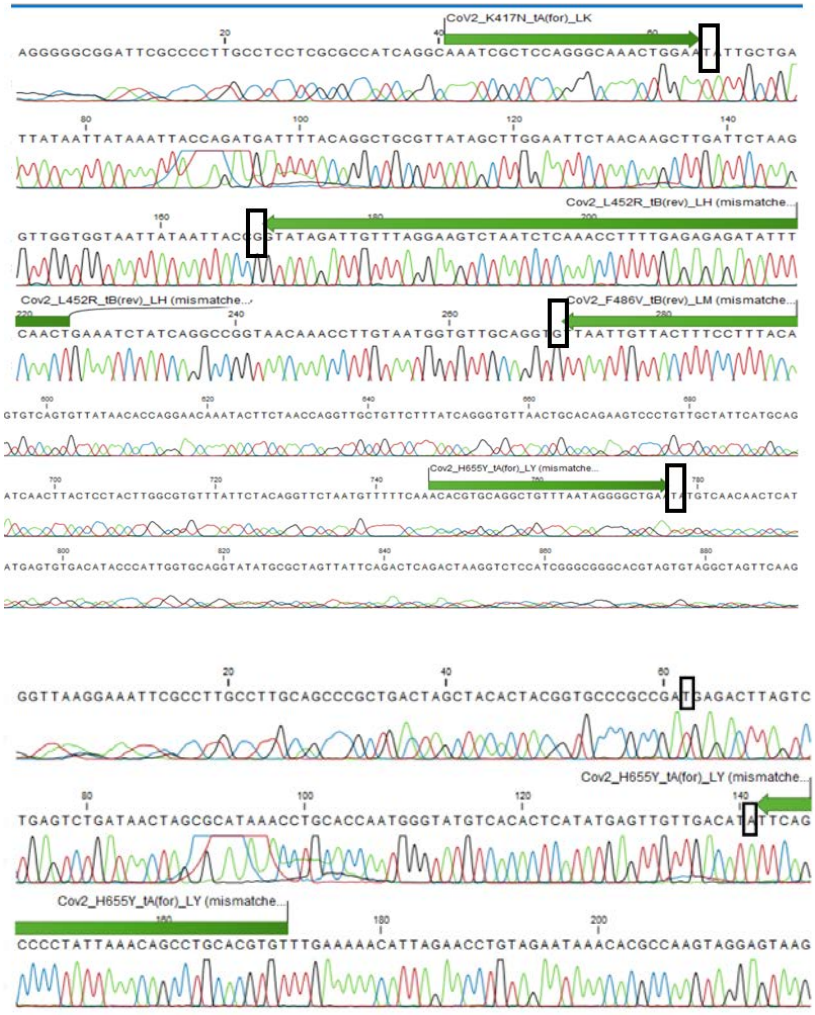

Figure A 11 This figure shows the binding sites of the primers CoV2_K417N_tA(for)_LK, CoV2_F486V_tB(rev)_LM, Cov2_L452R_tB(rev)_LH, Cov2_H655Y_tA(for)_LY, CoV2_P681H_tB(rev)_LK in the sequenced PCR product for variant BQ.1. The black boxes indicate the nucleotide alterations that correspond to the specific SNPs characteristic of variant BQ.1.

13. Table A 6: Summary of Snapshot results: Detection of Labelled LPs by Multiplex SNaPshot assay

Labelling Probe	Length	Wild Type	Mutation	Expected Peak Colour	Observed Peak Colour	Observed Peak Size (without tail A/B	Observed Peak size with tail A/B	Height
CoV2_H69&V70:-_tA(for)	56 (not LP)							
CoV2_H69&V70:-_tB(rev)_LY	52	A(TACATG)T	A()T	Green (A)/Red (T)	Red (T)	55.01	54.89	1409, 1302,
CoV2_G142D_-_tA(for)_LD	70	G, G(GTG)T	A,G()T	Green (A)/Blue (G)/Red (T)	Blue	69.27	69.29	6852,7676
CoV2_F157-_tB(rev)_LB	63	C, G(TTC)A	A, G()A	Green/Yellow/Blue	Blue(NTC)		62.55	2461
CoV2_K417N_tA(for)_LK	46	G	T	Blue/Red	Red	48.53	48.53	856/1219
Cov2_L452R_tB(rev)_LH	70	T	G/A	Green/Blue/Red	Blue	69.27	69.29	6852,7676
CoV2_F486V_tB(rev)_LM	65	T	G/C	Red/Blue/Yellow	Red	62.00	62.00	2168, 2103
CoV2_P681H_tB(rev)_LK	42	C	A	Yellow/Green	Yellow (NTC)	42.33, 42.25	42.25	2260, 2237
Cov2_H655Y_tA(for)_LY	45	C	T	Yellow/Red	Red	48.53	48.53	856, 1219

14. Table A 7 Fragment size analysis by capillary electrophoresis.

Labelling Primers	Sequences 5'-3'	Universal 15 bp tail A & B	Amplicon size (bp) (CLC Main Workbench)	Amplicon size (bp) (Capillary electrophoresis)
F-CoV2_H69&V70:-_tA(for)	F-GTTCTTACCTTTCTTTTCCAATGTTACTTGGTTCCATGITA	Forward primer A- gcctccctcgcgcca Reverse primer B- gccttgccagcccgc	114	104.52
R-CoV2_H69&V70:-_tB(rev)_LY	R-GGGTTATCAAACCTCTTAGTACCATTGGTCCCAGAGA			

F-CoV2_G142D_-_tA(for)_LD R- CoV2_F157-_tB(rev)_LB	F-ACTAATGTTGTTATTAAAGTCTGTGAATTTCAATTTTGTAATGATCCATTTTTGG R-CTGAGAGACATATTCAAAAGTGCAATTATTCGCACTAGAATAAACTCT	Forward primer A- gcctccctcgcgcca Reverse primer B- gccttgccagcccgc	180	177.1
F-CoV2_K417N_tA(for)_LK R-Cov2_L452R_tB(rev)_LH	F-TCAGICAAATCGCTCCAGGGCAAACTGGAAA R-AGTTGAAATATCTCTCTCAAAAGGTTTGAGATTAGACTTCCTAAACAATCTATAC	Forward primer A- gcctccctcgcgcca Reverse primer B- gccttgccagcccgc	221	219.11
F-CoV2_K417N_tA(for)_LK R-CoV2_F486V_tB(rev)_LM	F-TCAGICAAATCGCTCCAGGGCAAACTGGAAA R-ACCATIAGTGGGTIGGAAACIATATGATIGTAAAGGAAAGTAACAATTAA	Forward primer A- gcctccctcgcgcca Reverse primer B- gccttgccagcccgc	317	318.23

F-Cov2_H655Y_tA (for)_LY	F-ACACGTGCAGGCTGTTTAATAGGGGCTGAA	Forward primer A- gcctccctcgcgcca Reverse primer B- gccttgccagcccgc	167	163.95
R-CoV2_P681H_tB (rev)_LK	R-TGACTAGCTACACTACGTGCCCGCCGA			

15. LP and RP dissociation multiplex reaction in FAM and ROX channel for plasmid clones containing CoV2_H69&V70:-_tA and CoV2_F157-_tB(rev)_LB amplicons and CoV2_K417N_tA(for)_LK and CoV2_P681H_tB(rev)_LK amplicons from clinical sample variants BA.5.1.5

Table A 8 LP-RP duplex Tm analysis through FAM and ROX channel for plasmid containing clones of variant BA.5.1.5.

Labelling Probe	Reporter Probe	Fluoro phore	Theoretical Tm value	Expected Labelling Reaction	Labelled - ddNTP-Q	Observed Tm ℃
CoV2_H69& V70:- _tB(rev)_LY	CoV2_H69& V70:- _tB(rev)_RY	FAM	59.8ºC	U	U	64 & 53(NTC)
CoV2_G142D _-_tA(for)_LD	CoV2_G142D _-_tA(for)_RD	FAM	41.5ºC	A	A	48
CoV2_F157- _tB(rev)_LB	CoV2_F157- _tB(rev)_RB	FAM	50.6ºC	G	C	61(NTC)
CoV2_K417N _tA(for)_LK	CoV2_K417N _tA(for)_RK	FAM	69.8ºC	U	U/A	71
Cov2_H655Y _tA(for)_LY	Cov2_H655Y _tA(for)_RY	ROX	61.7ºC	U	U	66
CoV2_P681H _tB(rev)_LK	CoV2_P681H _tB(rev)_RK	ROX	68.3ºC	U	U	71
CoV2_F486V _tB(rev)_LM	CoV2_F486V _tB(rev)_RM	ROX	49.6ºC	C	Not labelled	No observed Tm
Cov2_L452R_ tB(rev)_LH	Cov2_L452R_ tB(rev)_RH	ROX	39.9ºC	C	C	48

16. LP and RP dissociation multiplex reaction in FAM and ROX channel for plasmid clones containing CoV2_H69&V70:-_tA and CoV2_F157-_tB(rev)_LB amplicons and CoV2_K417N_tA(for)_LK and CoV2_P681H_tB(rev)_LK amplicons from clinical sample variants BQ.1.

Table A 9 LP-RP duplex Tm analysis through FAM and ROX channel for plasmid containing clones of variant BQ.1.

Labelling Probe	Reporter Probe	Fluoro phore	Theoretical Tm value	Expected Labelling Reaction	Labelled-ddNTP-Q	Observed Tm°C
CoV2_H69&V70:-	CoV2_H69&V70:-	FAM	59.8ºC	U	U	64, 61(NTC)
CoV2_G142D_-	CoV2_G142D_-	FAM	41.5ºC	A	A	48
CoV2_F157-_tB(rev)_LB	CoV2_F157-_tB(rev)_RB	FAM	50.6ºC	G	C	55 (NTC)
CoV2_K417N_tA(for)_L	CoV2_K417N_tA(for)_R	FAM	69.8ºC	U	A/U	68,71
Cov2_H655Y_tA(for)_L	Cov2_H655Y_tA(for)_R	ROX	61.7ºC	U	U	66 &65(NTC)
CoV2_P681H_tB(rev)_L	CoV2_P681H_tB(rev)_R	ROX	68.3ºC	U	U	71
CoV2_F486V_tB(rev)_L	CoV2_F486V_tB(rev)_R	ROX	49.6ºC	C	Not labelled	No observed Tm
Cov2_L452R_tB(rev)_LH	Cov2_L452R_tB(rev)_RH	ROX	39.9ºC	C	C	48, 35(NTC)

17. Melting curves of reactions that involve the labeling probe LP CoV2_F157-_tB(rev)_LB and the RP CoV2_F157-_tB(rev)_RB

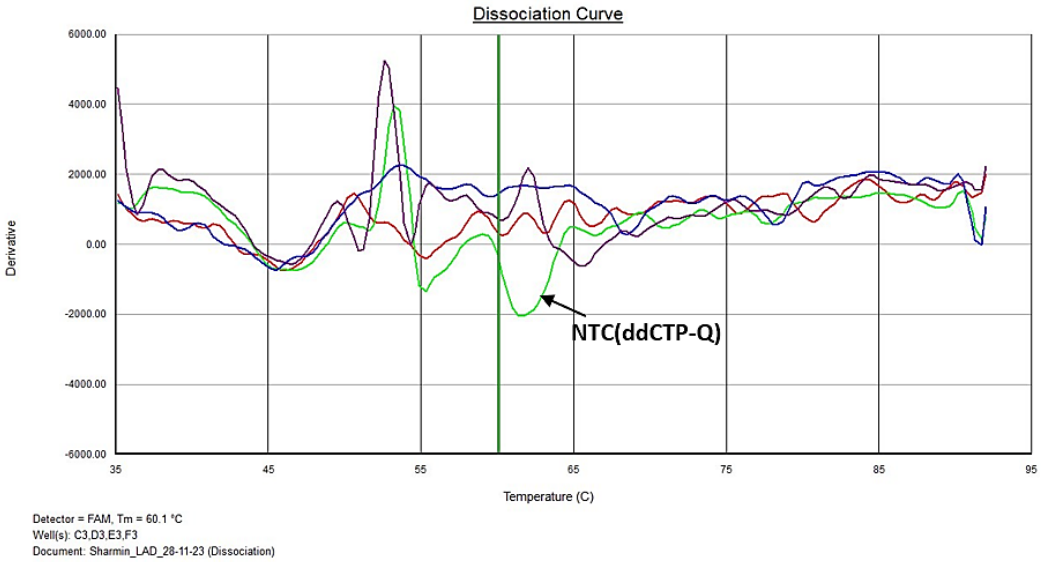

*Figure A 12: I**llustration of dissociation curves of reactions that involve the labeling probe LP CoV2_F157-_tB(rev)_LB and the reporter probe CoV2_F157-_tB(rev)_RB.** The green curve, which represents reactions without a template, showed a significant decrease in fluorescence signal of around -2000 relative fluorescence units at a Tm of 61°C. In contrast, the fluorescence units for the other colored curves were quite minor.*

A

Dimer Sequence:

5'- CTGAGAGACATATTCAAAAGTGCAATTATTCGCACTAGAATAAACTCT -3'

Maximum Delta G: -81.45 kcal/mol

Delta G: -4.77 kcal/mol **Base Pairs:** 4

```
5' CTGAGAGACATATTCAAAAGTGCAATTATTCGCACTAGAATAAACTCT
     ||||     :  :        : :        :  :     ::::
3'   TCTCAAATAAGATCACGCTTATTAACGTGAAAACTTATACAGAGAGTC
```

B

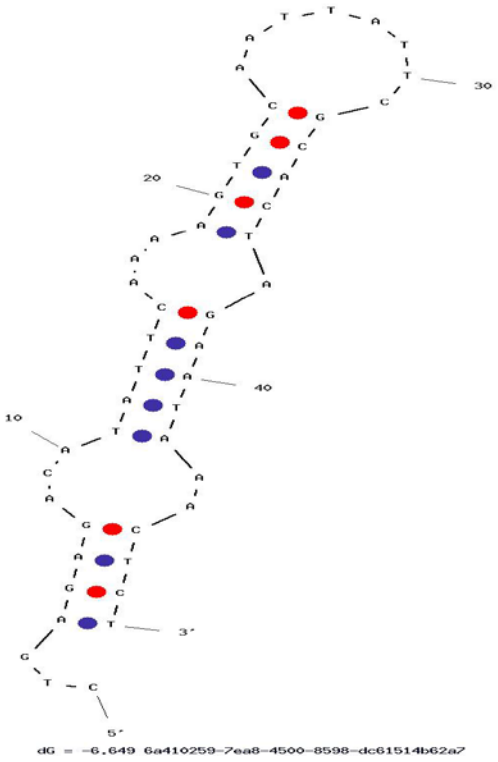

Figure A 13: ***Results of self-dimerization (A) and hairpin (B) structures of the labeling probe LP CoV2_F157-_tB(rev)_LB*** *calculated with the Oligoanalyzer 3.1 web-based bioinformatics tool: A) the maximum delta G of the probe (-81.45 kcal/mol) refers to the value of the total Gibbs free energy when it binds to its perfectly matched complementary sequence. The self-dimer structure (delta G of -4.77 kcal/mol), as presented in the bottom side of the panel, shows that the 3' ends of the probe are perfectly matched to the complementary sequence and can extend the probe with a ddCTP opposite to the G that is located in the third position from the 5' end; B) the hairpin structure of the probe (delta G of -6.65 kcal/mol in 45.3°C Tm) shows the same likelihood of the probe being extended with a ddCTP opposite to the G in the same position.*

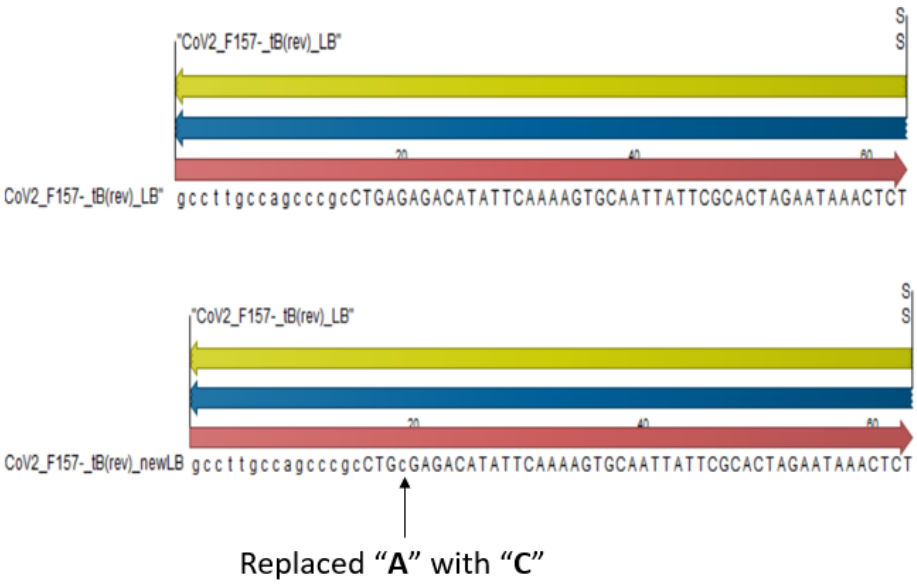

Figure A 14: ***New labelling probe sequence for LP CoV2_F157-_tB(rev)****. New LP was designed where the adenine "A" at the fourth position from the 5' end was replaced with a cytosine "C".*

18. New probe details:

Table A 10 New labelling probe sequences and their respective Tm values.

Labelling Probe	Labelling Primer with universal tail (5´-3´)	Length	Tm ℃
CoV2_F157-_tB(rev)_newLB	gccttgccagcccgcCTGcGAGACATATTCAAAAGTGCAATTATTCGCACTAGAATAAACTCT	63	68
CoV2_F157S-	gcctccctcgcgccaACCACAAAAACAACAAAAGTTGGATGGAAAGTGAGT	51	67

Table A 11 New reporter probe and its Tm value.

Reporter Probe	Fluorophore	Sequence 5´-3´	TmºC	Length

CoV2_F157S-tA(for)_RY	FAM	ACTCACTTTCCATCCAACTTTTGTTGTTTTTG	53	32

19.

Table A 12 Labelling Probe and Reporter Probe dissociation multiplex reaction in FAM and ROX channel (before and after treating with FastAP)

Labelling Probe	Reporter Probe	Fluorophore	Theoretical Tm value	Expected Labelling Reaction	Labelled		Treat with FastAP Tm Shifts	NTC	Treat with FastAP Tm Shifts		Treat with FastAP Tm Shifts	NTC	Treat with FastAP Tm Shifts		Treat with FastAP Tm Shifts	NTC	Treat with FastAP Tm Shifts		Treat with FastAP Tm Shifts	NTC	Treat with FastAP Tm Shifts
						A				C				G				U			
CoV2_H69&V70:-_tB(rev)_LY	CoV2_H69&V70:-_tB(rev)_LY	FAM	59.8ºC	U	U													66	63	61	
CoV2_G142D_-_tA(for)_LD	CoV2_G142D_-_tA(for)_LD	FAM	41.5ºC	A	A	49	45														
CoV2_F157S-tA(for)_LY	CoV2_F157S-tA(for)_RY	FAM	53ºC	U	U													64	61		
CoV2_F157-_tB(rev)_newLB	CoV2_F157-_tB(rev)_RB	FAM	50.6ºC	G	G																
CoV2_K417N_tA(for)_LK	CoV2_K417N_tA(for)_LK	FAM	69.8ºC	U	U													71	69		
Cov2_H655Y_tA(for)_LY	Cov2_H655Y_tA(for)_LY	ROX	61.7ºC	U	U	66	63											67	62		
CoV2_P681H_tB(rev)_LK	CoV2_P681H_tB(rev)_LK	ROX	68.3ºC	U	U											70	68	71	69		

CoV2_F486V_tB(rev)_LM	CoV2_F486V_tB(rev)_LM	ROX	49.6ºC	C	C	55,79	51.5	79
Cov2_L452R_tB(rev)_LH	Cov2_L452R_tB(rev)_LH	ROX	39.9ºC	C	C	49	47	

20. When running Fast 7500qPCR repeatedly, the same reactions provide different unexpected results.

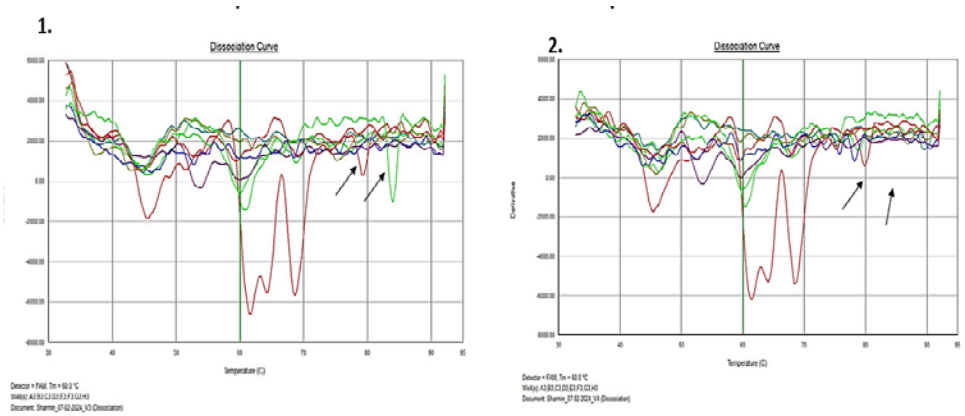

Figure A 15: ***FAM channel detector****: Panel 1 shows the results of the first run of the melting curve analysis. Two arrows indicate the presence of signals, represented by red and green, observed at temperatures of 80°C and 85°C, respectively. In contrast, Panel 2 shows the same reaction plate after two consecutive runs, when the previously observed signals were no longer visible at those specific temperatures.*

21. The variant specifics of the clinical samples along with their respective GenBank accession numbers.

Table A 13 Six clinical samples variant details and GenBank accession number

Variant	Accession number
CH1.1(sample 1)	OY814261.1
BE.1.1(sample 2)	OX331838
BF.7(sample 3)	OY832605.1
XBB1.5 (sample 4)	OY813584.1
CJ.1 (sample 5)	OY179166.1
BA.4.6.3 (sample 6)	OY816487

*Table A 14 Mutation and quencher labelled reactions of the selected variants CH1.1,BE1.1,BF.7, XBB1.5,CJ.1,BA.4.6.3 and BQ.1(using plasmid clones). *** SNP F157S exhibited no mutations across the selected variants.*

Labelling Primer	Labelling Primer with universal tail (5´-3´)	Wild Type	Mutation	Variant Labelled with ddNTPs						
		A(TACATG)T		CH 1.1	BE.1.1	BF.7	XBB 1.5	CJ.1	BA.4.6.3	BQ.1
CoV2_H69&V70:-_tB(rev)_LY	gccttgccagcccgcGGGTTATCAAACCTCTTAGTACCATTGGTCCCAGAGA		A (--)T	C	U	U	C	C	U	U
CoV2_G142D_-_tA(for)_LD	gcctccctcgcgccaACTAATGTTGTTATTAAAGTCTGTGAATTTCAATTTTGTAATGATCCATTTTTGG	G	A	A	A	A	A	A	A	A
CoV2_F157S-tA(for)_LY	gcctccctcgcgccaACCACAAAAACAACAAAAGTTGGATGGAAAGTGAGT	T	***	U	U	U	U	U	U	U
CoV2_F157-_tB(rev)_newLB	gccttgccagcccgcCTGcGAGACATATTCAAAAGTGCAATTATTCGCACTAGAATAAACTCT	C	A	U	G	G	G	U	G	G
CoV2_K417N_tA(for)_LK	gcctccctcgcgccaTCAGICAAATCGCTCCAGGGCAAACTGGAAA	G	T	U	U	U	U	U	U	U
Cov2_H655Y_tA(for)_LY	gcctccctcgcgccaACACGTGCAGGCTGTTTAATAGGGGCTGAA	C	T	U	U	U	U	U	U	U
CoV2_P681H_tB(rev)_LK	gccttgccagcccgcTGACTAGCTACACTACGTGCCCGCCGA	C	A	U	U	U	U	U	U	U
CoV2_F486V_tB(rev)_LM	gccttgccagcccgcACCATIAGTGGGTIGGAAACIATATGATIGTAAAGGAAAGTAACAATTAA	T	C/G	U	C	C	G	G	C	C

Cov2_L452R_tB(rev)_LH	gccttgccagcccgcAGTTGAAATATCTCTCTCAAAAGGTTTGAGATTAGACTTCCTAAACAATCTATAC	T	G	C	C	C	U	U	C	C